# 7.07 The Generation of Plate Tectonics from Mantle Dynamics

**D Bercovici**, Yale University, New Haven, CT, USA
**PJ Tackley**, Institut für Geophysik, ETH Zürich, Switzerland
**Y Ricard**, Ecole Normale Supérieure de Lyon, Université de Lyon-1, CNRS, Lyon, France





 http://dx.doi.org/10.1016/B978-0-444-53802-4.00135-4 

## 7.07.1 Introduction

Plate tectonics is arguably one of the most successful scientific theories in physical science, given its predictive capacity regarding, for example, the distribution and magnitude of seismic and volcanic disasters (see Abbott, 2011) or seafloor ages and hydrocarbon maturation (see McKenzie, 1981). However, it also plays a crucial role in planetary science since plate tectonics is a likely key ingredient for planetary habitability. In particular the plate-tectonic mode of mantle circulation drives chemical disequilibrium in the ocean and atmosphere by constantly bringing new mantle material to the surface. In this way, plate tectonics drives the geologic carbon cycle through erosion, weathering, and volcanism (Berner, 2004; Walker et al., 1981), which imposes a negative feedback and the long-term climate stability necessary for biological evolution over billions of years. Likewise, plate tectonics may also be necessary for the origin of life by providing an energy source for chemosynthetic life at the bottom of the ocean, that is, at mid-ocean ridges (e.g., Southam and Westall, 2007) (**Chapter 10.14**). The discovery of many terrestrial planets in other solar systems over the last 15 years (e.g., Charbonneau et al., 2009) has, therefore, emphasized that the existence of plate tectonics is possibly a necessary condition for biological habitability (Foley et al., 2012; Korenaga, 2010; Landuyt and Bercovici, 2009b; O'Neill and Lenardic, 2007; Valencia and O'Connell, 2009; Valencia et al., 2007; van Heck and Tackley, 2011).

However, understanding the conditions for plate tectonics requires a predictive theory for not only how it is driven but also how it arises during the evolution of a planet and in particular how it is generated on some but not all planets. For example, the occurrence of plate tectonics on Earth but not its putative twin Venus (or any of the other terrestrial planets in our solar system) is one of the major enigmas in Earth and planetary science. Thus, a comprehensive physical theory for the origin and generation of plate tectonics is one of the greatest challenges in geophysics yet remains an elusive goal despite 30 years of research (e.g., Bercovici, 1993, 1995b; Bercovici and Ricard, 2005; Davies and Richards, 1992; Foley and Becker, 2009; Hager and O'Connell, 1979, 1981; Kaula, 1980; Landuyt and Bercovici, 2009a; Landuyt et al., 2008; Ricard and Vigny, 1989; Tackley, 1998, 2000c,d; van Heck and Tackley, 2008; Vigny et al., 1991); see previous reviews by Bercovici et al. (2000), Gurnis et al. (2000), Tackley (2000b), Bercovici (2003), Lowman (2011), and Korenaga (2013).

In the late 1930s, following the introduction of Alfred Wegener's theory of continental drift (Wegener, 1924), several driving mechanisms for the Earth's apparent surface motions were proposed. While Wegener himself favored tidal and *pole fleeing* (i.e., centrifugal) forces, Arthur Holmes and others hypothesized that thermal convection in the Earth's mantle provided the necessary force to drive continental motions (Hales, 1936; Holmes, 1931; Pekeris, 1935; see Bercovici, 2007; Hallam, 1987; Lewis, 2002; and **Chapter 7.01**). Even after the rejection of the theory of continental drift, and its resurrection 30 years later in the form of 'plate tectonics' (Hess, 1962; Le Pichon, 1968; McKenzie and Parker, 1967; Morgan, 1968; Runcorn, 1962b), mantle convection was still invoked as the engine of surface motions (e.g., Oxburgh and Turcotte, 1978; Runcorn, 1962a; Turcotte and Oxburgh, 1972).

Indeed, more than 50 years since the discovery of seafloor spreading (Hess, 1962; Vine and Matthews, 1963), there remains little doubt that the direct energy source for plate tectonics and all its attendant features (mountain building, earthquakes, volcanoes, etc.) is the release of the mantle's gravitational potential energy through convective overturn (sustained by radiogenic heating and core cooling, which partially replenishes the mantle's gravitational potential energy).

With the recognition of the importance of slab pull (e.g., Forsyth and Uyeda, 1975) and that subducting slabs are essentially cold downwellings, it is widely accepted that the plates are not so much driven by convection but are an integral part of mantle circulation, or more to the point, they *are* mantle convection (e.g., Bercovici, 2003; Davies and Richards, 1992; Schubert, 1980). However, the notion that plates arise from a convective mantle yields many complications and new questions. The most difficult of these questions concerns the property of the mantle–lithosphere system that allows a form of convective flow that is unlike most forms of thermal convection in fluids (save perhaps lava lakes; see Duffield, 1972), and even rare for terrestrial planets, except Earth, that is, a convection that looks like plate tectonics at the surface. Indeed, understanding the complex properties of the mantle's convective 'fluid' has required an extensive collaboration of disciplines including experimental petrology, mineral physics, seismology, and geodynamics.

In this chapter, we review progress on the problem of how plate tectonics itself is explained by mantle convection theory. We begin by briefly surveying some essential features of plate tectonics that geodynamic theories seek to predict or explain, followed by aspects of basic convection in simple fluid systems that are applicable to plate tectonics (see also **Chapters 7.11** and **7.12**). We next discuss those features of plate tectonics that are reasonably well explained by basic convection theory and then examine the numerous features of plate tectonics that are poorly (or not at all) explained by simple convection. This is followed by an update on current research into the physics of plate generation and indeed how to unify the theories of plate tectonics and mantle convection. We close with a discussion of future directions regarding planetary evolution and the origin of plate tectonics itself.

## 7.07.2 Plate Tectonics

### 7.07.2.1 Present-Day Plate Motions

#### *7.07.2.1.1 Plate kinematics*

The Earth's surface motions are reasonably well described by solid-body rotations of spherical caps around an Euler pole wherein the motion of these caps is confined to the surface of a sphere (i.e., the Earth's surface). The Euler pole theory is the core premise of the working mathematical model of plate tectonics as originally prescribed by Morgan (1968) and McKenzie and Parker (1967) and continues to be used in present-day plate motion models (e.g., Argus and Gordon, 1991); (see **Chapter 6.08**). Plate-tectonic theory divides such surface motion into 12 major caps or plates, whose edges define the plate boundaries and a number of minor plate and microplates (**Figure 1**). The relative motion of these plates gives an accurate prediction of the deformation at plate boundaries, that is, whether they are convergent, divergent, or in shear. What is enigmatic about this description from a geodynamic perspective is not only that motion can be described with solid-body motion with narrow boundaries between plates but also that the Euler poles and hence directions of motion appear largely uncorrelated; for example, the motion of the Pacific and Austro-Indian Plates are essentially orthogonal to each other. These features lead to a system of plate boundaries where there is nearly as much strike-slip shear deformation as there is divergent and convergent motion (Olson and Bercovici, 1991), which is an important enigma about the plate-tectonic style of mantle convection.

Closely related to these modes of plate boundary deformation is the composition of the present-day velocity field in terms of poloidal and toroidal components (see **Section 7.07.3.7**). Poloidal flow is essentially the vertical convective circulation that expresses itself as convergent and divergent motion at the surface. Toroidal flow involves horizontal spinning or shearing motion about a vertical axis (e.g., cyclonic activity in the atmosphere), and in plate motions, this is manifested primarily as strike-slip shear. Decomposition of the present-day velocity field into poloidal and toroidal components (e.g., Forte and Peltier, 1987) shows that the poloidal and toroidal kinetic energies are comparable at most wavelengths (or spherical harmonic degree) (**Figure 2**). The largest energy for both fields occurs at spherical harmonic degree 1, for which the poloidal flow is from one hemisphere to the other and the toroidal flow involves net-lithospheric rotation relative to the mantle (Cadek and Ricard, 1992; Hager and O'Connell, 1978, 1979, 1981; O'Connell et al., 1991). Net-lithospheric rotation however depends on the choice of reference frame, the most common of which is the hot spot frame that is, in principle, fixed to the deep mantle. Although the lithosphere cannot have a net torque, net-lithospheric rotation in the hot spot reference frame is allowed and is even well predicted, given simple lateral viscosity variations associated with the contrast in oceanic and continental lithosphere (Ricard et al., 1991); in this frame of reference, the ratio of total toroidal to total poloidal kinetic energies is about 0.85, that is, the energies are roughly equal. The no-net-lithospheric-rotation frame is often chosen to remove the

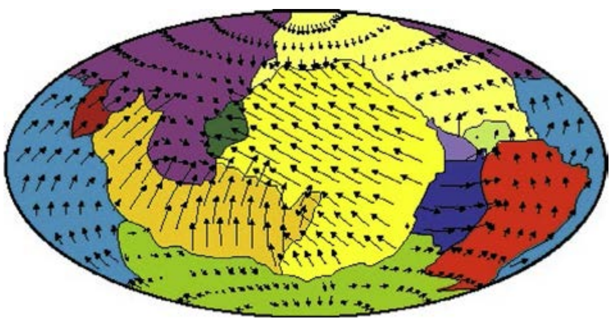

**Figure 1** Configuration of present-day plate tectonics with indicated directions of motion, on an equal-area projection map. Color code for each plate is as follows: Pacific, yellow; Austro-Indian, gold; N. American, light yellow; S. American, red; African, azure; Eurasian, purple; Antarctic, chartreuse; Nazca, indigo; Cocos, violet; Caribbean, light green; Philippine, dark green; Arabian, dark red.

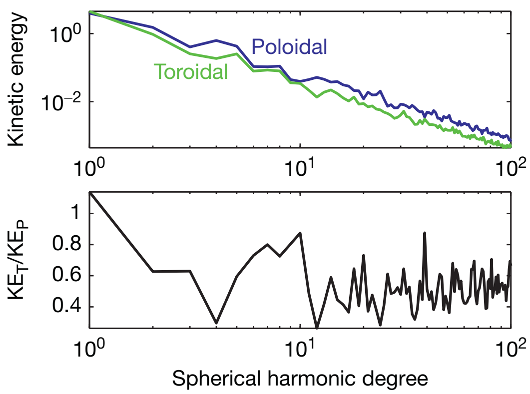


**Figure 2** Power spectrum (i.e., kinetic energy per mass) of poloidal and toroidal flow fields (top frame) and the ratio of energies (bottom frame) for present-day plate motions versus the spherical harmonic degree, which is equivalently the spherical wave number (wherein larger degrees represent smaller wavelengths). Velocity can be separated into poloidal and toroidal parts according to $\mathbf{v} = \mathbf{v}_p + \mathbf{v}_t$, in which the poloidal and toroidal velocities are represented in vector spherical harmonic series $\mathbf{v}_p = \sum_{l=1}^{\infty} \sum_{m=-l}^{l} \Phi_l^m r \nabla Y_l^m$ and $\mathbf{v}_t = \sum_{l=1}^{\infty} \sum_{m=-l}^{l} \Psi_l^m \mathbf{r} \times \nabla Y_l^m$ where $\Phi_l^m$ and $\Psi_l^m$ are spherical harmonic coefficients, $r$ is the radial distance from center of the planet, $\mathbf{r}$ is the position vector, and $Y_l^m$ is the normalized spherical harmonic of degree $l$ and order $m$. With these expansions, the kinetic energy (per unit mass) integrated over the surface of the globe separates into poloidal and toroidal energies according to $(KE_P, KE_T) = (1/2) \sum_{l=1}^{\infty} \sum_{m=-l}^{l} l(l+1)(|\Phi_{lm}|^2, |\Psi_{lm}|^2)$. The power spectrum shows the kinetic energies per degree $l$, that is, the components inside the summation over $l$.

reference frame but is only physically plausible in a mantle with laterally homogeneous viscosity (i.e., zero torque leads to zero net rotation if the Earth is spherically symmetric); in this case, the toroidal degree-1 field is zero, and the total toroidal energy is only about 0.28 of the total poloidal kinetic energy. However, it is most instructive to examine the ratio of energies for all spherical harmonic degree, rather than lump them all together. At longest wavelength, degree-1, the energies are roughly equal. At degrees 2 and 3, typical of the Pacific basin and Ring of Fire signature, the energies are comparable with the toroidal about 60% of the poloidal. At degrees 5–10, they are similarly comparable, with the toroidal energy peaking at about 90% of the poloidal energy at degree 10, and then are comparable again at its harmonics (degrees 20 and 40); these degrees are probably indicative of average plate sizes, and the harmonics provide sharpening associated with steplike structures. Thus, while the relevant ratio of total energies is still debated because of the frame dependence, higher-order wavelengths that are representative of plate-sized structures show that the fields are comparable.

The relation of the poloidal and toroidal velocity components to plate boundaries is most easily illustrated by the rate of horizontal divergence and vertical vorticity (i.e., rate of spin and strike-slip shear), which are associated with poloidal and toroidal fields, respectively (see Figure 3). On the Earth, no plate boundary is purely poloidal or toroidal but usually some

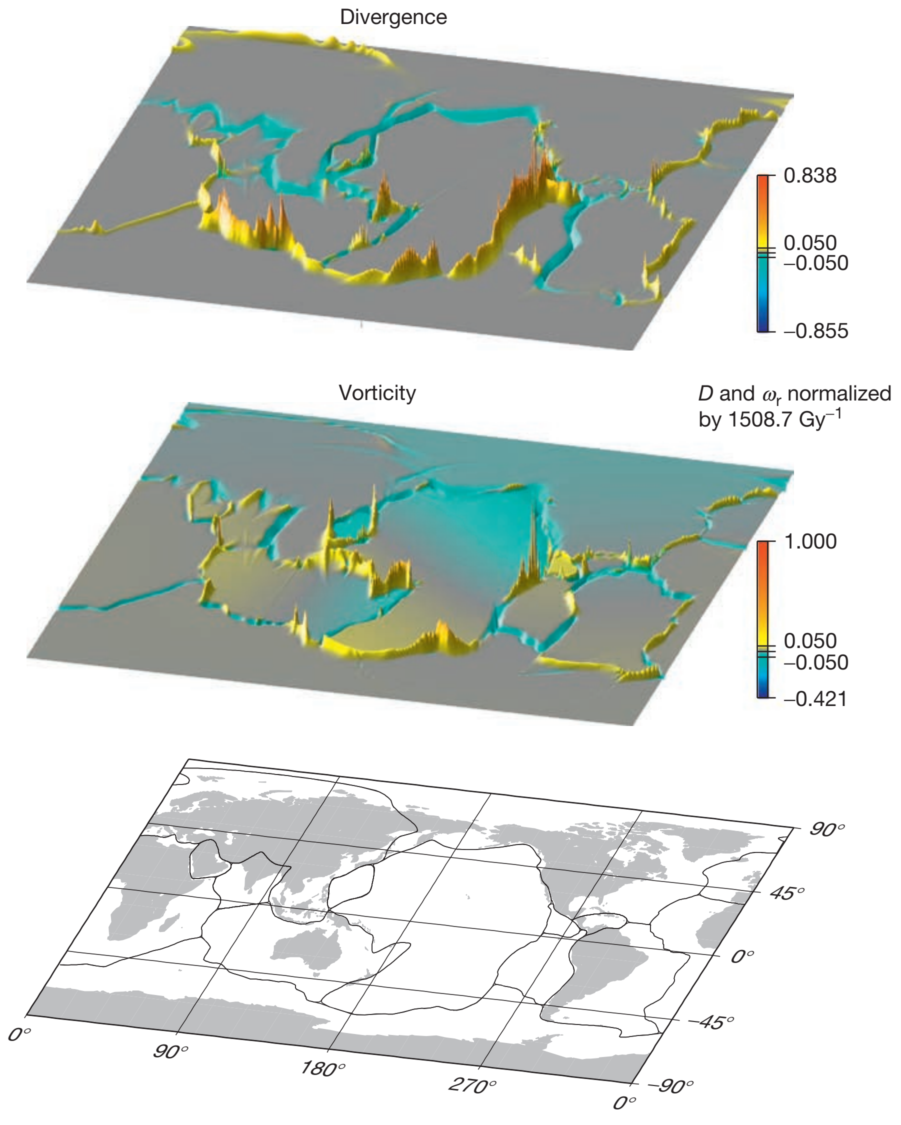


**Figure 3** Approximate horizontal divergence (top) and vertical vorticity (middle) fields of the Earth (plate and continental outlines are shown for reference in the bottom frame). Horizontal divergence is $\nabla_h \cdot \mathbf{v}$ (where $\mathbf{v}$ is the surface velocity); it is a fine-scaled representation of poloidal flow at the Earth's surface and represents the so-called rate of creation (divergence) and destruction (convergence or negative divergence) of the plates at ridges and subduction zones, respectively. Vertical vorticity is $\hat{\mathbf{r}} \cdot \nabla \times \mathbf{v}$; it is a fine-scaled representation of toroidal flow and represents the rate of strike-slip shear between plates and plate spin (vorticity is essentially a measure of the local angular velocity, that is, angular velocity of a point in the fluid). The divergence and vorticity fields shown are estimated directly from a model that uses finite-width plate margins based on seismicity distributions (Dumoulin et al., 1998); for the standard plate model with infinitesimally thin margins, these fields are all predicted to be singularities.

combination. However, the associated divergence and strike-slip vorticity are both equally and very strongly localized with comparable peak values. Moreover, using the model displayed in **Figure 2**, the ratio of root-mean-square net vorticity to that of the divergence is about 0.7 regardless of choice of reference frame. The vorticity field displays a weak expression of plate spin associated with rotations about various Euler poles, which are visible in vorticity gradients across plate interiors; but this is very weak relative to strike-slip vorticity.

#### *7.07.2.1.2 Plate forces*

The mathematical or Euler pole theory of plate tectonics is a kinematic depiction of motion, but not causative since it does not describe the dynamics or driving forces for plate tectonics. Much of this chapter is about how the mantle convective engine is related to or even causes plate tectonics. However, a budget of plate forces can be inferred by prescribing all plate forces – for example, edge forces like slab pull, ridge push and transform resistance, and areal forces like mantle drag – that when balanced give plate velocities; this amounts to an inverse problem in which the known input data vectors are the plate boundaries, the known outputs are the plate velocities or Euler poles, and from these, one solves or inverts for the unknown forces or torques that operate on the plates to yield plate motions. The classic demonstration of this force budget was done in the seminal paper of Forsyth and Uyeda (1975). The resulting inference of plate forces allowed an assessment of how plate motions are attributed to various forces. A very clear outcome of this analysis is that plate velocities are strongly correlated with the connectivity of a plate to a slab (i.e., the percent of its perimeter taken by subduction zones), which argues rather conclusively for the dominance of slab pull as a plate driving force (**Figure 4**). Other features such as plate size have little correlation with plate velocity, which is either due to the lack of mantle drag or that mantle drag and distributed ridge push balance each other (Hager and O'Connell, 1981).

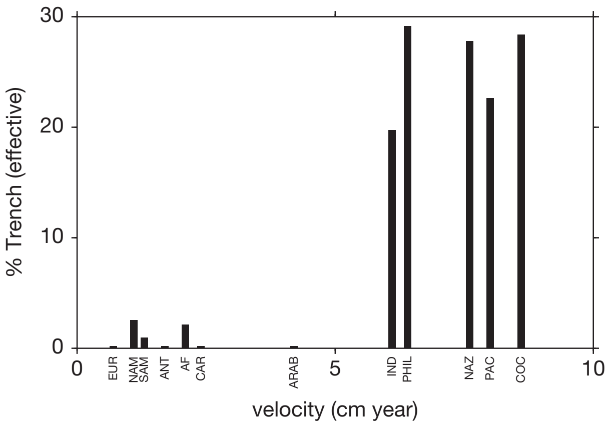


**Figure 4** Percent of plate boundary that is trench or subduction zone versus plate velocity for each plate. EUR, Eurasian Plate; NAM, North American Plate; SAM, South American Plate; ANT, Antarctic Plate; AF, African Plate; CAR, Caribbean Plate; ARAB, Arabian Plate; IND, Indo-Australian Plate; PHIL, Philippine Plate; NAZ, Nazca Plate; PAC, Pacific Plate; COC, Cocos Plate. The effective trench length corrects for subduction zones whose associated slab-pull forces are opposite in direction and presumably cancel. Data from Forsyth and Uyeda (1975).

#### *7.07.2.1.3 Plate age and size distributions*

The dominance of slab pull suggests that cold downwellings drive tectonics, that is, as the plates migrate, they get colder and heavier and eventually are convectively unstable and sink (which as we will see in the succeeding text is the description of a convective thermal boundary layer). However, plates are not all old and cold at subduction zones. In particular, the seafloor age distribution implies that subduction rates are independent of plate age; that is, the age of plates at subduction zones is distributed from age nearly 0 (i.e., subducting ridges) to the oldest ages of roughly 200 My (see Becker et al., 2009; Coltice et al., 2012) (see also the discussion in the succeeding text in **Section 7.07.5.5.3**). This observation represents an important paradox in linking plate tectonics to mantle convection.

The size distribution of plates is possibly also indicative of dynamic process in the mantle and lithosphere. A cumulative size distribution of present-day plates implies two statistical populations of large plates and smaller plates that follow different power-law or fractal distribution curves (Bird, 2003; Sornette and Pisarenko, 2003). This break in the distribution also appears to be a robust feature in time, extending back to at least 200 My (Morra et al., 2013). The larger plate distribution and its evolution have been proposed to reflect the spatial and temporal scales of mantle convective processes (Morra et al., 2013), while the smaller plate population follows a standard size–frequency power or fractal law indicative of progressive fragmentation (Bird, 2003; Sornette and Pisarenko, 2003). This interpretation however is somewhat at odds with the slab-pull correlation of Forsyth and Uyeda (1975) (**Figure 4**), which suggests that fast 'active' plates driven by subduction exist in both the large and the small distributions; hence, convection does not only drive large plates, and small plates are not simply being passively fragmented between larger plates.

### 7.07.2.2 Origin and History of Plate Tectonics

One of the most fundamental questions regarding Earth's evolution concerns the initiation of plate tectonics itself, even though evidence for the first appearance of plate tectonics is sparse and indirect at best. Geochemical analysis of zircons implies not only the existence of liquid water (Mojzsis et al., 2001; Valley et al., 2002) more than 4 Gy ago but also melting of sediments and formation of granites, possibly related to subduction zone melting, although perhaps as likely related to repeated melting events (Harrison et al., 2005; Shirey et al., 2008), the cause for which could be tectonic style recycling. Similar evidence suggests that subduction-related crustal production existed by 3.6 Ga (Hopkins et al., 2010; Jenner et al., 2013; Polat et al., 2011). Whether such possible protosubduction was localized or global is unknown (see Korenaga, 2013, who argued that geochemical data are too undersampled to be conclusive), but geochemical and petrologic evidence implies that tectonics was not widespread until 3.0–2.7 Ga (Condie and Kroner, 2008; Shirey and Richardson, 2011); see review by van Hunen and Moyen (2012).

Aside from plate initiation, the history of plate motions has only fairly recently extended into the Proterozoic through paleomagnetic plate reconstructions (e.g., Evans, 2009; Evans and Mitchell, 2011; Evans and Pisarevsky, 2008; Torsvik et al., 1996),but has yet to reach into the Archean; thus, information about early tectonic evolution largely comes from geochemical, petrologic, and geologic history of deformation belts (e.g., Brown, 2007; Condie and Kroner, 2008; Hamilton, 1998). However, the first indications of global tectonics appear to be associated with the Wilson cycle of supercontinent aggregation and dispersal (Shirey and Richardson, 2011), which continued through the Proterozoic with supercontinents such as Nuña and Rodinia (Evans, 2009; Evans and Mitchell, 2011) and on through the Phanerozoic with continental masses such as Pangaea.

#### 7.07.2.3 Planetary Tectonics

The lack of active plate tectonics on the other terrestrial planets of our solar system is an important constraint for inferring the conditions under which plate tectonics does or does not exist. Although Venus is very similar in size to Earth, and should thus have similar internal dynamics, it does not have recognizable plate tectonics. However, Venus' dearth of craters implies it was extensively resurfaced about 500 My ago, by either volcanic activity or lithospheric foundering (Turcotte, 1993; Turcotte et al., 1999). Moreover, the arcuate and topographic signatures of large Venus coronae are indicative of possible subduction, although other types of tectonic boundaries are not evident (Schubert and Sandwell, 1995). Although Mars is considerably smaller than Earth and thus more likely to have a colder and less active interior, it might have had tectonic activity in its early history; in particular, magnetic features and geologic reconstructions indicated the possibility of ancient spreading centers and strike-slip boundaries (Connerney et al., 1999, 2005; Yin, 2012). The lack of plate tectonics on Mars and Venus is typically attributed to the lack of liquid water, since Venus's water has been lost through a runaway greenhouse and Mars' water only likely existed in liquid form in its early history (Squyres et al., 2004), though perhaps coincident with surface tectonics. The mechanism by which liquid water provides a condition for plate tectonics remains enigmatic and debated since sustaining pore pressures, which reduce friction, to depths of 100 km is highly problematic, and the Earth's lithosphere might be as dry as Venus' due to dehydration melting at ridges (Hirth and Kohlstedt, 1996). Moreover, since plate tectonics is deemed necessary to stabilize Earth's temperate climate by a negative weathering feedback (Berner, 2004; Walker et al., 1981), whether liquid water or protoplate tectonics appeared first after magma ocean solidification remains an open question (e.g., Driscoll and Bercovici, 2013; Hamano et al., 2013; Lebrun et al., 2013).

## 7.07.3 Basic Convection

Basic thermal convection in fluids is perhaps the most fundamental paradigm of self-organization in nonlinear systems (see Nicolis, 1995). Such self-organization is characterized by the forcing of simple homogeneous yet perturbable or mobile systems (i.e., whose particles can move) far from equilibrium (e.g., by heating or imposition of chemical disequilibrium); in many cases, the systems can develop complex patterns and oscillatory or chaotic temporal behavior. In basic thermal convection, for example, a layer of fluid is heated uniformly and subsequently develops organized polygonal patterns and cells of cold and hot thermals. Indeed, the formation of tectonic plates is invariably a form of convective self-organization.

Although the phenomenon of convection was first recognized by Benjamin Thompson (Count Rumford) (1797), the first systematic experimental study of basic convection was carried out by Henri Bénard on layers of spermaceti (whale fat) and paraffin (Bénard, 1900, 1901), which yielded striking images of honeycombed patterns and vertical cellular structure (see **Chapter 7.03**). After John William Strutt (Lord Rayleigh) (1916) failed to theoretically explain the experiments with hydrodynamic stability theory, it was eventually deduced that Bénard's experiments were influenced by surface tension because of their open surface (Block, 1956; Pearson, 1958). When the thermal convection experiments were carried out with more controlled conditions, they were found to be well predicted by Rayleigh's theory (see Chandrasekhar, 1961, Chapter 2, Section 18). Nevertheless, convection in a layer of fluid heated along its base is still called Rayleigh–Bénard (and often just Bénard) convection (See **Chapter 7.01**).

#### 7.07.3.1 Convective Instability and the Rayleigh Number

Rayleigh's stability analysis of convection predicted the conditions necessary for the onset of convection, as well as the expected size of convection cells (relative to the layer thickness). The mathematics of his analysis has been summarized well elsewhere (Chandrasekhar, 1961), but in essence, the theory determines the infinitesimal thermal perturbations most likely to trigger convective overturn in a fluid layer that is gravitationally unstable (i.e., hotter, and thus less dense, on the bottom than the top). This most destabilizing perturbation is called the least-stable or most-unstable mode; its prediction and analysis are fundamental to the study of pattern selection in convection, as well as other nonlinear systems (see **Chapters 7.02** and **7.04**).

Depending on the nature of the binding top and bottom surfaces of the layer (i.e., whether they are freely mobile or adjacent to immobile surfaces), the most-unstable mode leads to convection cells that have a width approximately equal to (though as much as 50% larger than) the depth of the fluid layer. This result is quite relevant to plate tectonics since it is the first basic step in predicting the size of convection cells and thus the size of plates.

The perturbation that leads to this form of convection is deemed most unstable because, of all the possible perturbations, it will induce overturn with the smallest forcing. The forcing (i.e., deviation from conductive equilibrium) is driven by imposed heating, such that the resultant thermal buoyancy (proportional to density contrast times gravity) of a hot fluid parcel rising from the bottom surface through colder surroundings acts to drive convective overturn. However, such motion is also resisted or damped in two unique ways: viscous drag acts to slow down this parcel, and thermal diffusion acts to erase its hot anomaly (i.e., to lose heat to its colder surroundings). Thus, while the fluid layer might be gravitationally unstable, hot parcels rising might move too slowly against viscous drag before being erased by thermal diffusion. Similar arguments can be made for cold material sinking from the top surface through warmer surroundings. The competition between forcing by thermal buoyancy and damping by viscosity and thermal diffusion is characterized in dimensionless ratio called the Rayleigh number:

$$Ra = \frac{\rho g \alpha \Delta T d^3}{\mu \kappa} \qquad [1]$$

where $\rho$ is fluid density, $g$ is gravitational acceleration, $\alpha$ is thermal expansivity (units of $K^{-1}$), $\Delta T$ is the difference in temperature between the bottom and the top surfaces, $d$ is the layer thickness, $\mu$ is fluid viscosity (units of Pa s), and $\kappa$ is fluid thermal diffusivity (units of $m^2 s^{-1}$).

Even though $\Delta T > 0$ (i.e., heating is from below and causes gravitational instability), $Ra$ still must exceed a critical value $Ra_c$ for convection to occur. For $Ra < Ra_c$ the layer is stable and transports heat by conduction; for $Ra > Ra_c$, the layer will be convectively unstable and transport heat more rapidly via convection. Although $Ra_c$ varies depending on the mechanical nature of the horizontal boundaries (whether rigid or a free surface), it is typically of order 1000 (i.e., it varies between $Ra_c \approx 700$ for freely slipping – called *free-slip* – top and bottom boundaries and $Ra \approx 2000$ for the rigid or *no-slip* top and bottom boundaries).

This value can be roughly understood by considering the ascent of a hot (or descent of a cold) parcel of size $a$ and temperature anomaly $\Delta T$ against a viscous medium. Dimensional analysis shows that the parcel's typical ascent velocity is $\rho g \alpha \Delta T a^2/\mu$ (i.e., this combination of constants has units of meter per second). However, the rate that heat diffuses out of the parcel is $\kappa/a$ (i.e., smaller parcels lose heat faster). The critical state occurs when these two rates are equal; that is, if the buoyant ascent rate just exceeds the diffusion rate, the parcel should rise without being erased, but if the ascent rate is less than the diffusion rate, it will barely rise before being lost. Therefore, the critical state occurs if $\rho g \alpha T a^3/(\mu\kappa) \approx 1$. Scaling purely by orders of magnitude, a small parcel of fluid can be assumed to be of order ten times smaller than the entire layer; thus, assuming $a \approx d/10$ leads to a critical condition for onset of convection of $\rho g \alpha \Delta T d^3/(\mu\kappa) \approx 1000$.

For the Earth's mantle, the typical average properties from which the Rayleigh number is constructed are $\rho \approx 4000$ kg m$^{-3}$, $g = 10$ m s$^{-2}$, $\alpha = 3 \times 10^{-5}$ K$^{-1}$, $\Delta T \approx 3000$ K, $d = 2900$ km, $\mu = 10^{22}$ Pa s (dominated by the lower mantle), and $\kappa = 10^{-6}$ m$^2$ s$^{-1}$ (see Schubert et al., 2001) (see Chapter 7.02 and Volume 2). Taken together, these lead to a Rayleigh number of $\sim 10^7$, which is well beyond supercritical; although the mantle viscosity is extremely high, the mantle is also very hot and very large and hence convects vigorously. (See Chapters 7.02 and 7.04 for more thorough discussion.)

### 7.07.3.2 Vertical Structure of Simple Convection

#### 7.07.3.2.1 Symmetry

Once convection initiates and becomes fully developed, it is called *finite amplitude* convection, as opposed to the infinitesimal convection discussed earlier. The simplest form of such convection involves two-dimensional flow of constant-viscosity fluid in a plane layer that is heated on the bottom and cooled on the top (but whose upper and lower boundaries are otherwise mechanically identical, i.e., both free-slip or both no-slip). Such convection is a highly symmetrical system. This symmetry is prescribed by the fact that when convection reaches its final state (i.e., a steady state or time-averaged steady state), the top boundary is cooling the fluid by the same amount that the bottom boundary is heating the fluid; otherwise, the layer would heat up or cool down and is thus not in its final state. Thus, cold currents sinking from the top boundary will generally be equal and opposite in temperature and velocity to the hot currents emanating from the bottom boundary (Figure 5). The vertical cross section of such two-dimensional (2-D) steady convection therefore shows sequences of mirror image pairs of counterrotating convection cells; each cell's vertical wall is either a hot upwelling or a cold downwelling current, and the upwellings and downwellings are themselves symmetrical mirror images of each other through a 180° rotation (Figure 5). The breaking of this symmetry by various effects is vital to understanding the plate-tectonic style of mantle convection.

#### 7.07.3.2.2 Thermal boundary layers

When basally heated convection is vigorous (i.e., has moderate to high Rayleigh number $Ra$), it tends to stir the fluid until it is nearly homogeneous, that is, most of the fluid is at or near the average temperature of the top and bottom boundaries (this interior temperature is close to isothermal unless the fluid is significantly compressible over the depth of the layer, in which

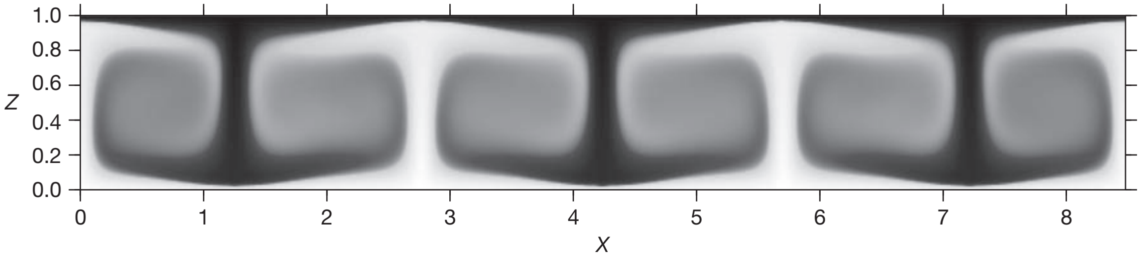


**Figure 5** A vertical cross section of the temperature field of a numerical simulation of two-dimensional plane-layer, basally heated, isoviscous (Bénard), convection, with free-slip top and bottom boundaries and $Ra = 10^5$. Black represents cold fluid; light gray is hot fluid. The temperature field shows symmetrical convection cells, upwellings, downwellings, and thermal boundary layers thickening in the direction of motion (at the top and bottom of the layer, in between the upwellings and the downwellings).

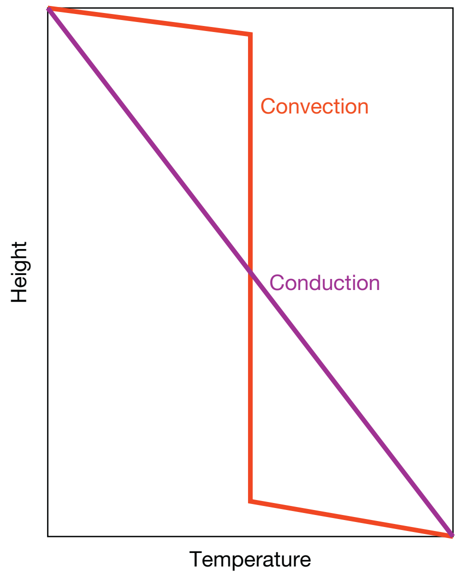


**Figure 6** Sketch of temperature profiles (i.e., horizontally averaged temperature vs. depth) for a simple isoviscous basally heated plane layer. Convective mixing homogenizes the conductive mean temperature into a nearly isothermal state (if the fluid is incompressible) with thermal boundary layers connecting it to the cold surface and hot base.

case the interior temperature follows an adiabat; see Chapter 7.02), thereby relieving the gravitational instability for the much of the layer (Figure 6). However, directly adjacent to the top and bottom boundaries, the fluid temperature must make a transition from the largely homogeneous interior value to the colder (at the top) or hotter (at the bottom) boundary value (again see Figure 6). These transition regions are the *thermal boundary layers*. In effect, convection confines the gravitationally unstable parts of the fluid to these relatively thin boundary layers, keeping most of the rest of the fluid gravitationally stable. The Earth's lithosphere and tectonic plates are essentially the horizontal thermal boundary layer along the top surface of the Earth's convecting mantle; thus, we will discuss thermal boundary layers in some detail and refer to them repeatedly.

Because of their large vertical temperature gradients, the thermal boundary layers control, via thermal conduction, the influx (through the bottom) and efflux (through the top) of heat. If the fluid is stirred by convection with increasing vigor, then more of the fluid will become homogeneous, and thus, the boundary layers will become thinner; although this leads to yet more gravitationally stable material, it also causes sharper thermal gradients in the boundary layers and thus even larger heat fluxes in to and/or out of the layer. Therefore, the more vigorous the convective stirring, the greater the heat flow through the layer. (For basally heated convection in which the top and bottom boundaries are isothermal, the heat flow through the layer is, in theory, unbounded; that is, convection can be so vigorous that the fluid would appear isothermal with two thermal boundaries reduced to simple temperature discontinuities. The same is not true for convection with only internal heating (see succeeding text) since the heat flow must balance the net rate of heat production in the layer regardless of fluid properties.)

As mentioned, the thermal boundary layers are where the gravitationally unstable material is confined, and thus, fluid in these layers must eventually either sink (if in the cold top boundary layer) or rise (if in the hot bottom boundary layer), thereby feeding the vertical convective currents, that is, downwellings and upwellings, respectively. The feeding of vertical currents induces motion of the boundary layers toward convergent zones (e.g., a downwelling for the top boundary layer) and away from divergent zones (e.g., over an upwelling). Such flow naturally causes the boundary layers to thicken in the direction of motion (see Figure 5). For example, in the top cold thermal boundary layer, fluid from hotter depths newly arrived at the divergent zone heats and thus thins the boundary layer; but as the fluid moves toward the convergent zone, it cools against the surface, and the boundary layer gradually thickens before eventually growing heavy enough to sink into the downwelling. We will revisit boundary layer thickening again when discussing subduction zones and seafloor topography.

#### 7.07.3.2.3 The size of convection cells

As discussed in Section 7.07.3.1, stability theory predicts that at the onset of overturn, convection cells are essentially as wide as the layer is thick. What determines the lateral extent of a single convection cell in finite amplitude convection is the length of the horizontal boundary layer currents. For example, as material in the top boundary layer flows laterally, it loses heat and buoyancy (being adjacent to the cold surface) and thus travels only a certain distance before it becomes so cold and negatively buoyant that it sinks and feeds the cold downwelling. The horizontal distance this boundary layer material travels before sinking determines the size of convection cells. For simple fluids, convection cell width is predicted by boundary layer theory to be the same as the layer height, that is, with an aspect ratio (width to height) of unity (Turcotte and Oxburgh, 1967; Turcotte and Schubert, 2002), as verified by experiments (e.g., see Figure 7 similar boundary layer arguments can be used to understand the structure of tectonic plates, although the aspect ratios of the major plates are much greater than unity, which reflects rheological complexities (see Section 7.07.3.5).

#### 7.07.3.2.4 Thermal boundary layer forces

What force makes the thermal boundary layer currents flow laterally? While it seems obvious that boundary layer fluid feeding a vertical current must flow horizontally (such as fluid going toward a drain), the forces behind these currents are of significance in regard to plate forces. First, buoyancy does not drive the boundary layer currents directly; buoyancy only acts vertically, while boundary layer currents move horizontally (buoyancy or gravity does eventually deflect these currents back into the convecting layer, but it cannot drive their lateral flow). Horizontal pressure gradients are the primary driving force for thermal boundary layers. For example, when hot upwelling fluid impinges on the top boundary, it induces a high-pressure region below the surface. As the top cooling thermal boundary layer material flows away from that region to its own downwelling, it gets heavier and acts to pull away from the surface; this induces a suction effect and thus, because of the boundary layer's growing weight, increasingly

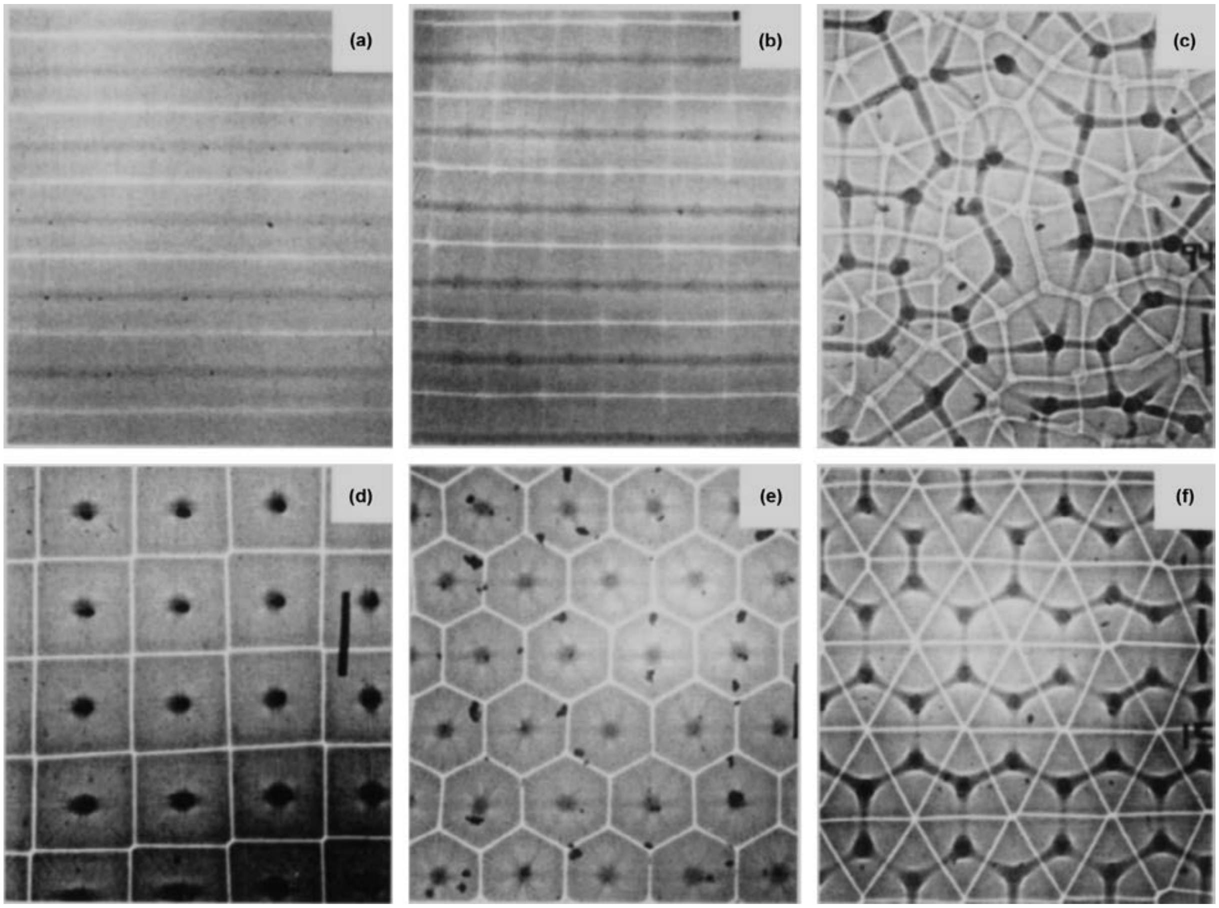


**Figure 7** Laboratory experiments on convection in viscous liquids in a plane layer, bounded between two horizontal rigid glass plates and heated from below. All images shown employ the shadowgraph technique (see text for discussion), and thus, dark regions are relatively hot, while light regions are colder. The roll pattern (a) is also called 2-D convection; this pattern becomes unstable to the bimodal pattern (b) at moderate Rayleigh numbers, which eventually gives way to the spoke pattern (c) at yet higher Rayleigh numbers (around $Ra = 10^5$). The roll, bimodal, and spoke patterns are typical for convection in isoviscous fluids, although they also occur in fluids with temperature-dependent viscosity ((a)–(c) are in fact for weakly temperature-dependent viscosity fluids). More unique to convection in temperature-dependent viscosity fluids are squares (d), hexagons (e), and even triangles (f ). Reproduced from White D (1988) The planforms and onset of convection with temperature-dependent viscosity. *Journal of Fluid Mechanics* 191: 247–286.

lower pressures in the direction of motion, eventually culminating in a concentrated low-pressure zone where the downwelling separates from the surface. Thus, the horizontal boundary layer current flows from the induced high pressure over the upwelling to the low pressure over the downwelling, that is, it flows down the pressure gradient. Invariably plate driving forces are related to these pressure gradients. Ridge push is the gradual pressure gradient going from the pressure high at a ridge outward; slab pull is effectively due to a concentrated pressure low caused by slabs pulling away from the surface. We discuss plate forces in greater detail later (**Section 7.07.4.1**).

### 7.07.3.3 Patterns of Convection

The 2-D convection described earlier is a special type of convective flow also known as convection with a roll planform; that is, the 2-D convection cells are infinitely long counter-rotating cylinders or rolls when extended into three dimensions. This pattern of convection is typically unstable at moderately high Rayleigh numbers (i.e., somewhat greater than the critical *Ra*) at which point convection becomes 3-D (Busse and Whitehead, 1971); that is, roll-like convection cells break down into more complicated geometric shapes. The study of convective planforms and pattern selection is a very rich and fundamental field in itself, although a full quantitative discussion is beyond the scope of this chapter; the interested reader should refer to Busse (1978) (and **Chapter 7.03**). However, we will briefly survey convective patterns in the context of plate tectonics and plate generation.

Much of the work on convective planforms was motivated by experimental studies of convection in thin layers (e.g., see Busse, 1978; Busse and Whitehead, 1971; Whitehead, 1976; Whitehead and Parsons, 1978) (see **Chapter 7.03**). Convection patterns displayed with experimental (and computational) techniques are quite varied. Purely basally heated, plane-layer isoviscous convection is a naturally symmetrical system; thus, even when convection is 3-D, the upwelling and downwelling currents retain some basic symmetry; for example, in *bimodal* convection, the upwellings assume the geometry of two adjacent sides of a square, while the downwellings form the other two sides of the square (Figure 7). However, the convection planform can also become highly irregular as with the *spoke* pattern that shows several nearly linear upwellings joined at a common vertex (and likewise with downwellings) (Figure 7); even in this irregular planform, the upwellings and downwellings are symmetrical in that, apart from the sign of their thermal anomalies, their general structure is indistinguishable, that is, they have the same irregular spoke shapes.

Other patterns of convection are also possible but are mostly seen with nonconstant-viscosity fluids. Even in this case, regular polyhedral patterns like squares and hexagons are common (as are irregular forms like the spoke pattern). One of the basic rules of the formation of regular planforms is that they obey a 'tiling pattern'; that is, if the fluid layer is to be filled with identical convection cells, then the cells must all fit together precisely (else a misfit would constitute a cell with an aberrant shape). There are only a few geometries that will allow identical cells to 'tile' together, that is, infinitely long rolls, rectangles, squares, triangles, and hexagons (see Figure 7). Even regular cells with hexagonal or square planforms are characteristic of weakly temperature-dependent viscosity and involve asymmetry between upwellings and downwellings, as we will discuss in the succeeding text (Section 7.07.3.5). Indeed, the symmetry breaking of basally heated, isoviscous convection by various effects, most notably internal heating and variable viscosity, is fundamental to understanding the nature of mantle convection and its relation to plate tectonics.

### 7.07.3.4 Influence of Internal Heating

As discussed earlier, purely basally heated convection in plane layers leads to upwellings and downwellings of equal intensity (equal and opposite thermal anomalies and velocities). However, one of the defining characteristics of convection in the Earth's mantle is that it is powered by the release of primordial heat, left over from planetary accretion, and radiogenic heating from the decay of uranium, thorium, and potassium distributed throughout the mantle. Thus, in addition to being heated along the core–mantle boundary by the hotter molten iron outer core, the mantle retains fossil heat while also being heated throughout its interior. Both primordial heat and radiogenic heating are referred to as internal heating – in contrast to boundary heating – and they effectively break the symmetry between upwellings and downwellings (Figure 8).

The simplest form of convection driven by internal heating is one in which the heat sources are distributed uniformly, the top boundary is kept cold and isothermal, and the bottom boundary is thermally insulated, that is, no heat passes through it; this is called purely internally heated convection. In this case, the bottom boundary cannot develop a thermal boundary layer, as this would carry heat-conducting thermal gradients, which are disallowed by the insulating condition of the boundary. Since there is no hot bottom thermal boundary layer to provide positive buoyancy, then there are no focused active upwellings emanating from the base of the layer. However, the top boundary is cold and thus develops a thermal boundary layer whose temperature gradients are responsible for conducting out all of the internally generated heat. Material in this boundary layer is cold and heavy and is pulled horizontally (again, via pressure gradients) toward a convergent zone where it eventually sinks to form cold downwellings, which cool the interior of the fluid layer. Thus, in purely internally heated convection, there are only concentrated downwelling currents; to compensate for the resulting downward mass flux, upwelling motion occurs, but it tends to be a broad background of diffuse flow, rising passively in response to the downward injection of cold material. Therefore, since the downwellings descend under their own negative buoyancy, they are typically called *active* currents, while the background upwelling is deemed *passive*.

Convection with both internal heating and basal heating (i.e., the bottom boundary is hot and isothermal – instead of insulating – and thus permits the passage of heat) is more complex than with either pure basal heating or pure internal heating. However, the nature of the resulting convection can be understood if one realizes that the bottom thermal boundary layer must conduct in the heat injected through the bottom, while the top thermal boundary layer must conduct out both the heat injected through the bottom and the heat generated internally (Figure 8). To accommodate this extra heat flux, the top thermal boundary layer develops a larger temperature drop

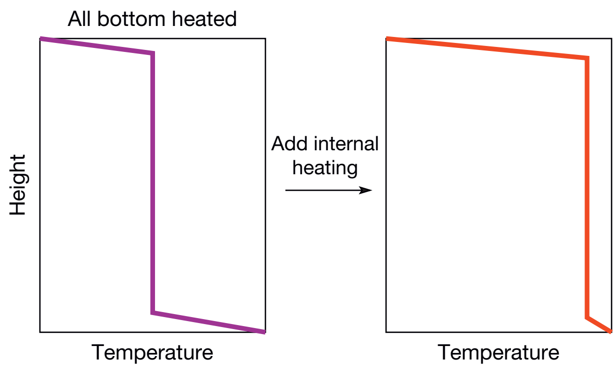


**Figure 8** Sketch of temperature profiles, as in Figure 6, for an isoviscous plane layer, with and without internal heating. With no internal heating, the interior mean temperature is the average of the top and bottom temperatures; the effect of adding internal heating is to increase the interior mean temperature and thus change the relative size and temperature drop across the top and bottom thermal boundary layers.

(to sustain a larger thermal gradient) than does the bottom boundary layer. In this way, the top boundary layer has a larger thermal anomaly than the bottom one, leading to larger, more numerous, and/or more intense cold downwellings than hot upwellings. Invariably, internal heating breaks the symmetry between upwellings and downwellings by leading to a preponderance of downwellings driving convective flow. In the case of Earth, the net surface heat flux is traditionally thought to be as much as 70–80% due to internal heating (with comparable parts radiogenic and primordial heat) and 20% basally heated (Turcotte and Schubert, 2002), although recent estimates of large thermal conductivity of liquid iron in the outer core imply a larger core heat flux and a mantle that is more than 25% basally heated. The mantle is, in any case, predominantly heated internally, with a smaller amount of basal heating. Thus, one can expect a top thermal boundary layer with a large temperature drop across it feeding downwellings that dominate the overall convective circulation; active upwellings from the heated bottom boundary provide only a small amount of the net outward heat flux and circulatory work. Indeed, this picture of convective circulation is borne out by both laboratory and numerical experiments (Figure 9).

Although we have yet to discuss many of the complexities leading to the plate-tectonic style of mantle convection, this simple picture of internally heated convection is in keeping with the idea that the large-scale circulation is driven by downwellings (slabs) fed by an intense thermal boundary layer (the lithosphere and plates), while active upwellings (mantle plumes) are relatively weak and/or few in number (Bercovici et al., 1989a; Bunge et al., 1997; Davies and Richards, 1992).

### 7.07.3.5 Influence of Temperature-Dependent Viscosity

Mantle material is known to have a highly temperature-dependent viscosity for subsolidus, or solid-state, flow.

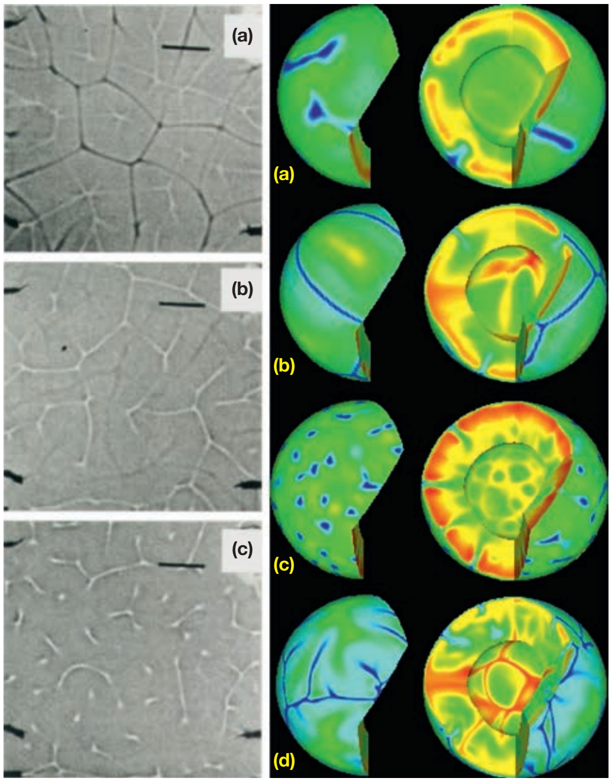


**Figure 9** Internally heated convection in examples of laboratory (left) and numerical (right) experiments. Laboratory experiments employ the shadowgraph technique (see Figure 7 and text for discussion), and apparent internal heating is accomplished by initiating basally heated convection and then steadily decreasing the temperature of the top and bottom surfaces; this causes the average fluid temperature to be greater than the average temperature of the two boundaries. The fluid thus loses its net heat and the rate of this bulk cooling is a proxy for internal heating. The frames show the convective pattern when the layer is all basally heated (a), and thus, upwellings (dark zones) and downwellings (light zones) are comparable; when bulk cooling (internal heating) is stronger than basal heating, the downwellings (light) are dominant (b); when bulk cooling is much stronger than basal heating, the upwellings are not distinct enough to register in the shadowgraph (c) (adapted from Weinstein S and Olson P (1990) Planforms in thermal convection with internal heat sources at large Rayleigh and Prandtl numbers. *Geophysical Research Letters* 17: 239–242). Numerical experiments are for purely internally heated convection in a spherical-shell model of the mantle with free-slip top and bottom surfaces, at moderate and high $Ra$, with and without a viscosity jump at 660 km depth. (a) Isoviscous mantle at $Ra = 1.6 \times 10^5$. (b) Same as (a) but with the viscosity of the upper mantle (above 660 km) reduced by a factor of 30. (c) Same as (a) except the entire mantle viscosity is reduced by 30 (thus, $Ra$ is larger by 30). (d) Same as (b) except the viscosity of both layers is reduced by 10. Note that even while an increase in $Ra$ causes more columnar downwellings (from (a) to (c)), a viscosity jump tends to reinforce or restore the tendency for sheetlike downwellings (d). Adapted from Bunge H, Richards M, and Baumgardner J (1996) Effect of depth-dependent viscosity on the planform of mantle-convection. *Nature* 379: 436–438.

Whether such subsolidus flow occurs by diffusion creep (deformation through the diffusion of atoms away from compressive stresses toward tensile stresses) or dislocation power-law creep (dislocations in the crystal lattice propagate to relieve compression and tension), the mobility of the atoms under applied stresses depends strongly on thermal activation; that is, the atom's thermal kinetic energy determines the probability that it will jump out of a lattice site (Evans and Kohlstedt, 1995; Karato, 2008; Ranalli, 1995; Weertman and Weertman, 1975). The viscosity law for silicates therefore contains a quantum-mechanical probability distribution in the form of the Arrhenius factor $e^{H_a/RT}$ where $H_a$ is the activation enthalpy (basically the height of the energy potential well of the lattice site out of which the mobilized atom must jump), $R$ is the gas constant, $T$ is temperature, and thus $RT$ represents the average kinetic energy of the atoms in the lattices sites. Because of this factor, a few hundred degree change in temperature can cause many orders of magnitude change in viscosity. Moreover, with the inverse dependence on $T$ in the Arrhenius exponent, viscosity is highly sensitive to temperature fluctuations at lower temperatures (i.e., the viscosity vs. temperature curve is steepest at low $T$). Thus, in the coldest region of the mantle, that is, the lithosphere, viscosity undergoes drastic changes: mantle viscosity goes from $10^{21}$ Pa s in the lower part of the upper mantle, to as low as $10^{18}$ Pa s in the asthenosphere (e.g., King, 1995), to an effective value of $10^{25}$ Pa s (e.g., Beaumont, 1976; Watts et al., 1982) or potentially much higher in the lithosphere. Thus, the viscosity may change by at least seven orders of magnitude in the top 200 hundred kilometers of the mantle. In the end, the effect of temperature-dependent viscosity on mantle convection is to make the top colder thermal boundary – that is, the lithosphere – much stronger than the rest of the mantle. This phenomenon helps make thermal convection in the mantle platelike at the surface in some respects, but it can also make convection *less* platelike in other respects.

A strong temperature-dependent viscosity can break the symmetry between upwellings and downwellings in much the same way as internal heating. This occurs because the top cold thermal boundary layer is mechanically much stronger and less mobile than the hotter bottom thermal boundary layer. The less mobile upper boundary induces a heat plug that forces the fluid interior to warm up; this in turn causes the temperature contrast between the fluid interior and the surface to increase and the contrast between the fluid interior and underlying medium (the core in the Earth's case) to decrease. This effect leads to a larger temperature jump across the top boundary layer (which partially reduces the boundary layer's stiffness by increasing its average temperature), and a smaller one across the bottom boundary layer (see **Figure 10**). Thus, the temperature-dependent viscosity can lead to an asymmetry in the thermal anomalies of the top and bottom boundary layers much as we see in the Earth.

The asymmetry of the boundary layers and related warming of the convective layer's interior is also related to the classical concept of 'self-regulation' in terrestrial planets (Tozer, 1972). In particular, if the mantle viscosity is too high for convection to be vigorous enough to remove the internally generated heat, then the mantle will simply heat up until the viscosity is reduced sufficiently to increase convective vigor. This effect plays an important role in the Earth's thermal evolution (Davies, 1980; Schubert et al., 1980), although it might be less profound if the radiogenic internal heating is less than originally thought and closer to that predicted by chondritic abundances (Korenaga, 2008).

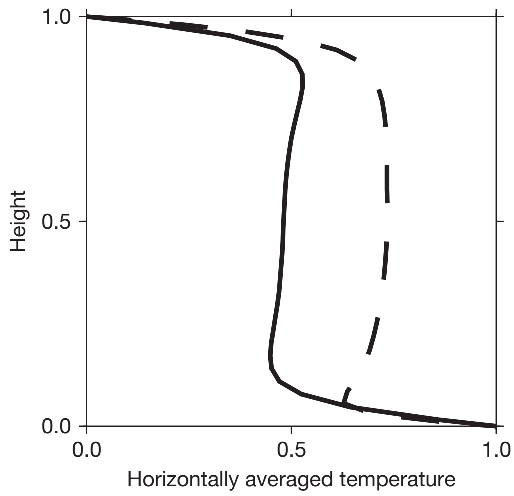


**Figure 10** Temperature profiles, as in **Figure 6**, for a basally heated plane layer of fluid undergoing thermal convection when its viscosity is constant (solid curve) and temperature-dependent (dashed). The fluid with temperature-dependent viscosity develops a stiffer upper thermal boundary layer that acts as a heat plug (i.e., it reduces convection's ability to eliminate heat), causing most of the rest of the fluid to heat up to a larger average temperature. Adapted from Tackley P (1996) Effects of strongly variable viscosity on three-dimensional compressible convection in planetary mantles. *Journal of Geophysical Research* 101: 3311–3332.

Temperature-dependent viscosity can also cause a significant change in the lateral extent of convection cells. Because material in the top thermal boundary must cool a great deal and thus for a long time to become negatively buoyant enough to sink against its cold, stiff surroundings, it must travel horizontally a long distance while waiting to cool sufficiently, assuming it travels at a reasonable convective velocity; this can cause the upper thermal boundary layer and thus its convection cell to have excessively large lateral extents relative to the layer depth (i.e., large *aspect ratios*). This effect has been verified in laboratory and numerical experiments (**Figure 11**) (Giannandrea and Christensen, 1993; Ratcliff et al., 1997; Tackley, 1996a; Weinstein and Christensen, 1991). As will be discussed later (**Section 7.07.4.6**), large aspect ratio convection cells are considered to occur in the Earth, especially if one assumes that the Pacific Plate and its subduction zones reflect the dominant convection cell in the mantle (i.e., a width of ~15 000 km for a maximum depth of ~3000 km). Thus, temperature-dependent viscosity can be used to explain the large aspect ratio of convection cells of mantle convection but with some significant qualifications.

With very strong temperature-dependent viscosity, the top thermal boundary layer can also become completely immobile and the large aspect ratio effect vanishes. The immobile boundary layer happens simply because it is so strong that it cannot move. As a result, the top boundary layer effectively imposes a rigid lid on the rest of the underlying fluid, which then

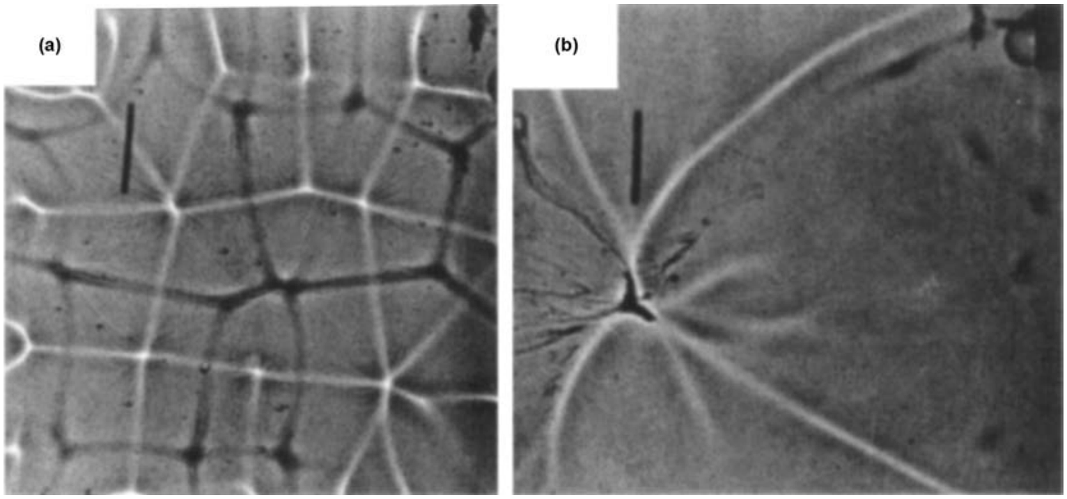


**Figure 11** Lab experiment for convection with temperature-dependent viscosity fluid and mobile top thermal boundary layer. The mobility of the top boundary layer is facilitated by a free-slip upper boundary, accomplished by inserting a layer of low-viscosity silicon oil between the working fluid (corn syrup) and the top cold glass plate. Without the oil, the rigidity of the top glass plate tends to help immobilize the cold and stiff top boundary layer. (a) For comparison, the experiment when the top boundary is rigid, yielding a predominantly spoke-like pattern. (b) The planform when the oil is used to make the free-slip top boundary, causing a dramatic increase in the convection cell size to what is deemed the *spider* planform. Adapted from Weinstein S and Christensen U (1991) Convection planforms in a fluid with a temperature-dependent viscosity beneath a stress-free upper boundary. *Geophysical Research Letters* 18: 2035–2038.

convects much as if it were nearly in isoviscous convection with a no-slip top boundary condition. Convection then has cells that are again about as wide as they are deep (i.e., with nearly unit aspect ratio). Moreover, in this form of convection, the planform can assume various simple geometries such as squares and hexagons (**Figure 7**); however, the upwellings and downwellings are not symmetrical in that the downwellings form the edges of the hexagons (or squares) and the hot, low-viscosity upwellings tend to rise as pipes or plumes through the center of the hexagons (or squares) (see Busse, 1978), similar in many respects to plumes in the Earth's mantle. Regardless of the pattern of convection, the immobilization of the top thermal boundary layer leads to convection that is unlike the Earth: unit aspect ratio cells and an immobile lithosphere.

Overall, three different styles or regimes of convection with temperature-dependent viscosity were first noted by Christensen (1984b) and elucidated and summarized by Solomatov (1995) with a basic scaling analysis (**Figure 12**). These regimes are as follows: (1) For weakly temperature-dependent viscosity, convection tends to appear as if it were nearly isoviscous (unit aspect ratio cells and a mobile top boundary); (2) with moderately temperature-dependent viscosity, convection develops a sluggish cold top boundary layer that is mobile but with large horizontal dimensions, that is, large aspect ratio cells; and (3) with strong temperature-dependent viscosity, the top boundary layer becomes rigid and immobile and convection assumes much of the appearance (apart from detailed patterns) of isoviscous convection beneath a rigid lid. The size of these regimes depends on the Rayleigh number since vigorous convection is more capable of mobilizing a cold top boundary layer than is gentle convection. These regimes have been deemed the nearly isoviscous or low-viscosity contrast regime, the sluggish convection regime, and the stagnant-lid regime. Although the sluggish regime is characterized by large aspect ratio cells suggestive of the Earth's plates, it is most likely that the Earth's Rayleigh number and viscosity variability would put the Earth's mantle in the stagnant-lid regime, that is, if the mantle were a fluid with only temperature-dependent viscosity. Indeed, both Venus and Mars, lacking unequivocal signs of active plate tectonics or continuously mobile lithospheres, appear to operate in the stagnant-lid mode. Indeed, considering the admittedly meager statistics of our own solar system, the stagnant lid might very well be the dominant mode of convection in terrestrial planets (e.g., see O'Rourke and Korenaga, 2012). However, the very presence of mobile plates on Earth shows that its lithosphere–mantle system has important effects that mitigate the demobilization of the top thermal boundary layer caused by temperature-dependent viscosity. In fact, it is not at all clear that the extreme Arrhenius-type temperature dependence of mantle or lithospheric viscosity actually occurs from a practical standpoint; that is, as will be discussed later (see **Sections 7.07.5.4** and **7.07.6.2**), there are multiple competing microscopic deformation mechanisms and the dominant one tends to be the weakest, that is, the one that relieves stress most efficiently.

### 7.07.3.6 A Brief Note on the Influence of Sphericity

Clearly because the Earth is primarily a sphere, models of convection in thick spherical fluid shells would appear to be most realistic (e.g., Bercovici et al., 1989a; Bunge et al., 1997; Choblet et al., 2007; Coltice et al., 2012; Foley and Becker, 2009; Tackley et al., 1993; van Heck and Tackley, 2008; Zhong et al., 2000). However, the effects of sphericity are possibly not so fundamental to the generation of plates. In particular, sphericity tends to break the symmetry between the top and the bottom boundary layers, and upwellings and downwellings in the opposite sense of what we think is relevant for the Earth. For purely basally heated spherical shells, conservation of energy prescribes that for a convective solution to be stable

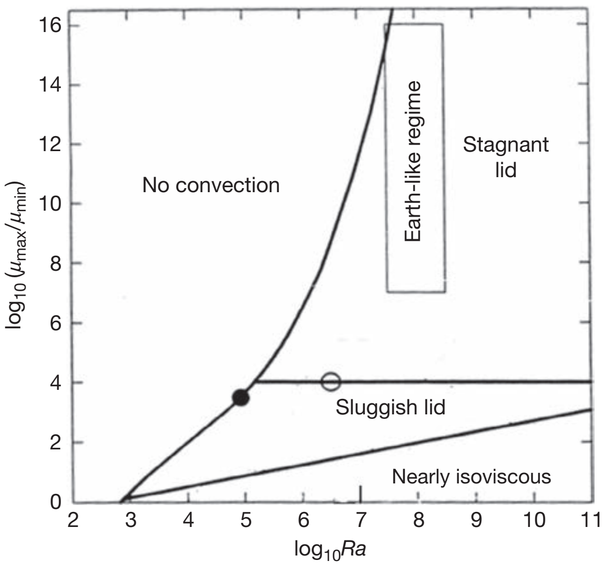


**Figure 12** Diagram showing the different convective regimes in '*Ra* versus viscosity ratio' space for convection in fluid with temperature-dependent viscosity; $\mu_{max}$ and $\mu_{min}$ are the maximum and minimum allowable viscosities of the fluid, respectively. See text for discussion. Adapted from Solomatov V (1995) Scaling of temperature dependent and stress dependent viscosity convection. *Physics of Fluids* 7: 266–274.

(i.e., steady or statistically steady), the total heat input through the bottom boundary must be equal to the heat output through the top. However, because of sphericity, the bottom boundary has approximately four times less surface area than the top boundary through which heat passes; to compensate for this smaller area, the bottom thermal boundary layer generally has a larger temperature drop (and thus larger thermal gradients) across it than does the top boundary layer. This asymmetry leads to upwellings with larger temperature anomalies and velocities than the downwellings, which is opposite to the asymmetry between upwellings and downwellings thought to exist in the Earth. Thus, effects like internal heating and temperature-dependent viscosity are even more important in order to overcome the asymmetry imposed by sphericity and to give a more Earth-like asymmetry.

### 7.07.3.7 Poloidal and Toroidal Flow

Convective motion, with its upwelling and downwelling currents, and the associated divergent and convergent zones at the surface and lower boundary, is also called *poloidal* flow. Basic convection in highly viscous fluids essentially has only poloidal flow. As already discussed in **Section 7.07.2.1.1**, a great deal of the Earth's plate motion is indeed poloidal (i.e., the motion associated with spreading centers and subduction zones), but much of it also involves strike-slip motion and spin of plates, which is, again, *toroidal* motion (Cadek and Ricard, 1992; Dumoulin et al., 1998; Hager and O'Connell, 1978, 1979, 1981; Kaula, 1980; Lithgow-Bertelloni et al., 1993; O'Connell et al., 1991). The existence of toroidal flow in the Earth's plate-tectonic style of mantle convection is a major quandary for geodynamicists and is at the heart of a unified theory of mantle convection and plate tectonics. Therefore, the reason that toroidal motion does not exist in basic convection deserves some explanation.

Most models of mantle convection treat the mantle as nearly incompressible, that is, as if it has constant density. In fact, convection models must allow for thermal buoyancy; thus, they really treat the mantle as a *Boussinesq* fluid; this means that while density is a function of temperature (and thus actually not constant), the density fluctuations are so small that the fluid is still essentially incompressible *except* when the density fluctuations are acted on by gravity (see **Chapters 7.02** and **7.04**). Thus, while the fluid behaves as if incompressible, it can still be driven by buoyancy. Moreover, even without thermal density anomalies, the mantle is still not really incompressible; due to increase in pressure, its density changes by almost a factor of 2 from the top to the bottom of the mantle (e.g., from the IASP91 reference Earth model, Kennet and Engdahl, 1991). However, mantle flow occurs on a much slower timescale than compressional phenomena – in particular acoustic waves – and thus, the mantle is really considered *anelastic* for which the separation of flow into poloidal and toroidal parts still applies (Bercovici et al., 1992; Glatzmaier, 1988; Jarvis and McKenzie, 1980; Tackley, 1996a). However, even the influence of this anelastic component of compressibility is rather small compared to other effects in thermal convection (Bercovici et al., 1992; Bunge et al., 1997; Tackley, 1996a) (see **Chapter 7.02**).

The incompressibility or Boussinesq condition requires that the rate at which mass is injected into a fixed volume must equal the rate at which the mass is ejected, since no mass can be compressed into the volume if it is incompressible; that is, what goes in must equal what goes out. Mathematically, when considering infinitesimal fixed volumes – the continuum mechanical equivalent, of a point in space – this condition is called the continuity equation and is written as

$$\nabla \cdot \mathbf{v} = 0 \qquad [2]$$

where $\mathbf{v}$ is the velocity vector and $\nabla$ is the gradient operator. This equation says that the net divergence of fluid away from or toward a point is zero; that is, if some fluid diverges away from the point, an equal amount must converge into it in order to make up for the loss of fluid. The most general velocity field that automatically satisfies this equation has the form (in Cartesian coordinates)

$$\mathbf{v} = \nabla \times \nabla \times (\phi \hat{\mathbf{z}}) + \nabla \times (\psi \hat{\mathbf{z}}) \qquad [3]$$

(where $\hat{\mathbf{z}}$ is the unit vector in the vertical direction) since $\nabla \cdot \nabla \times$ of any vector is zero. The velocity field in eqn [3] uses only two independent quantities, namely, $\phi$ and $\psi$, to account for three independent velocity components $v_x$, $v_y$, and $v_z$; this is allowed because eqn [2] enforces a dependence of one of the velocity components on the other two, and thus, there are really only two independent quantities. The quantity $\phi$ is called the poloidal potential that represents upwellings, downwellings, and surface divergence and convergence and (as we will show later) is typical of convective motion. The variable $\psi$ is the toroidal potential and involves horizontal rotational or vortex-type motion, such as strike-slip motion and spin about a vertical axis; toroidal flow is not typical of highly viscous convective motion (**Figure 13**).

What drives flow in a highly viscous fluid (where fluid particles are always at terminal velocity, i.e., acceleration is negligible) is the balance between buoyancy (i.e., gravitational) forces, pressure gradients, and viscous resistance; in simple convection with a constant-viscosity fluid, this force balance is expressed as

$$0 = -\nabla P + \mu \nabla^2 \mathbf{v} - \rho g \hat{\mathbf{z}} \qquad [4]$$

where $P$ is pressure, $\mu$ is viscosity, $\rho$ is density, and $g$ is gravitational attraction (on Earth's surface, $g = 9.8\ \mathrm{m\ s^{-2}}$). The viscous resistance term, proportional to $\mu$ in eqn [4], is due to an imbalance or gradients in stress, while stress is due to gradients in velocity – that is, relative motion between particles leading to shearing, stretching, and squeezing – imposed on a fluid with a certain stiffness or viscosity (see **Chapter 7.02** this volume). Taking $\hat{\mathbf{z}}\cdot\nabla\times\nabla\times$ of eqn [4] eventually leads to

$$\mu \nabla^4 \phi = -\rho' g \qquad [5]$$

where $\rho'$ is the density anomaly (e.g., due to horizontal variations in temperature). Equation [5] shows that the *poloidal* motion (left side of the equation) is directly driven by buoyancy forces (right side). However, if we take $\hat{\mathbf{z}}\cdot\nabla\times$ of eqn [4], we only obtain

$$\nabla^2 \psi = 0 \qquad [6]$$

which shows that there are no internal driving forces for toroidal flow. (Note that in deriving both eqns [5] and [6], we have removed a common operator $\nabla_H^2 = (\partial^2/\partial x^2) + (\partial^2/\partial y^2)$, which is the 2-D horizontal Laplacian, assuming the domain is horizontally uniform or periodic.) Thus, for isoviscous convection, toroidal motion does not occur naturally and the only way to generate it is to excite it from the top and/or the bottom boundaries; otherwise, toroidal motion does not exist. These same arguments hold for spherical geometry (e.g., see Busse, 1975; Bercovici et al., 1989b; Chandrasekhar, 1961), as well as for a compressible anelastic fluid (Bercovici et al., 1992; Glatzmaier, 1988; Jarvis and McKenzie, 1980), and even if the gravity $g$ and viscosity $\mu$ are functions of height $z$ (see **Section 7.07.5.7.2**).

Convective flow in a highly viscous medium can only drive toroidal motion by having platelike boundary conditions (Gable et al., 1991; Hager and O'Connell, 1978; Ricard and Vigny, 1989) or if there is a forcing term on the right side of eqn [6] related to the buoyancy or poloidal motion; as will be discussed later (**Section 7.07.5.7.2**), this forcing term only occurs if the viscosity varies laterally, that is, $\mu = \mu(x, y)$ (see **Figure 14** for a qualitative explanation). The problem of how to get buoyancy-driven poloidal motion to induce toroidal flow, either through boundary conditions or through horizontal viscosity variations, is called the *poloidal–toroidal coupling* problem. This will be discussed in more detail in the succeeding text (**Section 7.07.5.7**).

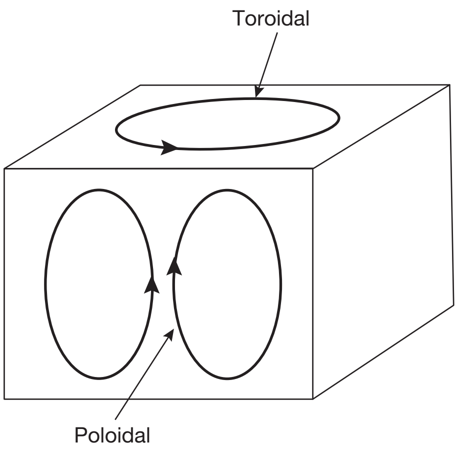


**Figure 13** Cartoon illustrating simple flow lines associated with toroidal and poloidal motion.

## 7.07.4 Where Does Basic Convection Theory Succeed in Explaining Plate Tectonics?

Given some of the essential aspects of simple viscous convection reviewed earlier, we can examine those features of plate tectonics that are characteristic of basic convective flow. Subsequently (**Section 7.07.5**), we discuss those aspects of plate tectonics that are *poorly* explained by basic convection.

### 7.07.4.1 Convective Forces and Plate Driving Forces

#### *7.07.4.1.1 Slab pull and convective downwellings*

If we are to draw any analogy between simple viscous convection and platelike mantle flow, then we must identify subducting slabs with the downwelling of a cold upper thermal boundary layer. As discussed earlier in **Section 7.07.2.1.2**, the

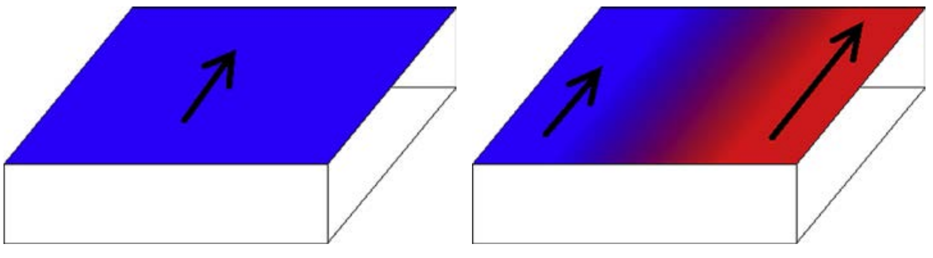

**Figure 14** Cartoon illustrating the need for variable viscosity to obtain toroidal flow. A floating viscous fluid is drawn down a linear drain like a subduction zone. If the layer is uniform in viscosity, then the flow is uniformly into the drain (left). But if the viscosity varies laterally, especially with a gradient perpendicular to the flow direction (right), then the more compliant fluid will be drawn into the drain faster than the stiffer regions. The relative motion between the compliant and the stiff regions establishes a strike-slip shear-type flow with a finite toroidal velocity field.

correlation between the connectivity of a plate to a slab (i.e., the percent of its perimeter taken by subduction zones) and the plate's velocity argues rather conclusively for the dominance of slab pull as a plate driving force (see **Figure 4**). Therefore, if slabs are simply cold downwellings, then the descent velocity of a downwelling in simple convection should be comparable to that of a slab and by inference the velocity of a plate (in particular a fast slab-connected or *active* plate). (As mentioned earlier (**Section 7.07.3.2**), the pull of a slab on a plate is in fact a horizontal pressure gradient acting in the cold upper thermal boundary layer and caused by the low pressure associated with a slab pulling away from the surface; invariably, the pressure gradient is established so that the boundary layer or plate feeds the slab steadily and thus leads to the appearance that the slab is pulling the plate.) We can estimate the force and velocity of such a cold downwelling with simple scaling analysis and compare the calculated velocity with tectonic plate velocities.

Generalizing the scaling analysis and boundary layer theory of Davies and Richards (1992), we consider a cold top thermal boundary layer that is $L$ long (from its creation at a divergent zone to its destruction at a convergent zone) and $W$ wide (**Figure 15**). As it moves from the divergent to the convergent zone, the boundary layer thickens by vertical heat loss, which, in the horizontally moving boundary layer, is only due to thermal diffusion.

To estimate the boundary layer thickness $\delta(t)$, we apply dimensional homogeneity (e.g., see Bridgman, 1922; Furbish, 1997) (see **Chapter 7.04**). Assuming that only thermal diffusivity $\kappa$ (with units of $\mathrm{m^2\,s^{-1}}$) and age $t$ (where $t=0$ at the divergent zone where the boundary layer is initiated) control the growth of the boundary layer, then we write $\delta(t)=A\kappa^a t^b$ where $A$ is a dimensionless constant ($A$ is dimensionless since we assume no other dimensional properties of the system have any influence on the cooling process). The constants $a$ and $b$ are then determined to match the dimensions of either side of the equation for $\delta$, leading to $a=b=1/2$. Indeed, a more careful analysis (see Turcotte and Schubert, 2002) shows that $\delta\approx\sqrt{\kappa t}$, within a factor of order unity.

When the boundary layer reaches the downwelling, its thickness is $\delta=\sqrt{\kappa L/v}$, where $v$ is the as yet undetermined velocity of the boundary layer. After downwelling, the descending vertical current extends to depth $D$. Moreover, because the boundary layer involves a temperature contrast of $\Delta T$ (from the deeper fluid interior to the surface), then the layer and the vertical current it feeds have an average thermal anomaly of $\Delta T/2$. The buoyancy force of the downwelling current is therefore

$$F_B=[\rho\alpha\Delta T/2][\delta WD]g \qquad [7]$$

where the first factor in the square brackets represents the density anomaly of the downwelling and the second factor in brackets is the volume of the downwelling. The drag force on the downwelling current is the viscous stress acting on the current (which, in this example, is approximately the viscosity times the strain rate of the fluid as it is sheared vertically between the downwelling and a stagnation point roughly halfway back to the divergent zone) times the area of the current on which the stress acts, that is,

$$F_D=\left[\mu\frac{v}{L/2}\right][DW]=2\mu vDW/L \qquad [8]$$

The force balance $F_B-F_D=0$ yields the downwelling velocity

$$v=\frac{\rho\alpha\Delta T\delta Lg}{4\mu} \qquad [9]$$

Substituting $\delta=\sqrt{\kappa L/v}$ and isolating $v$, we obtain

$$v=\left[\left(\frac{\rho\alpha\Delta Tg}{4\mu}\right)^2 L^3\kappa\right]^{1/3} \qquad [10]$$

As we have seen for most forms of basic convection, $L\approx D$ (i.e., convection cells are roughly unit aspect ratio), in which case [10] is equivalent to the classic scaling law $v\sim(\kappa/D)Ra^{2/3}$. Thus, using $D=3\times10^6$ m, $\kappa=10^{-6}\ \mathrm{m^2\,s^{-1}}$, $\rho=4000\ \mathrm{kg\,m^{-3}}$, $\alpha=3\times10^{-5}\ \mathrm{K^{-1}}$, $\Delta T=1400$ K, $g=10\ \mathrm{m\,s^{-2}}$, and $\mu=10^{22}$ Pa s (this viscosity represents the effective whole mantle viscosity that is dominated by the lower mantle), we obtain a velocity of $v\approx10\ \mathrm{cm\,year^{-1}}$. (We can adjust less well-constrained parameters, e.g., use, within reason, a lower or higher viscosity or a value of $L>D$; regardless the velocity remains of the order of 10 cm year.) This velocity is indeed the correct order of magnitude for velocities of active (i.e., slab-connected) plates,

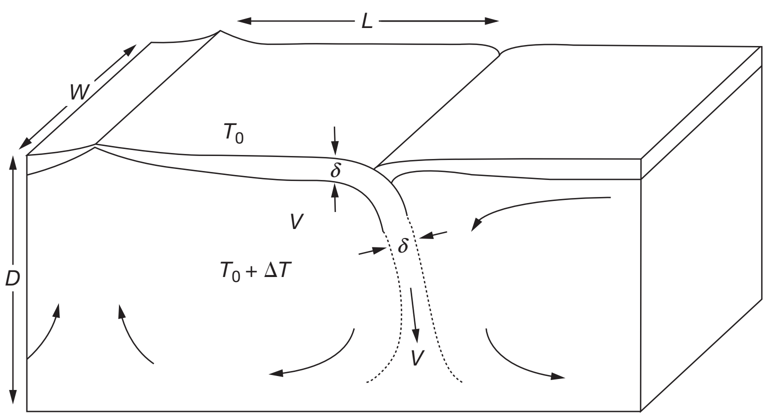


**Figure 15** Cartoon illustrating the slab-pull force problem discussed in **Section 7.07.4.1.1**. For definition of labeled variables, refer to text (see **Section 7.07.4.1.1**). Adapted from Davies G and Richards M (1992) Mantle convection. *Journal of Geology* 100: 151–206.

strongly suggesting that the plate force deemed ‘slab pull’ is well modeled by a simple cold downwelling current in basic convection. Moreover, simple heat-flux arguments lead to an identical result (see Section 7.07.4.4), showing that slabs not only drive plate motions and mantle flow but also are the primary means for cooling off the mantle.

#### 7.07.4.1.2 Ridge push is a convective lateral pressure gradient

The ridge-push plate force was initially conceived of as an edge force (i.e., acting on the edge of a plate at a mid-ocean ridge) due to the weight of a topographically high ridge (e.g., Forsyth and Uyeda, 1975). It has since been recognized as a force that is distributed across the area of the plate (Hager and O’Connell, 1981). Since plate area has little correlation with plate velocity (Forsyth and Uyeda, 1975), ridge push is typically assumed secondary to slab pull, or it is almost exactly canceled by mantle drag along the base of plates (Hager and O’Connell, 1981). Indeed, Lithgow-Bertelloni and Richards (1998) estimated that ridge push constitutes only 5–10% of the driving force due to subducted slabs. Nevertheless, after slab pull, ridge push is one of the more significant forces (and possibly the only driving force for plates lacking slabs, like the African and Antarctic Plates); thus, it deserves some discussion from the perspective of basic convection.

Ridges are topographically high because they are younger and composed of hotter more buoyant material than the surrounding material, which has cooled and grown heavier since moving away from the ridge. The subsidence of material away from a ridge is slow enough that the entire ridge–lithosphere system is essentially in isostatic balance, at least far from subduction zones. If topography is isostatic, then there is a *compensation depth* beneath the lithosphere at which every overlying, infinitely high, column of material with equal cross-sectional area weighs the same; this also means that hydrostatic pressure (i.e., weight per area) is the same at every horizontal position along and below the compensation level. However, columns that do not extend to the compensation depth do not weigh the same; in particular, the column centered on the ridge axis weighs the most since off-axis columns still include too much light material (like water) and not enough heavy material (like lithosphere) to equal the weight of the column of hot asthenosphere beneath the ridge. Thus, for depths less than the isostatic compensation depth, pressure is not horizontally uniform and is in fact highest beneath the ridge axis, thereby causing a pressure gradient pushing outward from the ridge (see Turcotte and Schubert, 2002); however, this pressure gradient exists everywhere within the lithosphere (i.e., wherever seafloor depth changes laterally) and not as a line force at the ridge axis.

How does this ridge-force pressure gradient relate to convective forces? As discussed previously (Section 7.07.3.2), the horizontal pressure gradient in a convective thermal boundary layer is what drives the lateral motion of the boundary layer. If the upper surface were deformable, the pressure highs at divergent zones would push up the surface, and the pressure lows at convergent zones would pull down on the surface. Thus, the pressure gradient in the thermal boundary layer would be manifested as surface subsidence from a divergent to convergent zone. In fact, as discussed in the next section, the resulting surface subsidence of a simple convective boundary layer is nearly identical to that observed for oceanic lithosphere. Thus, the ridge-push pressure gradient is essentially indistinguishable from the pressure gradient in a convective thermal boundary layer.

### 7.07.4.2 Structure of Ocean Basins

Large-scale variations in bathymetry, or seafloor topography, can be related to simple convective processes, in particular the cooling of the top thermal boundary layer. Although we have already discussed the cooling-boundary-layer concept in the previous section, we will reiterate the arguments in slightly more detail in order to examine the validity of the underlying assumptions.

As mentioned earlier (Section 7.07.3.2.2), when the top thermal boundary layer of a convection cell moves horizontally, it cools by heat loss to the colder surface. In simple convection, the surface is assumed impermeable, that is, no mass crosses it and thus, heat loss out of the top thermal boundary layer is assumed entirely due to thermal diffusion; that is, since the boundary layer abuts the impermeable surface, vertical heat loss due to ejection of hot mass or ingestion of cold mass across the surface is assumed negligible. While this assumption is reasonable for most of the extent of the thermal boundary layer, it causes convective theory to mispredict some details of ocean-basin topography and heat flow (see Section 7.07.5.2).

As discussed earlier in Section 7.07.3.2.2, the assumption of diffusive heat loss means that thickening of the boundary layer is controlled by thermal diffusivity $\kappa$, with units of $m^2\,s^{-1}$; thus, again by dimensional homogeneity (see Section 7.07.4.1.1), the boundary layer thickness $\delta \sim \sqrt{\kappa t}$. As the thermal boundary layer thickens, it weighs more and thereby pulls down on the surface with increasing force; if the surface is deformable, it will be deflected downward (until isostasy is established). The surface subsidence thus mirrors the increasing weight of the boundary layer; the weight increases only because $\delta$ grows, and thus, surface subsidence goes as $\sqrt{t}$. Therefore, seafloor subsidence is predicted by convective theory (more precisely convective boundary layer theory, Turcotte and Oxburgh, 1967) to increase as the square root of lithospheric age; this is called the $\sqrt{\text{age}}$ law. Moreover, this type of boundary layer theory predicts that the heat flow (units of $W\,m^{-2}$) out of the ocean floor should obey a $1/\sqrt{\text{age}}$ law, which can be inferred by the fact that the heat flow across the boundary layer is mostly conductive and thus goes as $k\Delta T/\delta$ (where $k$ is thermal conductivity and $\Delta T$ is the temperature drop across the thickening thermal boundary layer, as also defined in Section 7.07.4.1.1). Profiles, perpendicular to the spreading center, of seafloor bathymetry and heat flow versus age (Figure 16) show that, to first order, seafloor subsidence and heat flow do indeed follow boundary layer theory, that is, obey $\sqrt{\text{age}}$ and $1/\sqrt{\text{age}}$ laws, respectively (Parsons and Sclater, 1977; Sclater et al., 1980; Stein and Stein, 1992; Turcotte and Schubert, 2002), further emphasizing that the oceanic lithosphere is primarily a convective thermal boundary layer.

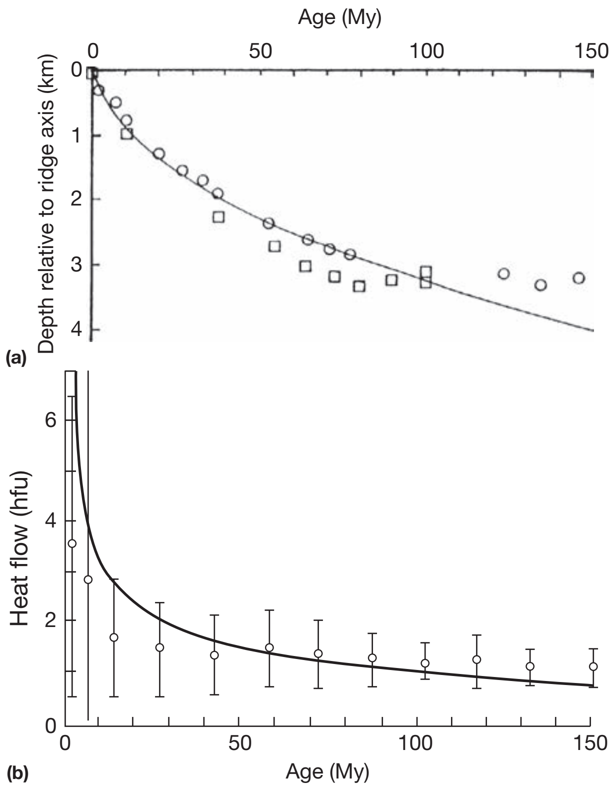


**Figure 16** Bathymetry – that is, seafloor topography – (a) and heat flow (b) versus age for typical ocean floor. Bathymetry is for the North Pacific (circles) and North Atlantic (squares) oceans; heat flow (in hfu = 41.84 mW $m^{-2}$) shows average global values (circles) and associated error bars. Both (a) and (b) show the predictions from convective boundary layer theory (solid curves), that is, a $\sqrt{\text{age}}$ law for bathymetry and a $1/\sqrt{\text{age}}$ law for heat flow. The theoretical curves fit the observations reasonably well, except near and far from the ridge axis (cf. Parsons and Sclater (1977); Sclater et al. (1980); Stein and Stein, 1992). Adapted from Turcotte D and Schubert G (2002) *Geodynamics*. Cambridge: Cambridge University Press.

However, at a greater level of detail, the $\sqrt{\text{age}}$ laws fail; this will be discussed later (**Section 7.07.5.2**).

### 7.07.4.3 Slablike Downwellings Are Characteristic of 3-D Convection

In simple, purely basally heated plane-layer convection, the convective pattern is often characterized by interconnected sheets of downwellings. For example, the hexagonal pattern is characterized by one upwelling at the center of each hexagon, surrounded by a hexagonal arrangement of downwelling walls (**Figure 7**). A similar situation occurs for spherical systems (Bercovici et al., 1989b; Busse, 1975; Busse and Riahi, 1982, 1988; Zhong et al., 2000). When internal heating of the fluid is included, the upwellings and downwellings can be so imbalanced as to destroy any trace of symmetry. Even so, the downwellings can persist as linear, albeit no longer interconnected, sheetlike downwellings at low to moderate Rayleigh numbers (Bercovici et al., 1989a; Weinstein and Olson, 1990), and give way to downwelling cylinders and blobs at high Rayleigh numbers (Bunge et al., 1996; Glatzmaier et al., 1990; Sotin and Labrosse, 1999); however, even at high Ra, the linearity of the downwellings is recovered by allowing viscosity to increase with depth, as is thought to occur in the Earth (Bunge et al., 1996) (see **Figure 9**). Thus, although sheetlike downwellings do not always occur in simple models of thermal convection, they are a very common feature. In that sense, the occurrence of slablike downwellings in mantle convection is characteristic of basic thermal convection. However, as we will discuss later, there are many other characteristics of subducting slabs that are unlike simple convective flow (see **Chapter 7.09**).

#### *7.07.4.3.1 Cylindrical upwellings and mantle plumes are also characteristic of 3-D convection*

Although mantle plumes and hot spots are not, strictly speaking, part of plate tectonics, they play an important role in our ability to measure absolute plate motions (e.g., because relative positions between hot spots appear to be fixed (Morgan, 1972) or change more slowly than plate motions (Molnar and Stock, 1987)) and in understanding the nature of mantle convection and the relative sizes of its thermal boundary layers.

As with sheetlike downwellings, cylindrical or plumelike upwellings are prevalent in simple thermal convection. (It is possible to get different shapes – for example, sheetlike – of upwellings, but they tend to break down into more columnar features before reaching the surface.) However, such upwellings always require a significant bottom thermal boundary layer heated from below by a relatively hot reservoir, such as the Earth's outer core; this boundary layer provides a source region for plumes, and its thickness therefore determines their size (Bercovici and Kelly, 1997; Christensen, 1984c). In basic convection with significant internal heating, the bottom thermal boundary layer typically has a much smaller temperature drop than does the top thermal boundary layer. In this case, upwellings still retain some plumelike quality though they are fewer in number and/or weak, relative to downwellings or slabs. However, the strength of plumes may depend on the large-scale style of convection; in particular, mobile-lid or platelike convection allows for a cooler mantle than in stagnant-lid convection, thus a bigger bottom thermal boundary layer, hence more robust plumes (Jellinek and Manga, 2004).

Overall, the existence of cylindrical upwelling plumes in the mantle – indirectly inferred from hot spot volcanism and geochemical analyses (Allégre, 1982; Duncan and Richards, 1991; Hofmann, 1997; Zindler and Hart, 1986) and perhaps most directly in seismic analysis (Montelli et al., 2004; Nataf and VanDecar, 1993; Shen et al., 1998; Wolfe et al., 1997, 2009) – is consistent with basic models of thermal convection. However, even the weak plumes appearing in 3-D models of internally heated convection are an integral part of the convective flow; that is, while they may not have much influence on the dynamics of the top cold boundary layer, they typically position themselves in accordance with the whole convective pattern, typically as far from downwellings as possible (Weinstein and Olson, 1989). Plumes well integrated into the global convective circulation are very unlikely to establish themselves where they must pass through adverse conditions (e.g., beneath a downwelling or across a strong 'mantle wind'), and even if they do, they can only exist as evanescent features

(Labrosse, 2002; Steinberger and O'Connell, 1998) (see Chapter 7.10).

### 7.07.4.4 Slab Heat Flux and Plate Velocities

The Earth's mantle is thought to be about 70–80% heated internally by primordial heat and radiogenic sources, and the rest from other sources, primarily from cooling of the core (see Chapter 7.11). As plumes are thought to carry the heat from the core (see next section), heat flow through the oceanic lithosphere, or equivalently cooling by slabs, accounts for most of the Earth's heat flow. Indeed, one can use these heat flow arguments to predict slab and plate velocities and check for self-consistency with the boundary layer force balance arguments of Section 7.07.4.1.1, which thus verifies that slabs are an integral part of convective heat transport (Bercovici, 2003).

At a few 100 km depth beneath the lithosphere, mantle heat loss is primarily due to the downward injection of cold material by subducting slabs (analogous to dropping ice cubes in hot water). The energy-flux balance would thus require that $fQ = wA\rho c_p \Delta T$ where $Q \approx 30$–$38$ TW is the net heat output through the top of the mantle (Schubert et al., 2001) $f = 0.8$–$0.9$ is the fraction of $Q$ accounted for by slab cooling (since the remaining heat transport by mantle plumes probably accounts for of order 10–20% of the net heat flux; Davies, 1988a; Jaupart et al., 2007; Lay et al., 2008; Pollack et al., 1993; Sleep, 1990), $\rho \approx 3000$ kg m$^{-3}$ is slab density, $c_p = 1000$ J kg K$^{-1}$ is heat capacity, $\Delta T \approx 700$ K is the average slab thermal anomaly as in Section 7.07.4.1.1, and $w$ is a typical vertical velocity of a slab. Lastly, $A \approx 2\pi R\delta$ is the total horizontal cross-sectional area of all slabs crossing this particular depth where $\delta \approx 100$ km is a typical slab thickness, and the horizontal length of all slabs is estimated by the circumference of the Earth since most slabs occur in a nearly large circle around the Pacific basin and thus $R \approx 6000$ km. Using these numbers, we can solve for slab velocity $w = fQ/(\rho c_p \Delta T \delta 2\pi R) \approx 10$ cm year$^{-1}$, which is precisely the typical velocity for fast, active plates and predicted by slab-pull arguments (Section 7.07.4.1.1). In the end, that 'active' plates cool, thicken, subside, and eventually sink as subducting slabs at plate velocities, while also cooling the mantle is tantamount to saying slabs and plates are convective currents.

### 7.07.4.5 Mantle Heterogeneity and the History of Subduction

Up to this point, one can construct a simple view of the connection between plate tectonics and mantle convection in which subduction zones are associated with convective downwellings and plumes with upwellings; whether ridges are also associated with active convective upwellings is less certain, if not doubtful (see Section 7.07.5.6). If heating is largely internal, then downwelling of the upper boundary layer, or lithosphere, at subduction zones would then be expected to dominate the structure of mantle temperature and density heterogeneity. Indeed, this seems to be the case, but the picture is complicated by the fact that plate motions, and hence subduction zones, are ephemeral on timescales of tens to hundreds of million years. Thus, one does not expect a perfect correspondence between present-day subduction zones and mantle downwellings, and it is necessary to invoke plate motion history in addressing this issue.

Averaged over the past 120–150 My, the locations of subduction zones (in a hot spot reference frame) correspond remarkably well to the location of high-seismic-velocity anomalies (cold material) in the mantle, at least at very long wavelengths (Richards and Engebretson, 1992) (Figure 17), a view supported in some detail by high-resolution tomographic studies of mantle structure (Fukao et al., 1992; Grand et al., 1997; van der Hilst et al., 1997; see also Volume 1). In fact, both the geoid (the Earth's gravitational equipotential surface; see Ricard et al., 1993) and global plate motions (Lithgow-Bertelloni and Richards, 1998) are well predicted using a mantle density model derived from slabs subducted during Cenozoic and Mesozoic times. However, there appears to be little evidence in these analyses of deeply seated upwellings beneath mid-ocean ridges that would provide plate driving forces of similar magnitude, although the African swell is a possible exception to this inference (Lithgow-Bertelloni and Silver, 1998). On the whole, one can infer a strong relationship between the mass of slabs injected at plate velocities since the Mesozoic with current observations of tomographic density

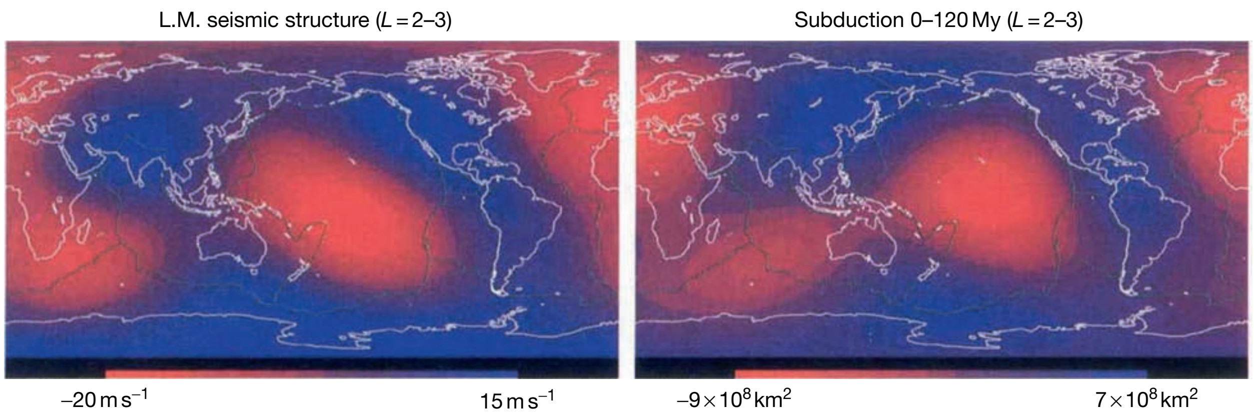


**Figure 17** Comparison of long-wavelength lower-mantle tomography (left) with time-integrated volume flux of slabs over the last 120 My (right). Reproduced from Richards MA and Engebretson DC (1992) Large-scale mantle convection and the history of subduction. *Nature* 355(6359): 437–440.

heterogeneity, and geoid anomalies, which confirms the linkage between mantle convection and plate tectonics. However, this inference bears little on the question of how the plates themselves are generated in the system.

#### 7.07.4.6 Temperature-Dependent Viscosity, Internal Resistive Boundaries, and the Aspect Ratio of Convection Cells

The Pacific Plate, with most of the kinetic energy and subduction zones of the plate-tectonic system, can in many ways be considered the top of the Earth's dominant convection cell. As such, it is a very large convection cell with an excessively large aspect ratio (much longer than it is possibly deep). (The size of several other massive plates could also be used to argue for large aspect ratio cells; however, except for the Indo-Australian plate – which in itself may be composed of several other plates (Gordon et al., 1998) – no other superlarge plate is considered *active*, i.e., slab-connected and 'fast,' and therefore does not really qualify as a possible convection cell.) Large aspect ratio or long-wavelength convection cells in the mantle are also inferred from seismic tomography (Su and Dziewonski, 1992) (see also **Figure 17**). Because of the dominance of such long-wavelength features, tomography and by inference convection are deemed to have a *reddened* spectrum.

Therefore, in many ways, mantle convection in the Earth is thought to be characterized by very large aspect ratio convection cells. As discussed previously (**Section 7.07.3.5**), convection with temperature-dependent viscosity can allow for large aspect ratio cells (e.g., Weinstein and Christensen, 1991), in particular in the *sluggish* convection regime (with moderately temperature-dependent viscosity and a sluggish but mobile upper thermal boundary layer; see Solomatov, 1995). This effect can theoretically allow for a Pacific-sized convection cell; however, if the Earth's mantle were only a temperature-dependent-viscosity fluid, estimates of its convective regime would place it in the *stagnant-lid* regime where the top thermal boundary layer is essentially frozen (Solomatov, 1995) and thus would be more characterized by unit aspect ratio convection cells.

However, other basic phenomena may also cause long-wavelength convection cells; these effects primarily involve an internal resistive boundary that, while not a feature of the fundamental fluid dynamics of convection, can be readily added to simple convection models to improve their correspondence with the Earth.

As is well known, the mantle is nominally divided into the upper mantle and the lower mantle at the 660 km seismic discontinuity (see review by Silver et al., 1988). This discontinuity is most likely a phase change from spinel to perovskite plus magnesiowiistite (Ito et al., 1990; Liu, 1979) and also involves a viscosity jump with depth by most likely a factor of 30–100 (e.g., Corrieu et al., 1994; Hager, 1984; King, 1995; Ricard et al., 1984, 1993; Richards and Hager, 1984). Although the nature of convective mass transfer across this 660 km boundary has been the subject of extensive debate, seismic tomography has given compelling evidence for transfer of both slabs (Creager and Jordan, 1984; Fukao et al., 1992; Grand, 1994; Grand et al., 1997; van der Hilst et al., 1991, 1997) and plumes (Shen et al., 1998; Wolfe et al., 2009) across the phase change. However, because of both the phase change and the viscosity jump, this boundary can still provide resistance to downwellings as they attempt to penetrate into the lower mantle. The phase change resists mass transfer because it is inferred to have a negative Clapeyron slope, which means that in relatively cold material, the phase transition will occur at a higher pressure than in hotter material. Thus, a cold downwelling moves the phase transition to greater pressures, causing a downward deflection of the phase boundary that acts to buoy the slab and resist its downward motion (Christensen and Yuen, 1985; Honda et al., 1993; Machetel and Weber, 1991; Schubert et al., 1975; Tackley et al., 1993, 1994; Weinstein, 1993). A viscosity jump retards the motion of downwellings because of the greater resistance of the material beneath the boundary. However, the viscosity jump need not be uniquely associated with the 660 km boundary; a low-viscosity asthenosphere or a smooth increase of viscosity with depth can induce similar effects (Ahmed and Lenardic, 2010; Lenardic et al., 2006). In any case, convection tends to develop large-volume downwellings – and thus large-wavelength convection cells – in order to gather enough negative buoyancy to penetrate more resistive lower layers. This 'reddening' of the convective spectrum (thus creating large aspect ratio, nearly Pacific size cells) has been well documented in 3-D models of spherical convection at reasonably high Rayleigh number for both the phase change (Tackley et al., 1993, 1994) and the viscosity-jump effects (Bunge et al., 1996; Tackley, 1996b).

In the end, a convecting mantle with either a moderately temperature-dependent viscosity or an internal resistive boundary can generate Earth-like, large-wavelength (or long aspect ratio) plate-sized convection cells. However, while these effects move us closer to obtaining platelike scales in convection models, none actually generate plates.

## 7.07.5 Where Does Basic Convection Theory Fail in Explaining Plate Tectonics?

Although models of basic thermal convection in the Earth's mantle can account for numerous features of plate tectonics, there remain many unresolved issues. Next, we survey some of the major apparent paradoxes and inconsistencies between convection and plate tectonics, as well as the progress in trying to solve them.

### 7.07.5.1 Plate Forces Not Well Explained by Basic Convection

While slab pull and to a large extent ridge push (really, distributed ridge push) are manifestations of simple convection, other forces are not. Most of the forces unaccounted for by convection are related to some feature of plate tectonics that convection does not (or does not easily) generate. One such force is transform resistance, as this involves strike-slip motion that cannot be readily generated, if generated at all, in simple convection. The lack of excitation of strike-slip motion is a major shortcoming of basic convection theory; however, we will defer discussion of this until later (see **Section 7.07.5.7**). The precise distribution of the *ridge push* force also cannot be predicted in simple convection models since they do not generate narrow passive divergent zones, that is, thin ridges fed by shallow nonbuoyant upwellings. The lack of formation of passive but focused upwellings is also a significant shortcoming of basic convection theory and will be discussed later as well (see **Section 7.07.5.6**). Finally, collision resistance does not explicitly occur in basic thermal convection models, which do not include chemical segregation and continental formation. This phenomenon can, in effect, be treated by thermochemical models that allow melting and surface emplacement of chemically buoyant continental material, which resists being drawn into downwellings (Lee et al., 2005; Lenardic and Kaula, 1996).

### 7.07.5.2 Structure of Ocean Basins (Deviations from the $\sqrt{age}$ Law)

As discussed earlier (**Section 7.07.4.2**), the classic bathymetry and heat flow profiles (**Figure 16**) show a predominant $\sqrt{age}$ dependence. However, bathymetry and especially heat flow deviate significantly from the $\sqrt{age}$ curve near the ridge axis itself and far from the ridge axis. In particular, the $\sqrt{age}$ prediction assumes that only diffusive transport of heat occurs in the upper thermal boundary layer, which likely becomes invalid both at and far from the ridge axis. At the ridge itself, heat transport by magma migration (e.g., see Katz, 2008) and hydrothermal circulation (Lister, 1972; Stein and Stein, 1992) are highly significant and likely account for suppression of axial bathymetry and heat flow profiles. Incorporation of realistic or more complete transport phenomena relevant to ridges (e.g., magmatism and/or water ingestion) into convection models is also related to the problem of how to generate focused but passive ridges (see **Section 7.07.5.6**).

The flattening of bathymetry, relative to the $\sqrt{age}$ law, far from the ridge axis has had various explanations. It has been proposed that flattening is the result of extra heating of the lithosphere (causing effective rejuvenation) brought on by (a) secondary small-scale convection and/or internal heating (Huang and Zhong, 2005; Parsons and McKenzie, 1978), (b) viscous heating (Schubert et al., 1976), and (c) mantle plumes (Davies, 1988b); nonthermal effects, such as due to high pressure associated with constricted asthenospheric flow, have also been proposed (Morgan and Smith, 1992). However, since 3-D convection itself differs significantly from the 2-D boundary layer theory from which the $\sqrt{age}$ law is derived (Turcotte and Oxburgh, 1967), such flattening and other deviations in the far-axis bathymetry are perhaps not altogether surprising from a mantle convection perspective.

### 7.07.5.3 Changes in Plate Motion

Plate motions evolve with various timescales. Some are clearly related to mantle convection, such as those associated with the Wilson cycle (Wilson, 1966), that is, the periodic formation and breakup of Pangaea, approximately every 500 My. Various hypotheses have been proposed to explain the dispersal of supercontinents. The conventional view is that supercontinents provide an insulating blanket, and thus, with radiogenic heating, they warm the underlying mantle, eventually inducing a hot upwelling that weakens and breaks up the overlying lithosphere (Coltice et al., 2007, 2009; Gurnis, 1988; Lowman and Jarvis, 1996). However, this mechanism requires more radiogenic heating than may actually exist (Korenaga, 2008). In the same vein, the present-day continents do not suggest that they stand above hotter than normal mantle; indeed, their basal heat flux appears very low (e.g., Guillou et al., 1994). However, this recent observation might not be generally relevant; in particular, Rolf et al. (2012) showed that while small subcontinental temperature anomalies occur as continents are drifting, they can become significantly larger when continents assemble into a supercontinent. Regardless, whether supercontinent insulation induces sufficient heating to induce dispersal remains a matter of debate (see Bercovici and Long, 2014; Heron and Lowman, 2011; Lenardic et al., 2005, 2011).

Plate motion changes that have occurred on shorter timescales are even more difficult to understand. The plate-tectonic history recorded in paleomagnetic data and hot spot tracks consists of long stages of quasisteady motions separated by abrupt reorganizations.

Stages of quasisteady motion are reasonably well explained in terms of plate forces (slab pull, ridge push, mantle drag, etc; Forsyth and Uyeda, 1975) or equivalently convective buoyancy from large-scale heterogeneities (e.g., Lithgow-Bertelloni and Richards, 1995; Ricard et al., 1989). Gradual reversals can also be explained by convective motion; for example, the notion of thermal blanketing can be extended to allow for plate reversals

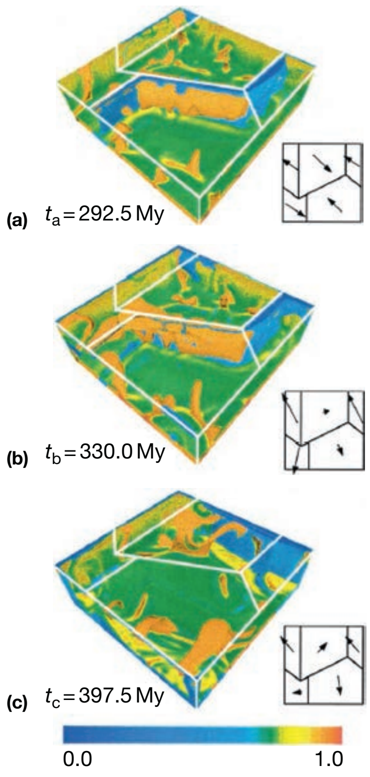


**Figure 18** The convection model of King et al. (2002) shows that reversals in plate motion can occur when converging flow over a cold downwelling (a) draws in hot subcontinental mantle (b) that annihilates the downwelling, subsequently changing the polarity of the convergent margin to a divergent one (c). Adapted from King SD, Lowman JP, and Gable CW (2002) Episodic tectonic plate reorganizations driven by mantle convection. *Earth and Planetary Science Letters* 203(1): 83–91.

in that hot subcontinental mantle anomalies can effectively annihilate slabs and thus cause radical changes in plate motion (King et al., 2002; Lowman et al., 2003) (see **Figure 18**).

Abrupt changes in plate motion, however, are not easily related to convective processes. The most dramatic plate motion change is recorded in the Hawaiian–Emperor bend, dated at 47 Ma (Sharp and Clague, 2006; Wessel and Kroenke, 2008); this bend suggests a velocity change of a major plate of ~45° during a period no longer than 5 My, as inferred from the sharpness of the bend. Convective plate driving forces, such as due to sinking slabs, cannot change directions much faster than the time to lose or erase a thermal anomaly, which is of order several tens of millions of years, based on descent at a typical convective velocity (see **Section 7.07.4.1.1**). Therefore, changing convective motions in less than ~5 My is physically implausible. Abrupt changes may be due to nonconvective sources such as rapid rheological response and fast adjustments in plate boundary geometries, such as due to fracture and rift propagation (e.g., Hey and Wilson, 1982; Hey et al., 1995). Plate reorganizations due to (a) the annihilation of a subduction boundary by rapid slab detachment and/or continental collision (e.g., Bercovici et al., 2015), (b) loss of a ridge and/or trench by subduction of a ridge (e.g., Thorkelson, 1996), or (c) the initiation of a new subduction zone (e.g., Hilde et al., 1977) possibly occur on relatively rapid timescales, although the timing of such mechanisms is not well constrained (Richards and Lithgow-Bertelloni, 1996). Offsets in plate age and thickness along already weak oceanic transform boundaries may provide excellent sites for the initiation of subduction (e.g., Hall et al., 2003; Stern, 2004; Stern and Bloomer, 1992; Toth and Gurnis, 1998) yielding a possible mechanism for plate motion changes; this, coupled with the notion of transform faults as long-lived weak 'motion guides' (see **Section 7.07.6.1.2**), emphasizes the importance of transform boundaries in the plate–mantle system. The possible mechanism for abrupt plate motion changes underscores the need to understand the interactions between the long timescale convective processes and the short timescale effects associated with the lithosphere's rheological response, for example, by fracture, fault sliding, and strain localization (see **Section 7.07.6**).

### 7.07.5.4 Platelike Strength Distributions: Weak Boundaries and Strong Interiors

One of the platelike characteristics of the Earth's top thermal boundary layer is its strength or viscosity distribution. Most of the boundary layer is strong or of high viscosity; on Earth, these strong regions are separated by narrow zones of intense deformation (i.e., the plate margins), which are necessarily weak to permit the observed levels of strain. The cause for such a strength distribution is at the heart of understanding how plate tectonics arises from convection.

#### 7.07.5.4.1 Do plates form because the lithosphere breaks?

It is often assumed that plates and their strength distribution form because the entire oceanic lithosphere is brittle and breaks under convective stresses. Thus, once the lithosphere is broken, it is not easily mended; the broken edges remain – more or less permanently – as sites of weakness and low-

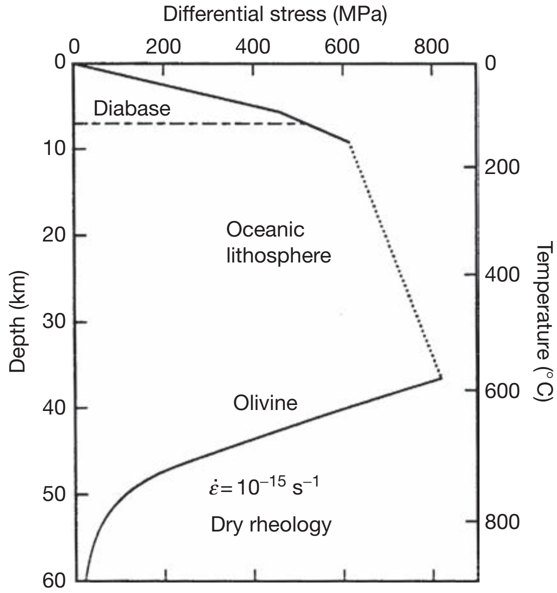


**Figure 19** Strength of oceanic lithosphere (in terms of differential stress necessary to cause failure) versus depth and temperature for a model lithosphere of ~60 My age. The top straight segment represents brittle failure; the central dashed segment is combined brittle–ductile behavior (the strength values of which are not well constrained; hence, the dashed line should not be interpreted literally), and the lower curved segment represents the transition to fully ductile behavior (with no strength). Adapted from Kohlstedt D, Evans B, and Mackwell S (1995) Strength of the lithosphere: Constraints imposed by laboratory experiments. *Journal of Geophysical Research* 100: 17587–17602.

frictional sliding (e.g., Davies and Richards, 1992). However, brittle failure cannot account for weakening over most of the oceanic lithosphere. Indeed, brittle failure and frictional sliding cease at shallow depths, on the order of 10 km (Kohlstedt et al., 1995), and give way to semiductile/semibrittle behavior that involves ductile cracking with noncontiguous distributions of microcracks (Evans and Kohlstedt, 1995; Kohlstedt et al., 1995). This semiductile behavior in fact exists over greater depths than does frictional sliding (**Figure 19**). Moreover, grain-size reduction in shear zones (through mechanisms like dynamic recrystallization) is thought to allow weakening and localization in the middle to deep lithosphere, as evident in peridotitic mylonites, that is, exposed mantle shear zones (Furusho and Kanagawa, 1999; Jin et al., 1998; White et al., 1980) (see also **Section 7.07.6.2.3**). The model of the broken lithosphere is therefore not valid. The lithospheric deformation mechanisms leading to plates are more likely controlled by other complex processes; this will be discussed further in **Section 7.07.6.2**.

#### 7.07.5.4.2 Plateness

Given the considerations mentioned earlier, many convection models seeking to generate plates employ a continuum approach; that is, they do not break the top cold boundary layer into pieces, but maintain its continuity while employing rheologies that allow parts of it to become weaker than other parts. In doing so, they try to obtain the property of a platelike strength (or viscosity) distribution for their top thermal boundary layer. This property is quantifiable and has been called *plateness* (Weinstein and Olson, 1992). A boundary layer with broad, strong, slowly deforming regions (representing strong plate interiors) separated by narrow zones of weak, rapidly deforming material (representing plate boundaries) have high plateness; clearly, convection in the Earth has a top thermal boundary layer with high plateness. A boundary layer with no strength variations, as occurs in basic convection with constant or only depth-dependent viscosity, has zero plateness.

Since plateness involves lateral variations in strength or viscosity, convection models can obviously only generate sufficient plateness if they employ a fully variable-viscosity law. Generally, viscosity is variable by virtue of being a function of the thermodynamic state (e.g., temperature and pressure), state of stress, and/or composition of the medium.

If viscosity is temperature-dependent, the top boundary layer will tend to be weakest at the divergent zone (where the boundary layer is thinnest), which approaches platelike behavior. However, the viscosity will be highest over the cold convergent zone, tending to immobilize it and eventually the entire boundary layer, which is of course one of the root causes for the subduction initiation problem (see **Section 7.07.5.5**); in the end, this also leads to a thermal boundary layer with little plateness. Therefore, it is a reasonable assumption that platelike strength distributions – or high plateness – require a lithospheric rheology that permits boundaries to be weak, independent of temperature.

At high stresses, mantle rocks undergo non-Newtonian dislocation creep wherein deformation responds nonlinearly to the applied stress; that is, the stress–strain rate constitutive law is nonlinear through a power-law relation such that

$$\dot{e} \sim \sigma^n \qquad [11]$$

where $\dot{e}$ is strain rate, $\sigma$ is stress, and $n$ is the *power-law index* (see **Figure 23**); for mantle rocks, $n=3$, typically (Evans and Kohlstedt, 1995; Weertman and Weertman, 1975). (Note that the mathematically correct constitutive law relates the strain-rate and stress tensors, and thus, strictly speaking, $\dot{e}$ and $\sigma$ are the square roots of the second scalar invariants of their respective tensors; see Malvern, 1969.) The effective viscosity is

$$\mu \sim \sigma/\dot{e} \sim \dot{e}^{1/n-1} \qquad [12]$$

which means that for $n>1$, viscosity decreases with increasing strain rate. The power-law rheology thus causes regions of the material that deform rapidly to become softer, while slowly deforming regions become relatively stiff. (Comparable effects can be caused with other rheologies such as Bingham plastics and biviscous laws; however, these are just further mathematical models for essentially the same strain-softening effect represented by a power-law rheology.) However, when such non-Newtonian rheologies with $n=3$ are incorporated into 2-D convection models, they yield very little platelike behavior (e.g., Christensen, 1984a; Parmentier et al., 1976).

Other models, concentrating on plate formation, placed a thin non-Newtonian 'lithospheric' fluid layer atop a thicker convecting layer or mathematically confined the non-Newtonian behavior to a near-surface layer or model lithosphere (Moresi and Solomatov, 1998; Richards et al., 2001; Schmeling and Jacoby, 1981; Weinstein, 1996; Weinstein and Olson, 1992); see **Figure 20**. In these models, the non-Newtonian effect does indeed yield an upper layer with reasonably high *plateness*. As noted by King et al. (1991), 2-D models with non-Newtonian lithospheres are almost indistinguishable from those with imposed plate geometries (e.g., Davies, 1988c; Olson and Corcos, 1980) and lithospheric weak zones (e.g., King and Hager, 1990; Zhong and Gurnis, 1995a), provided the non-Newtonian models employ a power-law index $n$ considerably higher than experimentally determined, that is, with $n>7$. Moreover, the simple power-law model even with large $n$ is less than successful in 3-D models where there are more than two types of boundaries (see succeeding text). Indeed, platelike behavior is more than simply generating weak boundaries, since each type of boundary, that is, convergent, divergent, and strike slip, develops under very different deformational and thermal environments. Obtaining sufficient platelike behavior is invariably related to the nature of how the different boundaries form. As

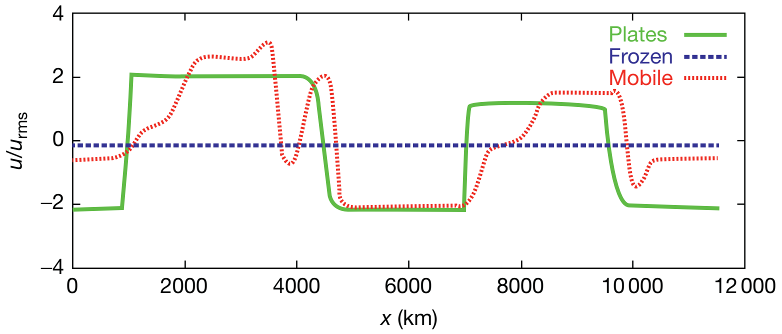


**Figure 20** Surface velocity above two-dimensional simulations of convection with a variable viscosity top boundary. A mobile top boundary (red) occurs when the fluid is entirely or nearly isoviscous such that the top thermal boundary layer acts viscously and deforms continuously and smoothly. The 'frozen' top boundary (blue) occurs when the fluid viscosity is strongly temperature-dependent and the cold top boundary layer becomes stiff and immobile. The platelike top boundary (green) occurs when the fluid has a strongly non-Newtonian or plastic rheology; here, the surface velocity is composed of nearly blocklike structures of almost constant velocity, separated by narrow zones of intense deformation. The mobile boundary (red) is defined to have 'plateness' near zero, while the platelike one (green) has 'plateness' near unity (Weinstein and Olson, 1992). Adapted from Richards M, Yang W-S, Baumgardner J, and Bunge H-P (2001) Role of a low-viscosity zone in stabilizing plate tectonics: Implications for comparative terrestrial planetology. *Geochemistry*, *Geophysics*, *Geosystems* 2: 1026. http://dx.doi.org/10.1029/2000GC000115.

each type of boundary is uniquely enigmatic, they warrant individual discussion and thus will be the focus of the following sections.

### 7.07.5.5 Convergent Margins and Subduction Zones

Cold subducting slabs sinking into the mantle are, as discussed earlier, a clear manifestation of thermal convection, in terms of both driving circulation and plate motion (**Section 7.07.4.1.1**) and cooling the mantle (**Section 7.07.4.4**). However, subduction zones remain a highly enigmatic feature of platelike convection, and we review some of the more outstanding questions later. Many of these topics are covered in **Chapter 7.09** of this volume, thus, we will only survey them briefly within the context of plate–mantle interactions and plate generation.

#### 7.07.5.5.1 Subduction initiation

How subduction zones initiate on Earth, but probably not the other terrestrial planets (the existence of subduction zones on Venus is, however, still arguable e.g., Schubert and Sandwell, 1995) is one of the most challenging issues in geodynamics (King, 2007; Mueller and Phillips, 1991; Stern, 2004). The fundamental difficulty with subduction initiation is that given mantle silicate's temperature-dependent viscosity, all terrestrial planets should be in a stagnant-lid regime of convection, that is, the extremely high viscosities of terrestrial lithospheres should prohibit them from being recycled into their underlying mantles, at least not on geologic timescales (**Section 7.07.3.5**).

The generation of weak zones on Earth that permit subduction of cold strong lithosphere is therefore a critical issue. Initiation and weakening mechanisms invoke, for example, rifting (Kemp and Stevenson, 1996; Nikolaeva et al., 2010; Schubert and Zhang, 1997) or sediment loading (Regenauer-Lieb et al., 2001) at passive margins and reactivation of preexisting fault zones from transform or spreading environments (Gurnis et al., 2004; Hall et al., 2003; Toth and Gurnis, 1998). All of these mechanisms have some observational motivation, although fault reactivation might be the most compelling (e.g., Lebrun et al., 2003). Nevertheless, each presupposes a rheological softening or shear-localizing mechanism that promotes lithospheric weakness specific to Earth; whether Earth's unique conditions involve the presence of liquid water, continental crust or cool enough surface temperatures remains an active area of debate.

#### 7.07.5.5.2 Asymmetry of subduction

The cause for asymmetrical downwellings, that is, one-sided subduction, is also an important area of research for which much progress has occurred in recent years. The downwelling currents in simple convection are largely symmetric; that is, one downwelling is composed of two cold thermal boundary layers converging on each other (**Figure 9**). In the Earth, the downwellings associated with plate motions – that is, subducting slabs – are highly asymmetrical, that is, only one side of the convergent zone, only one plate, subducts. A common explanation for the asymmetry is that it is caused by chemically light continents counteracting the negative buoyancy of one of the boundary layers approaching the convergent zone (e.g., see Lenardic and Kaula, 1996); however, this hypothesis is not universally valid since there are a significant number of purely oceanic subduction zones.

The asymmetry may also reflect an inequality of pressure on either side of the subducting slab if it deviates slightly out of vertical; that is, a more acute corner flow on one side of the subduction zone induces lower pressure than on the opposite side, thereby causing the slab to be torqued to the more acute side, that is, to enhance its obliquity (see Turcotte and Schubert, 2002). The oblique downwelling may then act to impede the motion and descent of the boundary layer approaching the acute angle, since it would have considerable resistance to making a $>90°$ downward turn, eventually leading to asymmetrical convergence. This effect is most significant for slabs that are effectively rigid relative to the surrounding mantle, in order that they act as stiff paddles while being lifted up; thus, if it occurs, the effect would theoretically be visible in basic convection calculations with strongly temperature-dependent viscosity. However, if the viscosity is so temperature-dependent that it induces such strong slabs, then it will also likely place convection itself into the *stagnant*-lid regime; that is, to make the slabs strong enough will also lock up the lithosphere (see **Sections 7.07.3.5** and **7.07.4.6**). To then adjust convection models to mitigate this extra problem requires proper initiation of subduction from cold, thick, and strong lithosphere (see **Section 7.07.5.5.1**).

Models with imposed weak zones in the lithosphere show that cold rigid lithosphere subducts readily and can even assume a fairly oblique slablike angle (Gurnis and Hager, 1988; Nakakuki et al., 2008; Zhong and Gurnis, 1995a), although both sides of the convergent margin usually undergo downwelling. Recent work has shown that permitting free surface deflection of the moving lithosphere as it bends into the subduction zone relieves much of the stress at this corner and promotes one-sided subduction (Crameri et al., 2012, results of which are displayed on the volume cover). One-sided subduction is further stabilized against eventual entrainment of the overriding lithosphere by including slab dehydration and subsequent mantle wedge hydration and melting (Gerya et al., 2008), which lubricates the acute corner flow adjacent to the slab (**Figure 21**).

#### 7.07.5.5.3 Age of subduction zones

As discussed in **Section 7.07.2.1.3**, a significant unresolved enigma concerns the age of subduction zones. In particular, while the convective picture of plate motions would have plates subduct when they get old, cold, and heavy, in fact, subduction zones are distributed in age from nearly 0 (i.e., subducting ridges) to roughly 200 My (see Becker et al., 2009; Coltice et al., 2012). One possible explanation is that dehydration-induced stiffening of the lithosphere occurs during ridge partial melting and is thus age-independent (i.e., it does not get any stiffer with time); subduction is thus age-independent if resistance to subduction is just from bending this strong lithosphere, which can occur any time there is sufficient negative buoyancy (Conrad and Hager, 2001). However, these concepts are based on 2-D steady-state models with imposed force balances. In fact, the dissipative

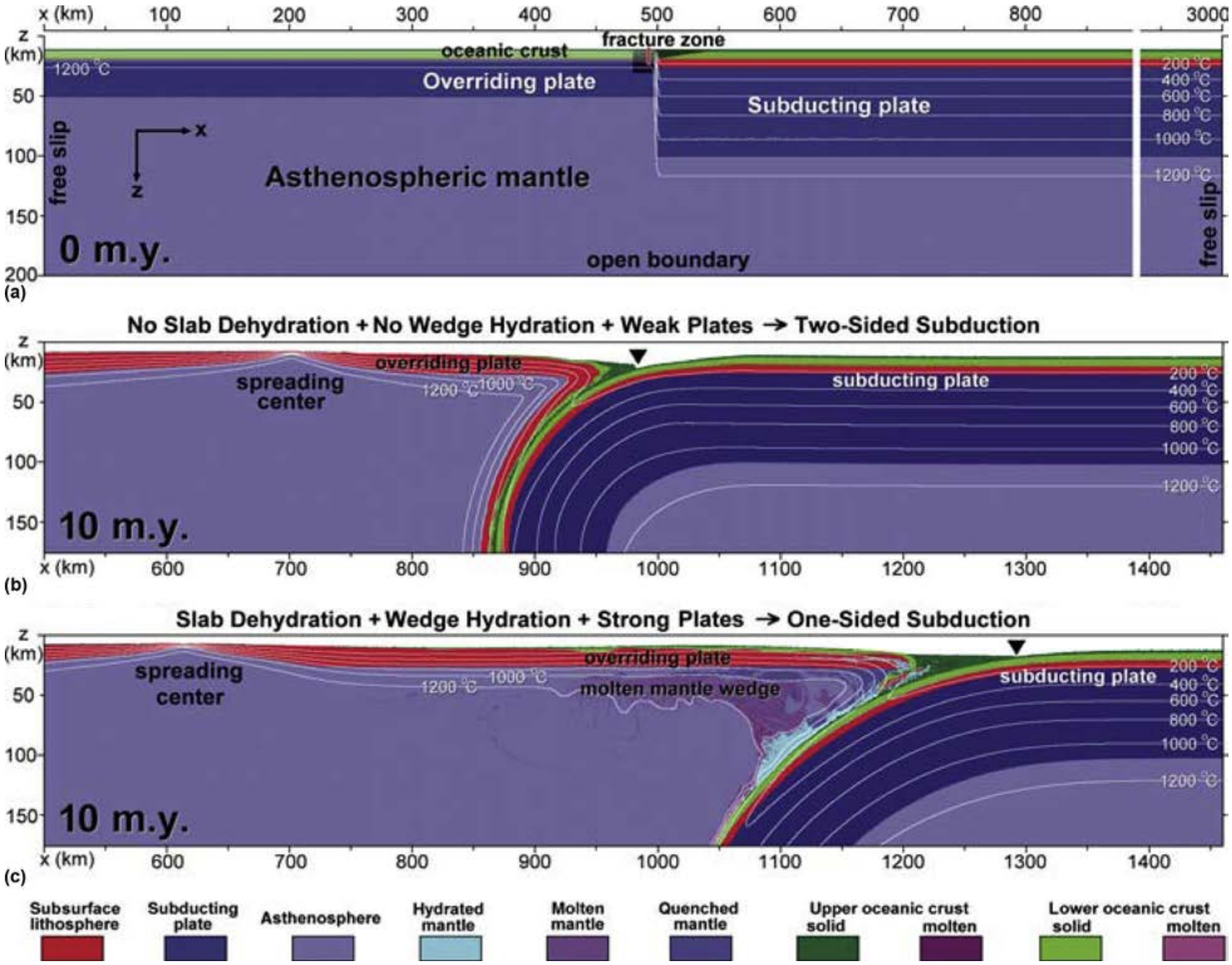


**Figure 21** Comparison of subduction flow calculations (model setup, (a)) with imposed weak zone and plastic softening and with (b) and without (c) the effect of water exchange between the slab and the wedge. Although subduction can initiate and proceed with weakening, it typically entrains the overriding plate (b); with slab dehydration, wedge hydration, and melting, the acute corner is lubricated and one-sided subduction is stable (c). Reproduced from Gerya TV, Connolly JA, and Yuen DA (2008) Why is terrestrial subduction one-sided? *Geology* 36(1): 43–46.

effect of such slab bending has recently been inferred to provide only minor resistance; for example, dissipation is minor when accounting for the bending radius of curvature being dependent on plate age and thickness rather than being constant as assumed by Conrad and Hager (2001); moreover, in three dimensions, the extra degree of freedom to evolve the length and curvature of the slab mitigates bending dissipation significantly (Buffett and Becker, 2012; Davies, 2009; Leng and Zhong, 2010). (See also **Chapter 7.09**).

Indeed, this phenomenon of age-independent subduction may just be mysterious from a 2-D and steady-state perspective of convection. A well-developed slab extending across the mantle is certainly capable of drawing a passive ridge into a subduction zone and thus consuming the plate; likewise, trench rollback due to plate foundering would also create 'young' subduction ages. Moreover, the presence of continents and passive margins might trigger subduction at younger than expected ages (Coltice et al., 2012). Thus, the age distribution of subduction zones is possibly a manifestation of time-dependent mantle convection and 3-D plate and crustal evolution. The treatment of temporal variations in plate–mantle systems is therefore a fertile area for future research.

#### *7.07.5.5.4 Melting, crust and depleted lithosphere buoyancy, and the eclogite transition*

Although the convective picture of tectonic plates is that they are thickening cold thermal boundary layers, partial melting at mid-ocean ridges induces two chemical effects that counter the plate's negative thermal buoyancy and tendency to sink at subduction zones. In particular, melt extrudes onto the seafloor as basalt, which is less dense than standard mantle peridotites. Moreover, melting extracts incompatible elements from the remaining solid lithosphere, and thus, it dries the lithosphere and depletes it of iron (Hirth and Kohlstedt, 1996), leaving it both stiffer and also chemically buoyant. The net effect is that the lithosphere is harder to subduct than a standard thermal boundary layer; indeed, the lithosphere is frequently not even negatively buoyant when it reaches subduction zones and by all rights should not even subduct. However, basalt reaching greater than about 60 km depth transforms to eclogite (Ahrens and Schubert, 1975a,b; Davies, 1992; Ito and Kennedy, 1971; Ringwood and Green, 1966), which is denser than lithospheric peridotites and promotes sinking. If basalt plus depleted lithosphere is nonsubductable, then it conceivably piles up over mantle downwellings until the basalt thickness exceeds the eclogite transition or the thermal boundary layer lengthens until its negative thermal buoyancy is sufficient to overcome the positive chemical buoyancy and sink (see also Davies, 1992, 2007a). Either way, once the basalt–eclogite transition is reached, the chemical buoyancy caused by melting is effectively erased and the downwelling current proceeds as a normal cold thermal; that is, in essence, the melting transition and eclogite transition cancel each other out. Therefore, claims that the eclogite transition drives tectonics (e.g., Ringwood, 1972; Ringwood and Green, 1966) tend to ignore the fact that ridge melting hinders it; likewise, claims that melting precludes normal convection neglect that the eclogite transition facilitates it. Taken together, these effects essentially negate each other.

#### *7.07.5.5.5 Trench-parallel flow and rollback*

During the 1980s and 1990s, seismic tomography was developed to infer mantle heterogeneity by resolving seismically fast and slow regions that are presumably associated with cold and warm anomalies, respectively (see Volume 1). Seismic tomography thus provides invaluable snapshots, primarily of the mantle temperature field; however, it does not indicate flow direction. In the last decade, measurements of seismic anisotropy have been refined through the analysis, for example, of shear-wave splitting, wherein the differences in velocity between vertical and horizontal polarizations of shear waves are used to infer material anisotropy. Although anisotropy can have many causes, its source in the deeper lithosphere and upper mantle is thought to originate from lattice-preferred orientation in olivine. Such olivine fabric tends to align in the direction of net integrated strain (Kaminski and Ribe, 2001) and thus is indicative of the direction of flow and deformation (see Volume 1 **Chapter 1.09**). One of the more remarkable observations stemming from global shear-wave splitting measurements and upper-mantle anisotropy is that mantle flow directly beneath many slabs at subduction zones is parallel to the trench, not perpendicular to it, as would be expected, given the direction of plate motion (Long and Becker, 2010; Long and Silver, 2008; Russo and Silver, 1994). Trench-parallel flow is perhaps best explained by retrograde slab motion, or trench rollback, whereby the foundering of the slab induces toroidal flow around the slab, that is, the mantle is squeezed sideways around the slab as it falls backward. As even this foundering motion involves a strong downward flow, the dominance of the trench-parallel signal appears to require that near the trench, the mantle is largely decoupled from the downward motion by some lubrication by either a low-viscosity asthenosphere or non-Newtonian behavior (see Long and Becker, 2010). Evidence that slab foundering and rollback are a major component of mantle flow implies that time-dependent plate evolution, such as retrograde motion and plate loss, plays a vital role in the generation and operation of plate tectonics on Earth (e.g., Bercovici and Long, 2014).

### 7.07.5.6 Divergent Margins: Ridges and Narrow, Passive Upwellings

Basic convection theory predicts that upwellings occur either as columnar plumes rising actively under their own buoyancy or as a very broad background of upwelling ascending passively in response to the downward flux of concentrated cold thermals. Basic convection theory and modeling do not predict focused, shallow, and passive upwellings (i.e., which rise in response to lithospheric spreading motion, rather than by their own buoyancy) analogous to ridges (Lachenbruch, 1976) (see **Chapter 7.08**). That all mid-ocean ridges involve passive upwelling is not necessarily universal (Lithgow-Bertelloni and Silver, 1998). However, the fastest and arguably the most significant ridge, the East Pacific Rise, is almost entirely devoid of a gravity anomaly or deep seismic structure (Forsyth et al., 1998), implying shallow, isostatic support and therefore no deep upwelling current lifting it up (see Davies, 1988a). (Although the interpretation of gravity by itself is nonunique, the lack of a significant free-air gravity anomaly over a topographic feature suggests that the gravity field of the topographic mass excess is being canceled by the field of a nearby mass deficit; this deficit is most readily associated with a buoyant and shallow isostatic root on which the topographic feature is floating.) Moreover, 90% of the structure of the Earth's geoid (the equipotential surface) can be explained by the gravitational attraction of the mass anomalies due only to slabs, implying that other mass anomalies, for example, those due to active buoyant upwellings, are much less significant (Ricard et al., 1993; Richards and Engebretson, 1992; see **Figure 17**). The absence of thermal anomalies beneath ridges is also in agreement with the fact that a simple model of isothermal half-space cooling with $\sqrt{\text{age}}$ satisfactorily predicts seafloor topography under all the oceans (see **Section 7.07.4.2**).

The cause and initiation of narrow ridges are easily as enigmatic as the problems with subduction. The orientation of ridges more or less mirrors the subduction zones that they eventually feed; thus, they may initiate as a strain localization, such as a self-focusing necking instability (Ricard and Froidevaux, 1986), or quite simply an effective tear in the lithosphere. This would suggest that the stresses in the lithosphere due to the pull of slabs are guided considerable distances such that they can be concentrated on particular regions (otherwise, continuous release and diffusion of stresses become manifested as distributed – and thus very unridge-like – deformation). A cold lithosphere, strong by virtue of its temperature-dependent viscosity, makes a plausible stress guide. Strain localization may be due to a variety of nonlinear feedback mechanisms, for example, necking in a non-Newtonian strain-softening medium and weakening due to melting (induced by pressure release melting within the passive upwelling; see Katz, 2008; Spiegelman and McKenzie, 1987; Tackley, 2000d; Turcotte and Morgan, 1992). Additional complexities involving hydrothermal circulation, melt production, and a healing timescale (see also **Section 7.07.6.2**) in non-Newtonian viscoplastic models also predict the formation of transform ridge offsets (Gerya, 2010, 2013).

Finally, while stress guides and strain localization are viable mechanisms for ridge formation, the physics that determines the distances to which the stresses are guided before causing a ridge – distances that also determine plate size – is not clear and remains a fruitful area of research.

### 7.07.5.7 Strike-Slip Margins: Generation of Toroidal Motion

While the upwellings, downwellings, divergent and convergent zones in basic convection may or may not appear exactly in the plate-tectonic form of convection seen on the Earth, they at least do exist in both forms of convection. However, while strike-slip motion (i.e., toroidal flow, which also includes plate spin) is very significant in the Earth's plate-tectonic style of convection (see **Sections 7.07.2.1.1** and **7.07.3.7**), it does not exist at all in basic convection with simple rheologies (i.e., with constant or depth-dependent viscosity) and is very weak in convection with slightly more complex rheologies (e.g., with temperature-dependent viscosity; Christensen and Harder, 1991). Thus, the correction to basic convection theory necessary to obtain strike-slip motion is nontrivial; this is because it is not simply a matter of adjusting the convective (poloidal) flow field, but involves generating an additional flow field that would not otherwise exist.

A very basic but important aspect of toroidal motion is that it cannot occur in 2-D models of convection (i.e., models with only $x$ and $z$ coordinates). Since toroidal flow occurs as vortex-type motion in the $x$–$y$ plane (see **Figure 13**), and since convection is driven by buoyancy forces that point in the $z$ direction, a flow model with convection and toroidal motion needs all three directions; thus, only 3-D convection models can obtain toroidal motion. Two-dimensional models of lithospheric motion in the $x$–$y$ plane are able to generate toroidal motion (Bercovici, 1993, 1995b, 1998; Bercovici and Ricard, 2005, 2013, 2014) as will be discussed later; however, these do not explicitly involve thermal convection. Another important criterion for platelike toroidal motion is that, apart from plate spin (including global rotation of the lithosphere, which has the largest toroidal power; see **Figure 2**), it is manifested in narrow but intense bands of strike-slip shear akin to a strike-slip margin or transform fault.

#### *7.07.5.7.1 Imposing plates or faults*

One way of inducing toroidal motion in mantle flow is to apply plate motion on the surface of an isoviscous mantle; the imposed strike-slip motion at the surface forces toroidal motion in the fluid, or mathematically speaking, it provides a boundary condition to eqn [6] that yields nonnull values of $\psi$ (Hager and O'Connell, 1978, 1979). This method of plate-driven mantle flow has yielded a variety of successful predictions, for example, the observation that the flow lines of the forced motion correlate with slab dip (Hager and O'Connell, 1978). A possibly more self-consistent approach is to drive the plate motion with buoyancy-driven (poloidal) flow; the tractions on the base of a plate are first provided by the poloidal flow, and then, the resulting plate motion subsequently drives toroidal flow. This method can be used to infer the mantle's density and viscosity structure by solving for the internal mass anomalies and viscosity stratification that gives the observed plate motions, as well as the observed geoid and topography (Hager and O'Connell, 1981; Lithgow-Bertelloni and Richards, 1998; Ricard and Froidevaux, 1991; Ricard and Vigny, 1989; Ricard and Wuming, 1991; Ricard et al., 1993; Vigny et al., 1991). It is also possible to use this technique to drive plates and toroidal motion with thermal convection (e.g., Gable et al., 1991; Monnereau and Quéré, 2001; Zhong et al., 2000), and models employing this method give insight into how toroidal and convective/poloidal flows interact. However, methods employing prescribed plate geometries cannot address the problem of how plates themselves are generated and evolve.

A still further step toward self-consistent generation of platelike toroidal motion is to impose faults or narrow weak zones in a model lithosphere, which either overlies a convecting mantle (Zhong and Gurnis, 1995a,b) or moves under its own pressure gradients (Gurnis et al., 2000; Zhong and Gurnis, 1996; Zhong et al., 1998). This approach is largely motivated by the fact that many weak zones persist within the lithosphere for long times and are always available to be reactivated by convective forces; this concept is also addressed later in **Section 7.07.6.1.3**. In these models, platelike motion is best generated by low-friction faults, and the

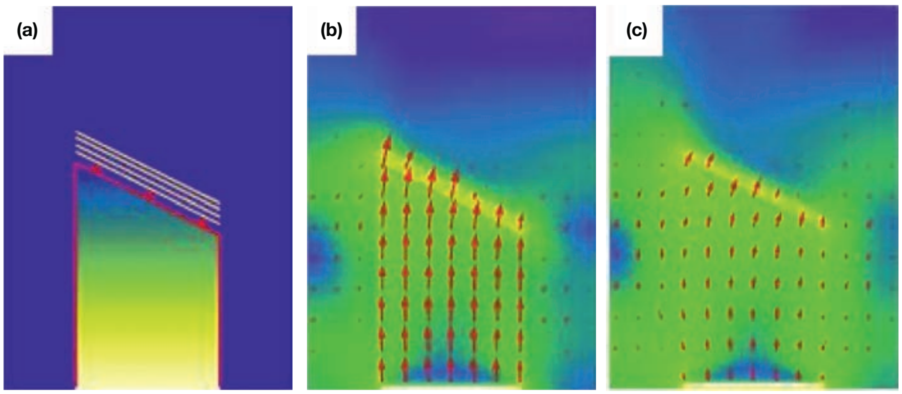


**Figure 22** A model of lithospheric flow driven by 'ridge push' (i.e., a lateral pressure gradient due to aging and thickening of the lithosphere) and slab pull with both non-Newtonian rheology and weak faults. (a) The color shading shows lithospheric age (proportional to thickening), slab dip (yellow contours indicate slab depth), and imposed weak faults (red lines). (b) Arrows show velocity field and color shows viscosity for the case with weak faults. (c) Same as (b) but for the case without faults. The weak faults provide lubricated tracks that facilitate much more platelike motion (b) than without the faults (c). See also Zhong et al. (1998). Adapted from Zhong S and Gurnis M (1996) Interaction of weak faults and non-Newtonian rheology produces plate tectonics in a 3d model of mantle flow. *Nature* 383: 245–247.

direction of motion is solely determined by neither the convective (or plate) forces nor the fault orientation; lithospheric motion instead assumes some optimum configuration that takes best advantage of the orientation of both the forces and the faults (Figure 22). Generally, the motion will arrange itself so that strike-slip shear occurs along the low-friction faults (see discussion later in Section 7.07.6.1.2 on the purpose of toroidal flow), and thus, the models generate significant toroidal motion.

However, the methods described earlier permanently prescribe the plate or fault geometries, and thus, these methods do not permit the plates or plate boundaries themselves to evolve from the convective flow. As with the 2-D convection models that strive to generate plateness, 3-D models that attempt to generate toroidal motion (as well as plateness) out of convective flow use a continuum approach with variable viscosity (e.g., Balachandar et al., 1995a; Bercovici, 1993, 1995a,b, 1996, 1998, 2003; Bercovici and Ricard, 2005, 2013, 2014; Cadek et al., 1993; Christensen and Harder, 1991; Foley and Becker, 2009; Kaula, 1980; Ribe, 1992; Stein et al., 2004; Tackley, 1998, 2000a,b,c,d; Trompert and Hansen, 1998; van Heck and Tackley, 2008; Weinstein, 1998; Zhang and Yuen, 1995).

#### 7.07.5.7.2 Why is variable viscosity necessary for toroidal motion?

The reason that the generation of toroidal motion in continuum models requires variable viscosity is somewhat mathematical and thus warrants some theoretical development. As shown earlier (Section 7.07.3.7), if viscosity is constant in viscous buoyancy-driven flows (with homogeneous boundaries), the toroidal motion is zero (see eqn [6]). If viscosity $\mu$ is variable, then instead of the equation for toroidal flow being homogeneous as in eqn [6], we have

$$\mu\nabla^2\nabla_{\mathrm{H}}^2\psi = \hat{\mathbf{z}}\cdot\nabla\mu\times\nabla^2\mathbf{v} + \hat{\mathbf{z}}\cdot\nabla\times\left(\nabla\mu\cdot\left(\nabla\mathbf{v}+[\nabla\mathbf{v}]^t\right)\right) \qquad [13]$$

(where $[..]^t$ implies transpose of a tensor). Thus, the toroidal field is forced internally (i.e., within the fluid) if $\boldsymbol{\nabla}\mu\neq 0$; if this condition is not met, then the right side of eqn [13] is zero leading to a null solution for $\psi$ as in eqn [6]. This might lead one to believe that toroidal motion can be generated for any variable viscosity, including one that is dependent only on depth (which might occur because of the natural stratification and compression of mantle rock). However, this is not the case. In order to guarantee that the toroidal field obtains some energy from convection, even indirectly, we require that the convective poloidal field $\phi$ appears on the right side of eqn [13]; that is, the poloidal field gets energy from convective buoyancy (see eqn [5]) and then passes on some of this energy to the toroidal field via viscosity gradients. However, after some algebra, it can be shown that the poloidal field $\phi$ does not appear at all in eqn [13] if $\mu$ is only a function of height $z$. Therefore, the toroidal field only couples to thermal convection through the poloidal field if $\nabla_{\mathrm{H}}\mu\neq 0$, that is, if viscosity is at least horizontally variable (see also Bercovici, 1993; Hager and O'Connell, 1981; Kaula, 1980; Ribe, 1992; Ricard and Vigny, 1989).

Equation [13] suggests another important condition for generating toroidal motion; in particular, the first term on the right side will be most significant if the horizontal viscosity gradient is orthogonal to the horizontal velocity. A weak zone striking parallel to surface flow will of course satisfy this condition and will thus be a source of toroidal motion and strike-slip shear.

The effect of laterally variable viscosity can be understood qualitatively as well. If convective forces pull or push the upper thermal boundary layer, and part of this boundary layer is weak, then the weak area tends to get moved or deformed more easily than the neighboring stronger zones. The differential motion between the strong and the weak zones can lead to strike slip-type shear and toroidal motion (see Figure 14). However, the mechanism leading to laterally varying viscosity that is sufficient to generate platelike toroidal motion is perhaps the most critical issue in understanding the generation of plate tectonics; this question will be the focus of the rest of the chapter.

## 7.07.6 Plate Generation Physics

### 7.07.6.1 Non-Newtonian Mechanics

#### 7.07.6.1.1 What variable viscosities give both plateness and toroidal flow?

As already noted, viscosity is variable by virtue of being possibly dependent on the thermodynamic state, state of stress, grain size, and composition of the medium. Nevertheless, a temperature-dependent viscosity by itself is probably not capable of generating the requisite toroidal flow and plateness. Numerous studies of basic 3-D convection with temperature-dependent viscosity yielded little platelike motion, usually with negligible plateness and toroidal kinetic energies on the order of 10% or less of the total (Christensen and Harder, 1991; Ogawa et al., 1991). The reason these models yielded little toroidal motion is likely due to the upper thermal boundary layer being too cold and stiff to permit any additional motion such as toroidal flow. It may also reflect the fact that since both viscosity and buoyancy are dependent on temperature, the viscosity and poloidal flow fields are in phase, whereas viscosity gradients orthogonal to the poloidal flow are probably optimal for generating toroidal flow (see Section 7.07.5.7.2). Thus, the necessary heterogeneities in viscosity likely arise from other nonlinear rheological mechanisms.

Given the success of creating respectable *plateness* from non-Newtonian power-law or plastic rheologies in 2-D convection models, it stands to reason that similar rheologies would generate significant toroidal motion in 3-D convection models. However, this appears not to be the case. Models using power-law rheologies (even with an excessively large power-law index $n>3$) or plastic rheologies yield modest platelike toroidal power, although the strike-slip shear zones tend to be broad and diffuse (Bercovici, 1993, 1995b; Cadek et al., 1993; Christensen and Harder, 1991; Stein et al., 2004; Tackley, 1998; Trompert and Hansen, 1998; Weinstein, 1998).

It has been proposed that strain softening-type power-law rheologies are not sufficient to excite the necessary shear-localizing behavior and platelike flow and instead that *velocity-weakening* or equivalently *pseudo-stick-slip rheologies* are necessary to generate such motion (Bercovici, 1993, 1995b). A velocity-weakening rheology involves a constitutive law that acts like a normal, highly viscous fluid at low strain rates, but at larger strain rates, the viscosity weakens so rapidly with increasing strain rate that the very resistance to flow itself – that is, the

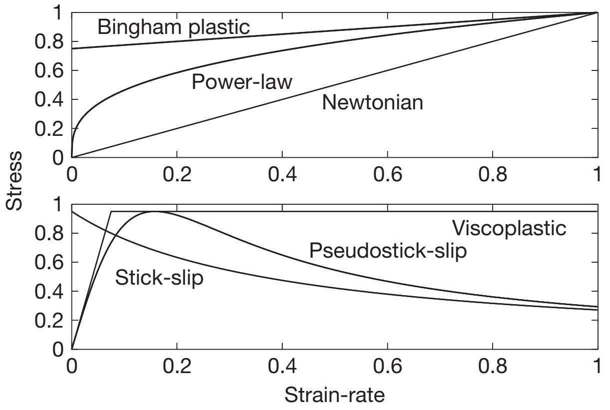


**Figure 23** The stress versus strain-rate curves for various rheologies. A Newtonian rheology is represented by a linear constitutive relation between stress and strain rate. A non-Newtonian power-law rheology has a nonlinear constitutive relation in which strain rate goes as stress to some power $n > 1$ (the curve shows the case for $n = 3$ that is typical of deep mantle silicates). Both Bingham plastic and viscoplastic rheologies describe discontinuous stress–strain rate relations whereby, at a particular yield stress, an abrupt transition in flow behavior occurs from strong (immobile or highly viscous) to weak (viscous or with only a maximum strength or allowable stress). Stick-slip and pseudo-stick-slip behaviors make transitions at a peak stress from strong (immobile or highly viscous) to one where strength (i.e., the allowable stress or resistance to deformation) is lost with faster deformation.

stress – decreases; this rheology is most simply represented by the constitutive law

$$\sigma \sim \frac{\dot{e}}{1 + \dot{e}^2/\gamma^2} \qquad [14]$$

where $\gamma$ is the strain rate at which the stress $\sigma$ reaches a maximum and begins to decrease with increasing strain rate (Figure 23). When employed in various flow models (which permit motion in the $x$–$y$ plane and thus toroidal flow), the velocity-weakening rheology yields much more platelike toroidal motion and high plateness than do the power-law rheologies (Bercovici, 1993, 1995b; Tackley, 1998) (see Figures 24 and 25).

The velocity-weakening rheology, however, has proved difficult to implement in mantle convection simulations because of its double-valued strain rate (i.e., any given stress has two possible values of strain rate). Convection studies have been, in general, more successful using a simple viscoplastic lithosphere overlying a viscous convecting mantle (Moresi and Solomatov, 1998; Tackley, 2000c; Trompert and Hansen, 1998) including fully 3-D spherical models (Foley and Becker, 2009; Richards et al., 2001; van Heck and Tackley, 2008) (Figure 26). The viscoplastic rheology dictates that at low strain rates, material deforms like a very stiff, viscous fluid, but at a given stress (a 'yield stress'), the resistance to motion stops increasing with strain rate and remains constant (Figure 23). However, these models produce only moderate platelike behavior (Tackley, 2000c; Trompert and Hansen, 1998), unless used in conjunction with an imposed low-viscosity asthenospheric channel (Richards et al., 2001; Tackley, 2000d) or viscosity reduction due to melting in near-surface mantle upwellings (Tackley, 2000d) (Figure 27). Although these viscoplastic models still have difficulty generating isolated strike-slip (toroidal) zones, the inclusion of melting leads to very localized spreading centers with shallow passive upwellings (Figure 27). Nevertheless, instantaneous or 'steady-state' rheologies, including the velocity-weakening one, fail to allow inactive or dormant weak zones that can be reactivated, which is possibly a critical feature of plate tectonics; this is discussed further in Section 7.07.6.1.3.

#### 7.07.6.1.2 What is the purpose of toroidal motion?

Continuum models that generate toroidal motion from first principles allow us to address an important question: Why does toroidal motion form in the first place, and what role does it play? Since poloidal motion involves upwellings and downwellings, it can enhance its own energy uptake by increasing the rate at which gravitational potential energy is released; this feedback effect is the reason that heated layers go convectively unstable in the first place. However, toroidal flow only dissipates the energy provided: since it involves purely horizontal motion, it does not explicitly enhance gravitational energy release, nor does it, by the same token, transport heat and directly facilitate cooling of the fluid. By all appearances, the toroidal field is superfluous. And yet it is omnipresent in the Earth and is readily generated in fluid models with non-Newtonian (especially velocity-weakening) rheologies.

The reason that toroidal motion is generated appears to relate to the thermodynamic efficiency of surface flow. Examination of the total viscous dissipation in the continuum models of Bercovici (1993, 1995b) shows that even though the toroidal flow field is added to the convectively driven poloidal field, it actually makes the system *less* dissipative than if it were not present (Bercovici, 1995a); that is, generation of toroidal motion *enhances* the efficiency of surface motion. Indeed, the toroidal field establishes itself in focused zones of strike-slip shear that act as lubricated motion guides. The bulk of the fluid outside of these zones of intense toroidal motion remains relatively undeformed and thus entails little dissipation. Within these zones, deformation may be intense, but the viscosity is so low that the dissipation is small. Moreover, the zones of deformation are ideally so narrow and involve so little volume that they make little contribution to the total dissipation generated throughout the whole medium.

#### 7.07.6.1.3 Instantaneous rheologies and plate boundary history

Strongly non-Newtonian rheologies, such as those in the plasticity or velocity-weakening limit, appear to be reasonably successful at generating platelike motion. However, there are a few fundamental problems with this approach. First, these very nonlinear rheologies tend to be ad hoc. For example, while the plasticity formalism is based on known plastic yielding of rocks, it requires a much lower low yield stress or friction coefficient relative to the actual strength of rocks. Moreover, the velocity-weakening mechanism is an assumed law since there is no steady-state creep law that displays this behavior; it is if anything a steady-state representation of a more complex time-dependent self-softening mechanisms (see Section 7.07.6.2). Indeed, laboratory experiments on rock deformation at moderate temperatures show much more complex behavior than simple instantaneous rheologies (e.g., time

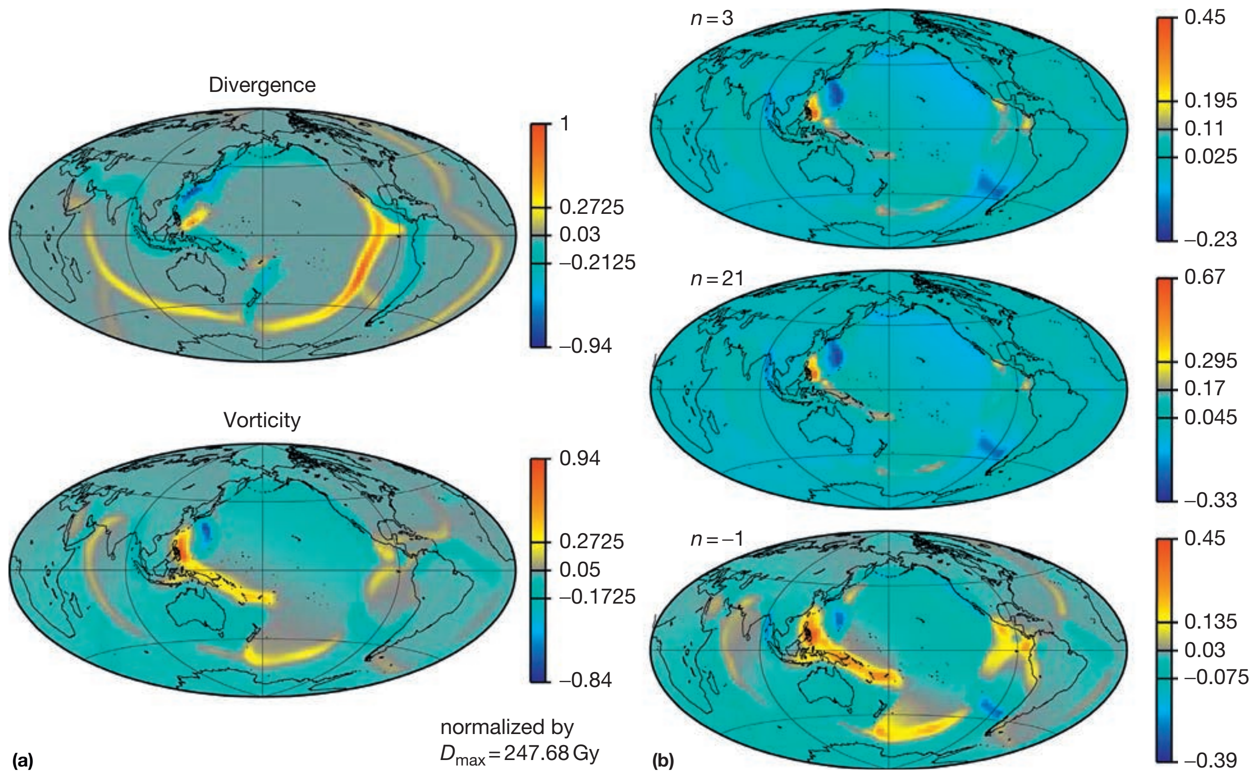


**Figure 24** Divergence rate and vertical vorticity (rate of spin and strike-slip shear) of present-day plate motions (a), representing poloidal and toroidal motion, respectively. Red and yellow divergence is positive over spreading centers and blue is negative, or convergent, over subduction zones. Red and yellow vorticity represents left-lateral strike-slip motion and counterclockwise spin, while blue is right-lateral motion and clockwise spin. Fluid-dynamic calculations use the Earth's divergence as a source–sink field to drive flow in various non-Newtonian shallow-layer model lithospheres, thereby generating toroidal motion that is shown in terms of vorticity (b). Power-law rheologies with indexes $n = 3$ and even as high as $n = 21$ (where stress goes as strain rate to the $1/n$ power; see eqn [11]) generate vorticity fields that do not compare well with the Earth's vorticity field. A self-lubricating or pseudo-stick-slip rheology, represented by $n = -1$ (see eqn [14]), however, generates vorticity that compares well with the Earth's present-day case. Adapted from Bercovici D (1995) A source–sink model of the generation of plate tectonics from non-Newtonian mantle flow. *Journal of Geophysical Research* 100: 2013–2030.

evolution of grain size and texture, as well as interaction between different deformation mechanisms; see Karato, 2008).

Second, these non-Newtonian rheologies involve an *instantaneous* response because viscosity responds only on the instantaneous strain-rate field. Thus, weak zones, as proxies for plate boundaries, only exist as long as they are being deformed; once deformation ceases, the boundaries instantaneously vanish (Gurnis et al., 2000; Zhong et al., 1998). However, it is known that while new plate boundaries continue to be formed, old inactive ones persist as fabric in the lithosphere and even provide intrinsic weak zones that are preferred sites at which to reactivate deformation, especially for the initiation of new subduction zones in cold strong lithosphere (Gurnis et al., 2000; Hall et al., 2003; Lebrun et al., 2003; Toth and Gurnis, 1998). Thus, plate boundaries have memory: they can remain weak even without being deformed and be advected with the material in which they are embedded. This implies that the weakness is an actual transportable property, like temperature, chemical concentration, or grain size. Moreover, such weak zones can persist for extremely long times, possibly much longer than the typical convective timescale of $10^8$ years (a typical convective overturn time) (Gurnis et al., 2000); this suggests that the property that determines plate boundary weakness obeys a much longer timescale than does convection.

### 7.07.6.2 Dynamic Weakening and Damage Physics

That plate boundaries are caused by some weakening property rather than an instantaneous rheological response correlates with the origins of the velocity-weakening and localizing feedback. There are various candidate feedback mechanisms that we discuss next.

#### *7.07.6.2.1 Thermal self-weakening*

The velocity-weakening rheological law expressed in eqn [14] is a simplified, 1-D, steady-state representation (Bercovici, 1993; Whitehead and Gans, 1974) of the classical self-softening feedback arising from the coupling of viscous heating with temperature-dependent viscosity (Schubert and Turcotte, 1972). With this feedback mechanism, deformation causes frictional heating, which warms and weakens the material; the weak zone is more readily deformed causing a concentration of deformation and therefore more heating, weakening, etc. In this case, a weak zone corresponds to a temperature anomaly, and thus, temperature acts as the transportable time-

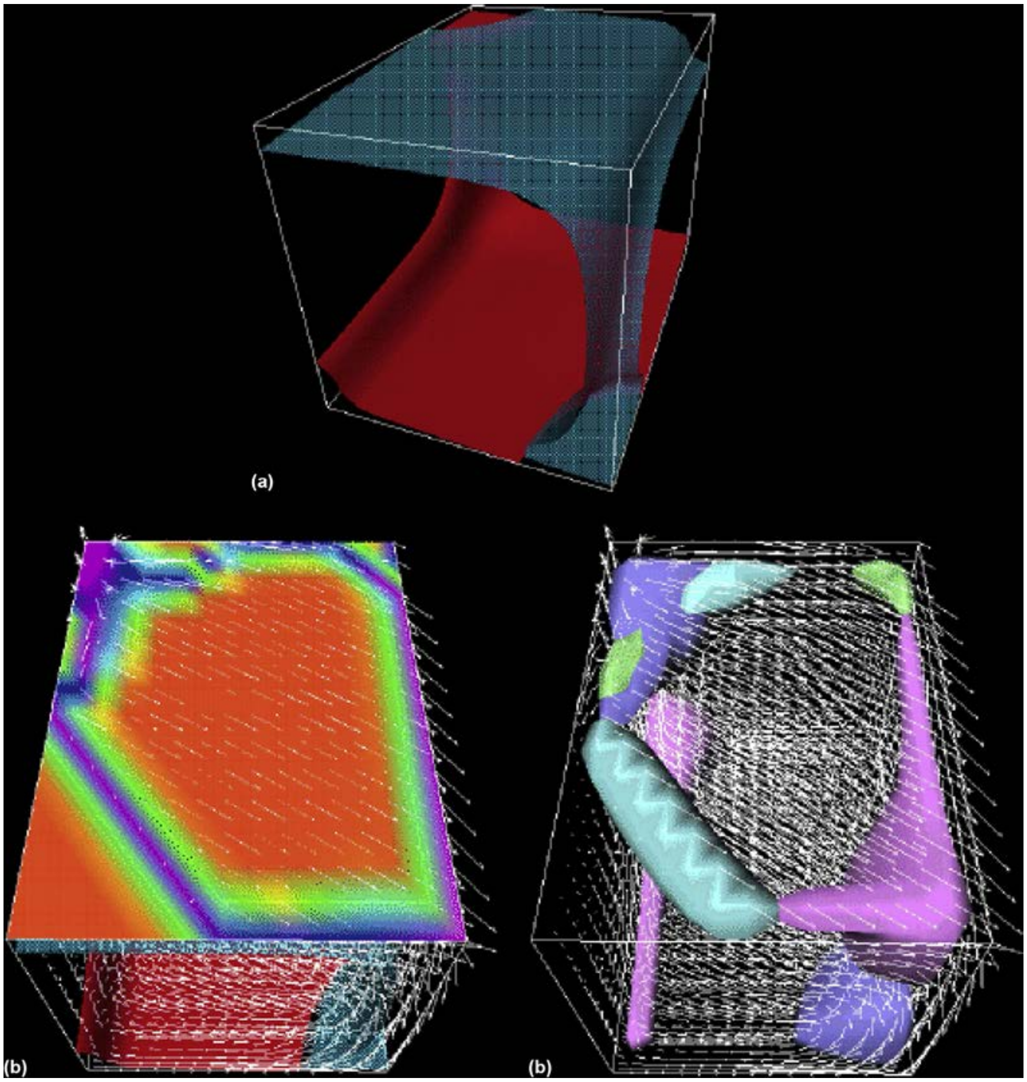


**Figure 25** Generation of platelike motion in lithospheric flow driven from below by a convective-type buoyancy field. (a) The temperature field from simple basally heated convection. This is used as a static source of buoyancy to drive flow that then drags an overlying layer of fluid with stick-slip rheology (eqn [14]). The sharp changes in viscosity (b) surrounding nearly isoviscous (red) blocks, along with nearly uniform velocity fields in these blocks, are suggestive of highly platelike flow. (c) Isosurfaces of horizontal divergence (poloidal flow) in the lithospheric layer (pink and purple) and vertical vorticity or toroidal flow (light blue and green). The elongated blue surface corresponds to a long, fault-like concentration of strike-slip shear. Adapted from Tackley P (1998) Self-consistent generation of tectonic plates in three-dimensional mantle convection. *Earth and Planetary Science Letters* 157: 9–22.

dependent property whose history can be retained for a finite period of time.

?A3B2 tlsb=0.01w?>However, when this viscous heating-based mechanism is incorporated into flow models, it is not overly successful at generating large-scale platelike motions. In lithospheric flow models, this mechanism gives relatively weak localization and diffuse toroidal motion (Bercovici, 1998) (see **Figure 28**). In convection models, viscous heating can be significant on small scales in the lithosphere and, with temperature-dependent viscosity, can lead to modest local concentrations of toroidal motion (Balachandar et al., 1995a,b; Zhang and Yuen, 1995); however, the surface motions and strength distributions are not platelike, and the global toroidal energy is typically very small. This lack of platelike motion probably occurs for several reasons. First, the temperature anomalies necessary to reach a velocity-weakening regime are excessively large, near the melting temperature, which is well beyond that attainable with viscous heating in these systems (Bercovici and Karato, 2003); that is, dissipative thermal anomalies are self-limiting because dissipative heating is proportional to the local viscosity, which drops precipitously with increasing temperature (Fleitout and Froidevaux, 1980; Yuen et al., 1978). Secondly, and for similar reasons, the temperature anomalies due to viscous dissipation are generally much smaller than temperature anomalies due to heat that powers convection (e.g., radiogenic heating). Thus, the temperature drop across the cold upper thermal boundary layer is usually much larger than any temperature anomaly due to viscous heating, causing this boundary layer to continue to be stiff and immobile.

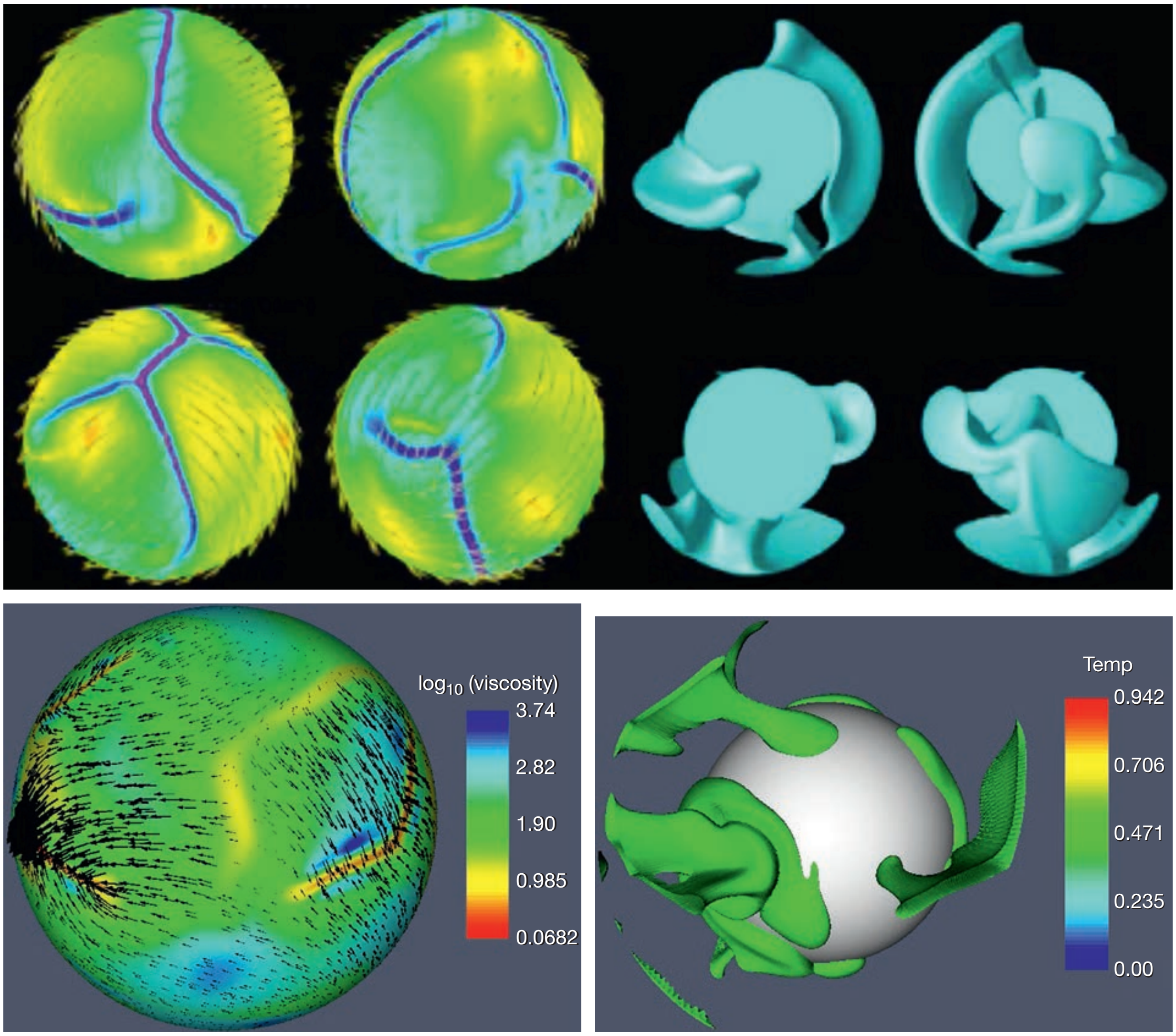


**Figure 26** Three-dimensional spherical-shell convection with a plastic-type lithospheric rheology from two different studies of van Heck and Tackley (2008) (top) and Foley and Becker (2009) (bottom) showing platelike behavior. Left panels show surface viscosity with velocity vectors superimposed. Right panels show isothermal surfaces and in particular cold downwellings. Note the passive divergent and rheological weak zone forming midway between the two major downwelling regions.

Moreover, if the Earth's weak zones were due to temperature anomalies (and were fortuitously not overwhelmed by convective temperature anomalies), they would diffuse away on the order of a few million years (assuming plate boundaries are of order 10 km wide and thermal diffusivity is $10^{-6}\ \mathrm{m^2\,s^{-1}}$), which is not observed (Gurnis et al., 2000). Finally, if plate boundaries, in particular strike-slip margins, were caused by viscous heating, then they should be perceptible with heat flow measurements; however, this is generally thought not to be the case (Lachenbruch and Sass, 1980) (cf. Thatcher and England, 1998).

Nevertheless, while viscous heating alone is unlikely to provide a sufficient sustained localizing feedback mechanism, it could play a role in assisting localization associated with grain-size reduction (Kameyama et al., 1997) (see also **Section 7.07.6.2.3**) and in helping initiate subduction (Thielmann and Kaus, 2012) (see also **Section 7.07.5.5.1**).

#### *7.07.6.2.2 Water and void weakening*

An appealing yet speculative plate generation model invokes water as the weakening agent; this is motivated by the oft-stated hypothesis that plate tectonics only exists because water lubricates plate boundaries, which also partially explains the lack of plate tectonics on the terrestrial planets devoid of water (Lenardic and Kaula, 1994, 1996; Tozer, 1985). In particular, water is assumed to provide pore pressure reduction of friction and/or lubrication of slip zones by, for example, serpentinization (Escartin et al., 2001). Moreover, if weak zones are due to water, then their longevity would be controlled by chemical diffusivity of hydrogen in minerals, which is faster than most chemical diffusivities but much slower than thermal diffusivity (Brady, 1995), in which case weak zones could survive over geologic timescales.

Water is certainly ingested by subducting slabs and plays a critical role in maintaining sufficient weakness at subduction

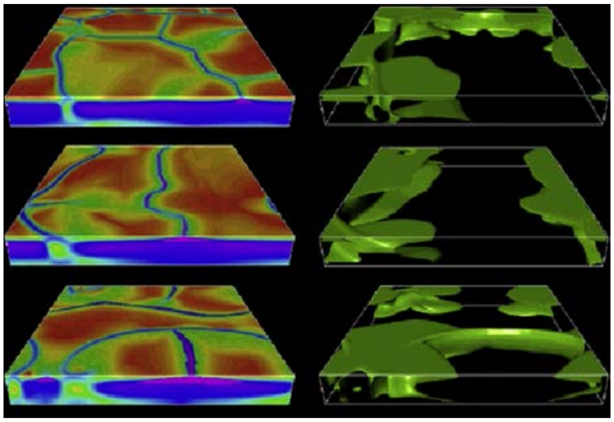

**Figure 27** Three-dimensional simulations of convection with a viscoplastic rheology and including viscosity reduction by melting. Convection is driven entirely by internal heating, and thus, cold downwellings are the dominant current. The left panels show the viscosity fields, where purple and blue are low viscosity and red and yellow are high viscosity. The right panels show the associated cold isothermal surfaces that outline the downwelling convecting currents that drive motion in the system; therefore, any low-viscosity surface region coinciding with a cold isotherm is a convergent zone. The platelike geometry is apparent in the surface viscosity fields (left panels); in particular, the focused spreading centers overlying melt lenses (purple zones) are diverging passively, that is, they are not associated with any active upwelling rising from deep in the layer. However, strike-slip motion is relatively weak and not isolated, being associated primarily with obliquity and offsets in the spreading centers. Adapted from Tackley P (2000) Self-consistent generation of tectonic plates in time-dependent, three-dimensional mantle convection simulations: 2. Strain weakening and asthenosphere. *Geochemistry*, *Geophysics*, *Geosystems* 1: 1026. http://dx.doi.org/10.1029/2000GC000043.

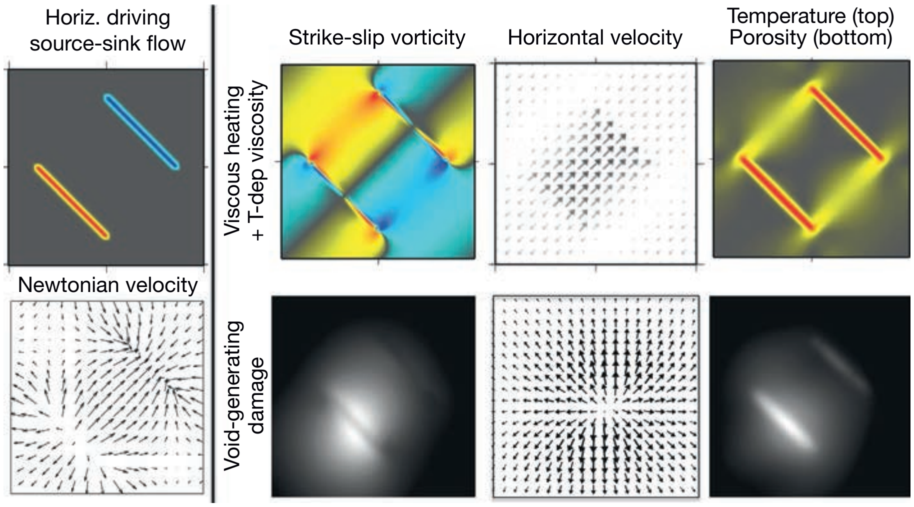


**Figure 28** Summary of two separate source–sink model studies of shallow lithospheric flow with different localization mechanisms. The driving source–sink field equals the horizontal velocity divergence and has amplitude of $\pm 1$; the velocity field corresponding to pure source–sink flow, as occurs with a Newtonian uniform rheology, is shown for comparison. The top row of calculated fields (right of the vertical line) is for the case with viscous heating and temperature-dependent viscosity; the generated toroidal vorticity field is relatively weak with an amplitude of $\pm 0.2$ (i.e., only 20% of the driving source–sink field), leading to modest platelike flow yet still diffuse strike-slip shear in the corresponding velocity field and weak temperature and viscosity anomalies over the strike-slip margins. The bottom row of calculated fields is for the case of void-generating damage, as a model for opening up cracks and pore space with which to ingest a weak phase such as water; in this case, dilational flow augments poloidal motion over the driving source and leads to very unplatelike monopolar flow, with poor platelike structure in both the vorticity field and the porosity field (which controls the effective viscosity). Adapted from Bercovici D (1998) Generation of plate tectonics from lithosphere-mantle flow and void-volatile self-lubrication. *Earth and Planetary Science Letters* 154: 139–151; Bercovici D and Ricard Y (2005) Tectonic plate generation and two-phase damage: Void growth versus grainsize reduction. *Journal of Geophysical Research* 110: B03401. http://dx.doi.org/10.1029/2004JB003181.

zones, in addition to the asymmetry of slab downwelling (Crameri et al., 2012; Faccenda et al., 2009, 2012; Gerya et al., 2008; Ranero et al., 2003; see also **Section 7.07.5.5.2**). However, applying the water weakening mechanism to understand shear localization at all plate boundaries is fraught with various limitations. First, frictional reduction by pore pressure is relevant for brittle failure and frictional sliding, which occurs only over shallow depths that are already the weakest portions of the lithosphere (**Figure 19**). The lithosphere reaches its peak strength well below the top roughly 10 km and undergoes complex transitions to semiductile and ductile behavior, where frictional sliding plays little to no role. Second, the availability of water to weaken the deep strong lithosphere is problematic. Given melting at ridges and extraction of water into the melt phase, most of the lithosphere is probably as dry as on nonplate planets such as Venus (Hirth and Kohlstedt, 1996). Thus, if water is to play a weakening role, it must be ingested from the surface to great depths, down to 100 km or so. The great pressures at these depths cause a very large lithostatic pressure gradient against which fluid has to be pushed, in addition to closing down fluid pathways to negligible permeabilities; given that tectonic stresses are orders of magnitude smaller than lithostatic pressures, it is unlikely they can induce deep pressure lows and hold open fluid pathways against the weight of the lithosphere. One possible solution to this quandary is deep thermal cracking at fracture zones emanating from mid-ocean ridges, which can possibly allow water to be ingested to moderate depths and serpentinize lithosphere in these zones (Korenaga, 2007). However, thermal stresses at best allow water to be ingested to moderate depths (a few tens of kilometers), leaving much of the lower strong lithosphere, and lithosphere far from fracture zones, unaffected. Moreover, the ingestion of water and serpentinization occur only before thermal stresses relax away moderately rapidly, and thus, there is no feedback by which weakening focuses deformation, which causes more weakening, thus focusing deformation further, etc.

Indeed, in order for water to induce a shear-localizing feedback, it must not only weaken the material into which it is ingested, but the ingestion and water content must, in turn, be enhanced by the deformation itself. In particular, ingestion of water may be controlled by rate of deformation when voids are created by damaging of the material, such that these voids take up water, which causes weakening, which in turn focuses deformation, more damage, etc. The physics of this process was elaborated on by 'two-phase damage' theory (Bercovici and Ricard, 2003; Bercovici et al., 2001a,b; Ricard and Bercovici, 2003; Ricard et al., 2001) wherein the energy necessary to create a void or a microcrack (Griffith, 1921) is treated as the surface energy on the interface between a host phase (rock) and the void-filling phase (e.g., water). Deformational work is used to create this interfacial energy by generating more voids, thus inducing weak zones on which deformation localizes. This mechanism leads to a spectrum of shear-localizing behavior, from diffuse to very sharp shear zones (Bercovici and Ricard, 2003; Bercovici et al., 2001b), and also predicts failure in low-cohesion rocks that undergo dilational or compactive/cataclastic damage (Ricard and Bercovici, 2003). However, when this mechanism is placed at high lithostatic pressures typical of the mid-to-deep lithosphere, it is suppressed relative to other deformation mechanisms, given the difficulty of opening new pores (Landuyt and Bercovici, 2009a). Moreover, when this mechanism is employed in 2-D lithospheric flow models, wherein imposed source–sink poloidal flow is used to generate strike-slip toroidal motion, it does not yield platelike solutions (Bercovici and Ricard, 2005); in particular, the dilational motion from void generation augments poloidal flow at the expense of toroidal motion, thereby leading to very unplatelike flow (see **Figure 28**).

In the end, water weakening remains problematic for generating weak zones that extend across the entire lithosphere and for generating toroidal motion. Certainly, water-enhanced melting is likely critical for melt localization at ridges and weakening of the mantle wedges at subduction zones (see **Sections 7.07.5.5.2** and **7.07.5.6**). Whether water directly leads to the formation of all plate boundaries especially the most enigmatic 'toroidal' ones is, however, doubtful, although its indirect effect on surface conditions remains a possibility (see **Section 7.07.7.3**).

#### *7.07.6.2.3 Grain-size weakening*

Observations of localized shear in mantle peridotitic mylonites – where large strain correlates to highly reduced mineral grain sizes – at all types of plate boundaries (e.g., Dijkstra et al., 2004; Etheridge and Wilkie, 1979; Furusho and Kanagawa, 1999; Ildefonse et al., 2007; Jin et al., 1998; Skemer et al., 2010; Warren and Hirth, 2006; White et al., 1980) have prompted much activity in exploring grain size-dependent shear-localizing feedback mechanisms (e.g., Braun et al., 1999; Kameyama et al., 1997; Montési and Hirth, 2003). In this case, a self-weakening positive feedback occurs because of the interaction of grain size-dependent rheologies (such as diffusion creep or grain-boundary sliding; see Hirth and Kohlstedt 2003) and grain-size reduction driven by deformation through dynamic recrystallization (e.g., Derby and Ashby, 1987; Doherty et al., 1997; Karato et al., 1980; Lee et al., 2002; Shimizu, 1998; Urai et al., 1986). However, this localizing feedback mechanism is paradoxical because grain-size reduction by recrystallization is generally thought to occur only in dislocation creep, which is independent of grain size, while rheological softening by grain-size reduction only occurs in diffusion creep, when the grains cannot be reduced (De Bresser et al., 1998, 2001; Etheridge and Wilkie, 1979; Karato and Wu, 1993; see **Figure 29**). Large grains undergoing dislocation creep can shrink through dynamic recrystallization, while small grains undergoing diffusion creep coarsen by normal grain growth; grain sizes thus tend to evolve toward the boundary between diffusion and dislocation creep, and the rheology therefore tends to become anchored closed to the boundary, on the piezometric curve. Near this boundary, complex interactions can ensue, leading to effective rheologies that are dependent on both grain size and stress. Such interactions can be due either to mixing of creep mechanisms over grain-size distributions that span the boundary (e.g., Rozel et al., 2011) or to unique mechanisms like grain-boundary sliding (e.g., see Hansen et al., 2012; Hirth and Kohlstedt, 2003); however, these effects are not necessarily distinguishable in that both mixing and grain-boundary sliding lead to similar grain-size and stress dependence (see Hansen et al., 2012; Rozel et al., 2011). Nevertheless, these interactions are bound close to the diffusion–dislocation boundary where grain-size reduction and thus localization feedbacks are restricted (Rozel et al., 2011).

In addition to problems with the grain softening feedback mechanism, grain growth and healing of weak zones in single-mineral or single-phase systems are quite fast (Karato, 1989), which would cause fine-grained weak zones in the lower lithosphere to vanish in less than a million years (see Bercovici and Ricard, 2012). Thus, grain-size reduction in these simple systems cannot by itself support long-lived plate boundaries.

However, many of the problems with this mechanism stem from its basis in monomineralic single-phase systems. That lithospheric and crustal rocks are polymineralic multiphase systems like peridotite (with at least both olivine and pyroxenes) may play an important role in localization and plate

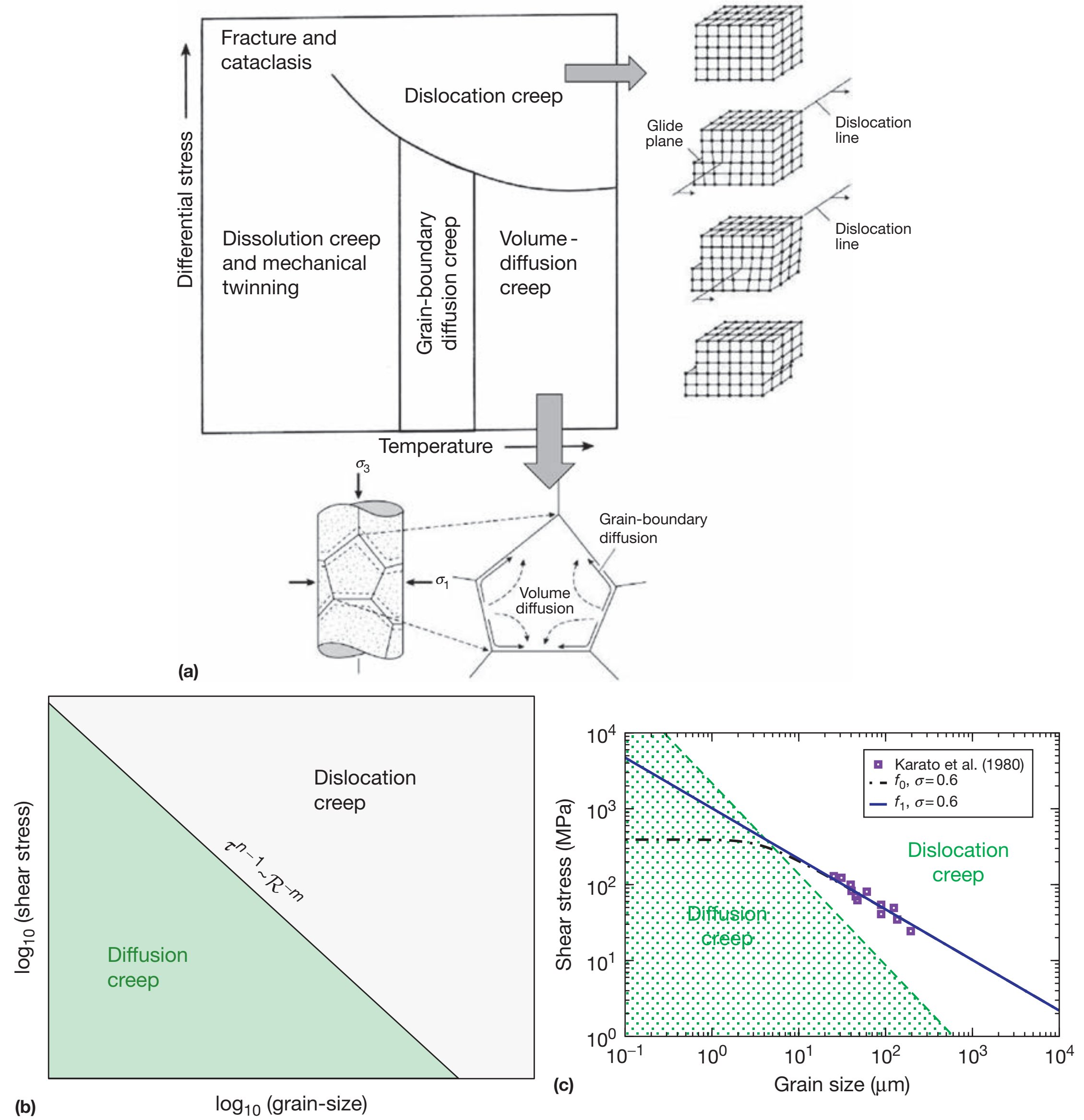


**Figure 29** (a) Deformation map of stress–temperature space showing different creep and failure mechanisms; (b) stress–grain size space sketch to show typical creep mechanism transition as a function of grain size (the transition occurs where the strain rates of each mechanism are equal and thus, $\dot{e} \sim \tau^n \sim \tau/\mathcal{R}^m$ and thus, the boundary is given by $\tau^{n-1} \sim \mathcal{R}^{-m}$); and (c) a stress–grain size deformation map and steady-state rheology predicted by the single-phase grain-damage theory of Rozel et al. (2011), where the solid blue curve is for the case where damage only exists in dislocation creep (as expected) and the black dashed-dot curve is if damage can somehow persist into the diffusion creep regime. The two-phase Zener pinning damage model (Bercovici and Ricard, 2012) provides a mechanism for damage to persist well into the diffusion creep regime.

boundary formation. Indeed, many observations of peridotitic mylonites show evidence of secondary-phase pinning in which reduced pyroxene grains appear to hold the olivine in permanent diffusion creep (Herwegh et al., 2011; Linckens et al., 2011; Mehl and Hirth, 2008; Olgaard, 1990; Warren and Hirth, 2006). In this regard, Bercovici and Ricard (2012) recently proposed a generalized two-phase grain evolution and damage theory, which provides a new mechanism that potentially solves the grain-weakening paradox. This theory treats the coupling between damage and Zener pinning in two-phase rock mixtures like peridotite. In essence, pinning in mixtures arises because immiscible phases block each others' grain-boundary migration and hence stunt grain growth. In two-phase theory, the pinning or blocking surface is represented by the interface between phases. This interface undergoes damage by stretching or rending, which reduces the size of the pinning surfaces, which in turn pins grains to smaller sizes regardless of creep mechanism. Damage thus indirectly reduces grain size even in diffusion creep, wherein the material gets weaker as grains shrink, thereby allowing a very effective shear-localizing feedback consistent with observations of mylonites.

This two-phase grain-damage and pinning model has also been tested in 2-D lithospheric source–sink flow models

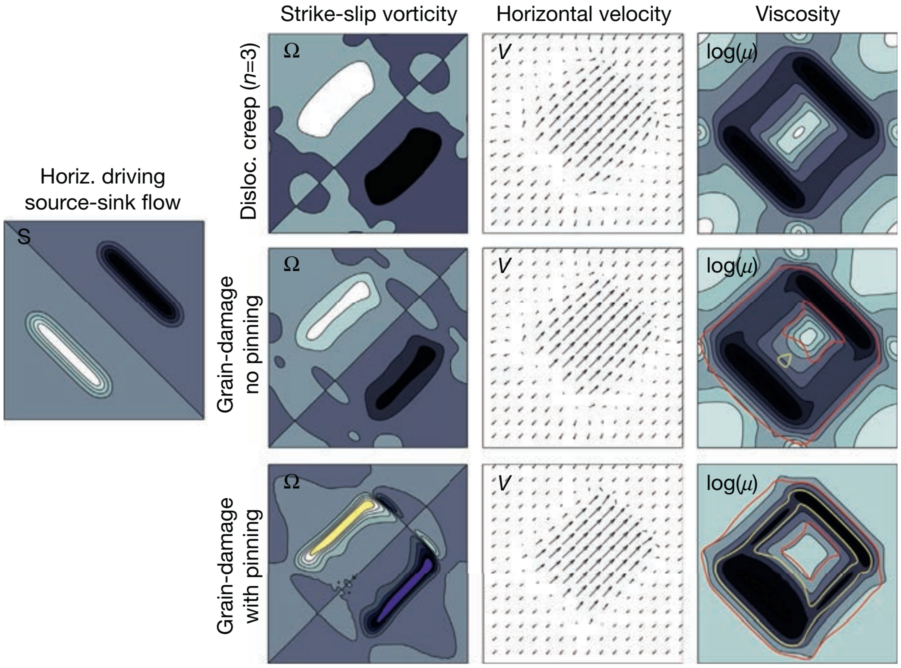


**Figure 30** Source–sink-driven flow with simple dislocation-creep power-law rheology ($n=3$), grain damage without pinning, and grain damage with pinning. Yellow and indigo on the $\Omega$ contours show saturation above $\pm 1$. Yellow contours on $\mu$ plots bound where the medium is more than 99% in diffusion creep (red is the 75% bound). Adapted from Bercovici D and Ricard Y (2013) Generation of plate tectonics with two-phase grain-damage and pinning: Source–sink model and toroidal flow. *Earth and Planetary Science Letters* 365: 275–288.

(Bercovici and Ricard, 2013). Grain-size reduction and damage without pinning (as in Rozel et al., 2011) lead to very weak localization and toroidal motion, similar to that for basic dislocation-creep power-law rheologies (**Figure 30**, top rows). However, the inclusion of pinning and interface damage allows for intense localization and toroidal motion and highly platelike behavior (**Figure 30**, bottom row).

The pinning effect also promotes the longevity of inactive weak zones; in particular, after deformation ceases, grain growth and healing are essentially stopped or retarded by the small pinning bodies, which in themselves grow extremely slowly (especially if moderately dispersed) (Bercovici and Ricard, 2012). Moreover, the damage model shows that the inheritance of weak zones can have a major influence on plate and plate boundary evolution after plate motion changes in 2-D flow models (Bercovici and Ricard, 2013, 2014); this effect provides a simple theory for both the emergence of plate tectonics in the Archean and modern and even abrupt plate reorganizations (Bercovici and Ricard, 2014; Bercovici et al., 2015) (see **Figures 31** and **32**). In the end, the presence of pinning in polycrystalline or two-phase materials permits damage and softening to coexist in a positive shear-localizing feedback while also allowing for long-lived dormant weak zones.

#### *7.07.6.2.4 Summary thoughts on weakening and damage*

It is unlikely that any one shear-localizing mechanism will be the so-called magic bullet of plate boundary formation and plate generation. A distinct possibility may be that a combination of rheological mechanisms will be necessary. While brittle failure at shallow depths does not dictate the major weakening effect (since it is occurring in the weakest region of the lithosphere), shallow and intermediate-depth cracks sustained by water might help nucleate self-weakening zones at greater depth. The pervasiveness of mylonitic shear zones, however, is evidence that grain size-dependent damage mechanisms are acting across the deeper strongest part of the lithosphere, and these are likely the rate-limiting processes to generate plate boundaries. Grain damage with pinning in polycrystalline or two-phase mixtures appears to be a promising mechanism for such localization and boundary formation, although it requires further testing in global geodynamic models.

In the end, the simplest ingredients for plate generation might be damage and grain-size reduction (augmented by pinning, as mentioned earlier) in addition to melt-induced weakening at divergent and convergent zones. Although the effect of water on melt weakening is manifested by its reduction of melting temperature, its influence on grain damage is less obvious. One possibility is that water on Earth's surface promotes the carbon cycle and a cool surface, which thus impedes healing and advances the influence of damage and weakening; this hypothesis is central to one explanation for the dichotomy between Earth and Venus (Landuyt and Bercovici, 2009b) and for predicting the occurrence of plate tectonics on super-Earths (Foley et al., 2012), as will be discussed later (see **Section 7.07.7.3**).

## 7.07.7 Plate Generation on Earth and Other Planets

### 7.07.7.1 Origin of Plate Tectonics and Archean Tectonics

As discussed in **Section 7.07.2.2**, a critical moment in Earth's evolution is the initiation of plate tectonics itself. Although evidence for the first appearance of plate tectonics is sparse

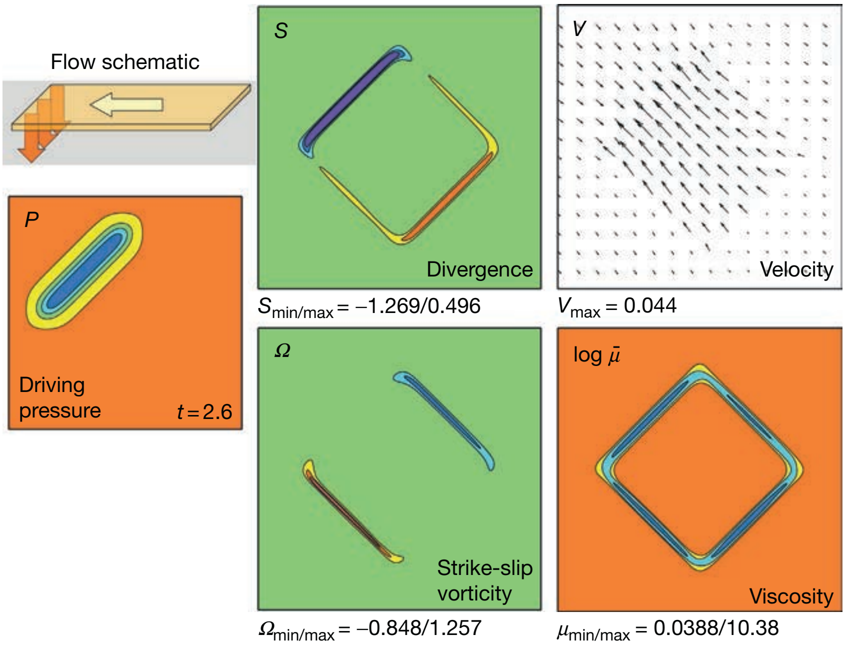


**Figure 31** A calculation of pressure-driven flow in a thin 2-D horizontal-layer model of the lithosphere, where the pressure low is akin to a single subduction zone (see schematic frame). The rheology of the layer is governed by the grain evolution, damage, and pinning model of Bercovici and Ricard (2012, 2013), which is also shown in **Figure 30**. In this case, the low-pressure zone $P$ is imposed and then rotated about a vertical axis by 90° three times (with roughly 10 My dimensional time between rotations to develop damaged weak zones) as an idealization of intermittent and chaotic subduction during the early Archean. The bands of damage induced by the pressure low from a previous orientation are long-lived, inherited, and amplified by the lithospheric flow of the next orientation, resulting in localized but passive bands of strike-slip vorticity $\Omega$ and positive divergence $S$ (red and yellow contours; convergence with $S<0$, indicated by blue contours, is actively driven by the pressure low). Thus, a complete plate arises with a contiguous weak plate boundary (indicated by viscosity $\overline{\mu}$) while only being driven by subduction, which is the final state shown (with final dimensionless time indicated on the $P$ frame). Dimensionless extrema for contours or vectors are indicated below each frame, save $P$, which is always between 0 and 1. This model is proposed to explain the emergence of plate tectonics in the Archean, from protosubduction 4Ga to global tectonics by ~3 Ga. Adapted from Bercovici D and Ricard Y (2014) Plate tectonics, damage and inheritance. *Nature* 506: 513–516. http://dx.doi.org/10.1038/nature13072.

and indirect, it appears that protosubduction existed roughly 4Ga, but global tectonics possibly did not become pervasive for a billion years later (see **Section 7.07.2.2**). Plate generation models have recently begun to explore this question of the onset of subduction and plate tectonics, and it remains a fruitful area of future research (e.g., Bercovici and Ricard, 2014; Korenaga, 2006, 2013; Moyen and van Hunen, 2012; Sizova et al., 2010; van Hunen and Moyen, 2012; van Hunen and van den Berg, 2008) (see also **Figure 31**).

The nature and evolution of the plate–mantle system during the Archean also remain enigmatic. Various lines of evidence imply that plate velocities and crustal production were slower in the Archean (see Korenaga, 2006). Thus, plate motions may have been impeded by greater lithospheric stability and strength through melting and production of buoyant crust and depleted lithosphere (Davies, 1992; van Hunen and van den Berg, 2008) and/or dehydration-induced stiffening and larger resistance to slab bending (Conrad and Hager, 2001; Korenaga, 2003, 2006). These stabilizing effects, however, have recently been questioned either because of greater upper-mantle depletion in the Archean that limited melting (Davies, 2006, 2007b) or because plate bending provides only minor resistance in convective circulation (Buffett and Becker, 2012; Davies, 2009; Leng and Zhong, 2010; see also **Section 7.07.5.5.3** and **Chapter 7.09**).

In the end, future plate generation theories that allow for thermal and petrologic evolution and inherited plate boundary weakness will be necessary to understand tectonic evolution and history.

### 7.07.7.2 Plates, Continents, and the Wilson Cycle

A major phase of petrologic evolution on Earth was the growth of continental crust through the Precambrian, which played a major role in the evolution of the plate–mantle system. In particular, with fully evolved continental crust, the dynamics of the mantle and lithosphere is influenced by the contrast between continents and oceans in myriad ways. First, while the ocean floor is continuously being created and destroyed, continents are essentially passive and permanent rafts floating at the surface of the Earth. In terms of basic physics, the continents impose a heterogeneous thermal boundary condition at the top of the mantle, which can significantly affect convective circulation (Kelly and Pal, 1978). Because of their thicker lithosphere, the heat flow across continents is around 65 mW m$^{-2}$, with values as low as 15 mW m$^{-2}$ over Precambrian areas (Pinet et al., 1991). These heat flow values include the large radiogenic contribution in continental crust, which suggests that the heat flow across the Moho in cratonic lithosphere is roughly an order of magnitude smaller than

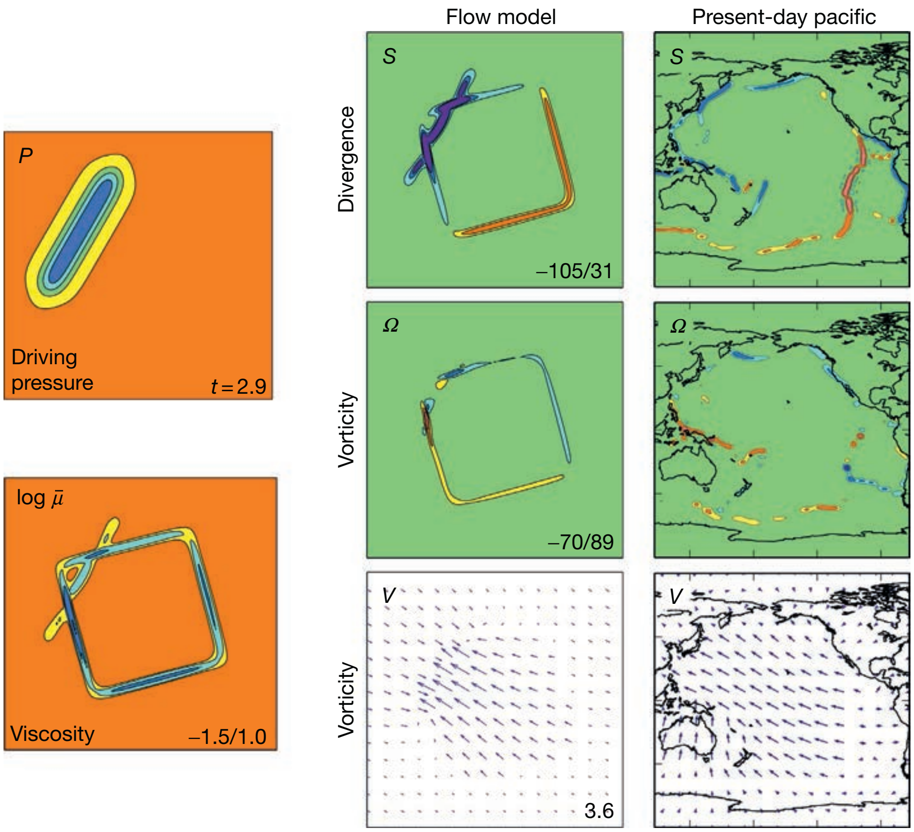


**Figure 32** A similar model calculation to that shown in **Figure 31**, but now an abstraction of the rotation of the Pacific Plate associated with the Emperor–Hawaiian bend 47 Ma. The initial condition is a platelike flow similar to that shown in **Figure 31** but with velocity oriented along azimuth W15N, similar to the Emperor seamount track. The driving pressure is then rotated 45 degrees to drive flow W60N, similar to the Hawaiian Islands track, which is the final state shown. The weakened damaged zones that determined the configuration of the plate before the rotation are inherited and maintained after rotation and create oblique subduction, divergence, and strike-slip boundaries, in addition to spalling of minor plates. Although the calculation is highly idealized, it has significant resemblance to the structure of the current-day Pacific Plate and minor Philippine Plate (right column). (Extrema of contours or vectors are indicated on each frame.) Adapted from Bercovici D and Ricard Y (2014) Plate tectonics, damage and inheritance. *Nature* 506: 513–516. http://dx.doi.org/10.1038/nature13072.

that across the seafloor, which is on average around 100 mW m$^{-2}$. This heterogeneity in heat flow has various consequences for plate tectonics.

Because the thick continental lithosphere acts as a partial insulator, the underlying mantle tends to be hotter. This thermal blanketing has been observed experimentally and numerically (Guillou and Jaupart, 1995; Lenardic et al., 2011). The temperature increase depends on the size of the continents (Grigne et al., 2007; Phillips and Coltice, 2010) and could reach anomalies of 100 K under supercontinents (Coltice et al., 2007). This effect causes large-scale convective instabilities, which in turn induce rapid drift of continental rafts and subsequent supercontinent reorganization. This mantle–continent interaction provides a mechanism for the Wilson cycle – wherein continental plates aggregate over cold downwellings, inhibit subduction, overheat the underlying mantle, and then fragment over the resulting hot upwelling mantle – and has been modeled by Gurnis (1988) with simple 2-D Cartesian geometry, as well as with 3-D spherical geometry with platelike rheology (e.g., Rolf et al., 2012). According to the models and scaling analysis of Zhong and Gurnis (1993), the periodicity of this cycle, 300–500 My, corresponds to observed Wilson cycle periods. The instability and dispersal of supercontinents above a hotter mantle may also be reinforced when the subcontinental mantle is isolated by a sheet of subducting slabs (Heron and Lowman, 2011; Yoshida, 2013). However, as discussed in Section 7.07.5.3, recent work suggests the supercontinent insulation effect may be insufficient to drive continent dispersal, which thus remains an open question.

The large contrast in strength between oceanic and continental lithospheres also tends to localize stresses at their junction and facilitate development of weak zones and new plate boundaries. Convection models with plastic lithospheres (see **Section 7.07.6.1**) allow for such weakening at larger yield stresses with continents present than without them; this allows for better agreement with the experimental values of yield stress (Rolf and Tackley, 2011). Although the effects of continent/ocean heterogeneities have not been considered in damage models, a similar weakening and localization near heterogeneities can be expected. The presence of continents likely also affects the seafloor age–area distribution (see **Section 7.07.2.1.3**). In particular, without continents, subduction ideally happens once it reaches a critical age (i.e., it is old, cold, and heavy enough to sink); but the imposition of continents could cause subduction to occur preferentially at passive margins that facilitated weakening and thus could be independent of seafloor age, which is in agreement with observations of present-day Earth (Becker et al., 2009; Coltice et al., 2012).

### 7.07.7.3 Plates, Climate, and Divergent Evolution of Planets

That Earth has plate tectonics but her ostensible twin Venus does not has been one of the key mysteries in the plate generation problem, and it has motivated much speculation about planetary conditions, including the requirement of liquid water, for plate tectonics to exist. While a traditional view has been that water lubricates plates by, for example, introduction of sediments at subduction zones or serpentinization along faults (e.g., Hilairet et al., 2007; Korenaga, 2007; Lenardic and Kaula, 1994; Tozer, 1985), the Earth's lithosphere might be as dry as that of Venus, because of dehydration melting at ridges (Hirth and Kohlstedt, 1996; see also **Section 7.07.6.2.2**). This paradox has prompted arguments that water's role is not in weakening the lithosphere but is instead in keeping Earth's surface temperature cool. In particular, Lenardic et al. (2008) posited that cooler surface temperatures on Earth lead to a more negatively buoyant top thermal boundary layer than on Venus; thus, Earth's lithospheric stress state is able to exceed its yield stress and fail, while Venus's lithosphere cannot. Alternatively, Landuyt and Bercovici (2009b) argued that surface temperature controls the competition between shear-localizing damage and healing (i.e., grain growth); that is, a cool surface retards healing and promotes damage and plate boundary formation, while a hot surface does the opposite and yields a stagnant lithosphere (**Figure 33**). These studies both suggest that Earth has plate tectonics because water drives the carbon cycle, which leads to a cool surface and the right conditions for plate tectonics, while Venus's loss of water and runaway greenhouse inhibits plate formation. However, this finding leads to the even deeper question of whether plate tectonics (which stabilizes a temperate climate) or a temperate climate (which is a necessary condition for tectonics) came first. Very recent coupled mantle-climate models suggest that the coupled feedbacks between tectonics, degassing, weathering, and greenhouse evolution occur simultaneously and can account for the divergent evolution between Earth and Venus (Driscoll and Bercovici, 2013).

### 7.07.7.4 Plates, Super-Earths, and Habitability

Plate tectonics is presumed to be a necessary condition for a temperate climate, by the carbon buffer and negative feedbacks associated with resurfacing and mineral exposure, erosion, weathering, and volcanism (Berner, 2004; Walker et al., 1981); the reciprocal dependence of plate tectonics on climate (**Section 7.07.7.3**) thus implies that a clement, habitable surface, and plate tectonics are mutually required. Plate tectonics may also be necessary for the existence of life by providing a source of thermodynamic disequilibrium through continuous recycling of the surface (e.g., Martin et al., 2008; Southam and Westall, 2007). The discovery of many terrestrial planets in other solar systems over the last 15 years (e.g., Charbonneau et al., 2009) has, therefore, emphasized the importance of understanding the conditions for plate tectonics as one

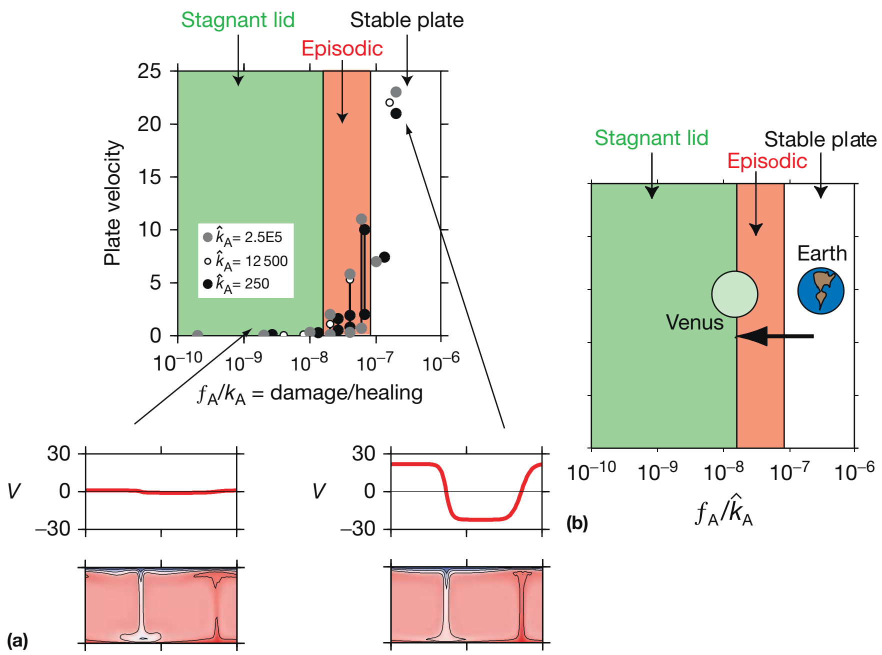


**Figure 33** Convection with damage – transition from stagnant, to episodic, to platelike as a function of the damage–healing ratio (a). Healing is a function of surface temperature, and thus, high temperatures enhance healing relative to damage, while low surface temperature is opposite. This ostensibly explains why Venus is stagnant or episodic and Earth has plate tectonics (b). Adapted from Landuyt W and Bercovici D (2009) Variations in planetary convection via the effect of climate on damage. *Earth and Planetary Science Letters* 277: 29–37.

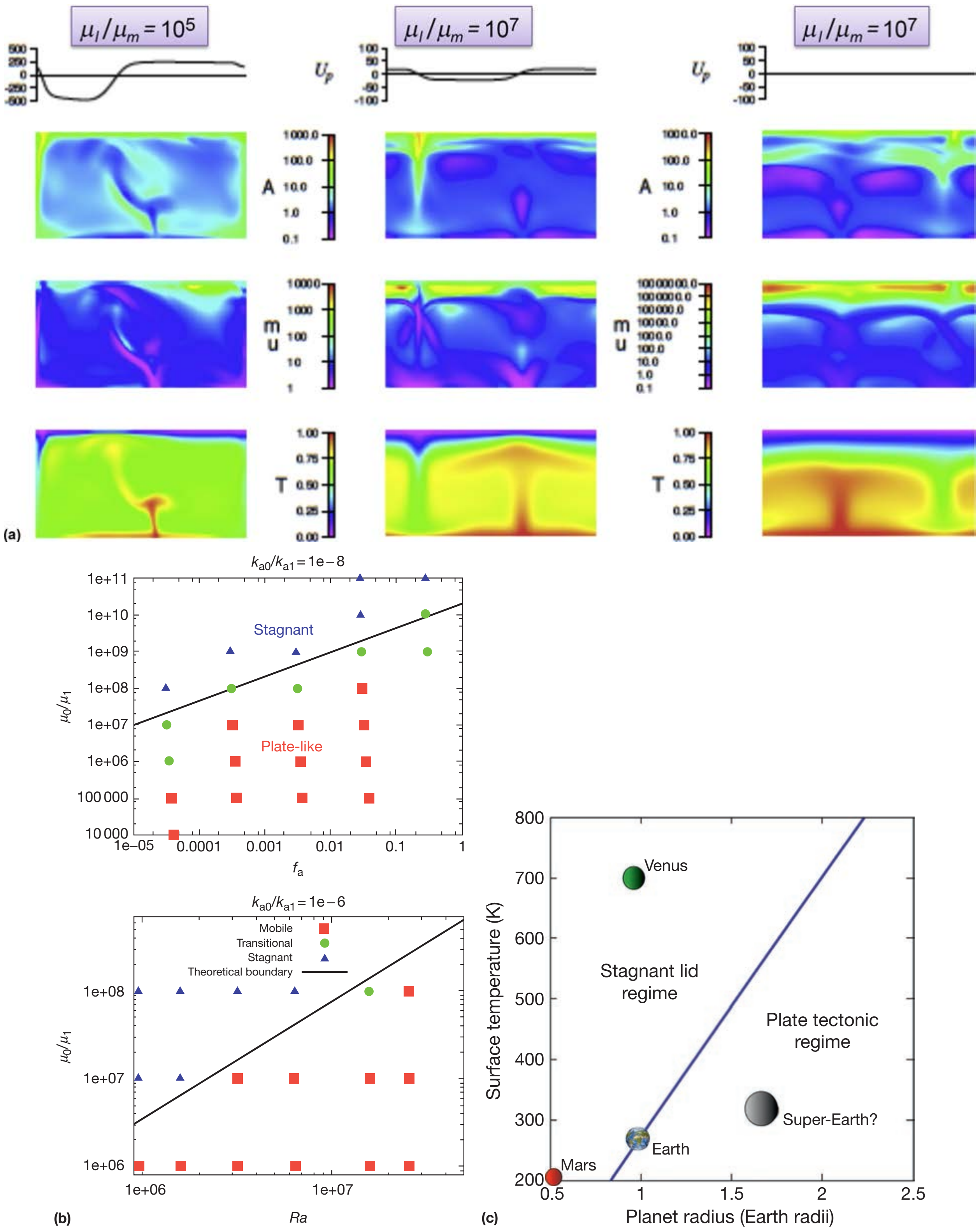


**Figure 34** Convection with damage: the transition from stagnant to platelike or mobile surface flow occurs at a critical lithosphere–mantle viscosity ratio $\mu_l/\mu_m$ (a). This ratio is itself a function of damage (for a given healing) and Rayleigh number (b) for which a scaling law for the transition can be inferred analytically. This can be compared to the predicted viscosity ratio of a planet with a certain size and internal and surface temperatures. Equivalence of these viscosity ratios occurs at a unique surface temperature for a given planet size (and internal temperature, not shown) and thus yields a phase diagram for planetary plate tectonics (c). Adapted from Foley BJ, Bercovici D, and Landuyt W (2012) The conditions for plate tectonics on super-earths: Inferences from convection models with damage. *Earth and Planetary Science Letters* 331–332: 281–290.

(although perhaps not a unique) requirement for liquid water and presumed habitability. The most readily available observation of terrestrial exoplanets is their mass, which has caused some debate as to whether size is more or less conducive to plate tectonics. Indeed, the first studies of this issue came to opposite conclusions, that is, plate tectonics on super-Earths is either inevitable (Valencia and O'Connell, 2009; Valencia et al., 2007) or impossible (O'Neill and Lenardic, 2007). More recent studies suggest that other factors such as surface temperature are equally or more important (Foley et al., 2012; Korenaga, 2010; van Heck and Tackley, 2011), which corresponds more closely to the Earth–Venus–Mars comparison (**Figure 34**). Overall, it appears that planet size is possibly more conducive to tectonics, depending on the surface conditions (Foley et al., 2012; Korenaga, 2010), interior composition and rheology (Tackley et al., 2013), and age in the planets thermal history (Lenardic and Crowley, 2012). However, this debate has highlighted the importance of understanding the physics of plate generation in order to predict how planetary conditions facilitate or inhibit plate-tectonic formation.

## 7.07.8 Closing and Future Directions

Although the theory of plate tectonics has provided one of the greatest predictive tools in the solid-Earth sciences, it is by no means a complete theory. Plate tectonics is a kinematic model in that it describes motions, but it does not involve dynamics, that is, either the forces or energy behind plate motions; nor does it explain the cause and generation of the plates themselves. In contrast, mantle convection theory describes and incorporates the essential dynamics and energy source for plate motions, but does not in itself predict the formation of the plates – with weak boundaries, strong plate interiors, asymmetrical subduction, passive spreading centers, sudden and sometimes global changes in plate motions, and toroidal motion. A theory of mantle convection that generates plates – in essence a unified theory of mantle dynamics and plate tectonics – remains one of the grand challenges of geodynamics.

Considerable progress has been made in the last 20 years on obtaining fluid mantle flow models that yield platelike behavior. The earlier successes come about by prescribing lithospheric weak zones and ad hoc rheologies (or rheologies like brittle failure that, while empirically based, are not applicable to the entire lithosphere) that yield more or less the correct behavior. While these ad hoc formulations gave important clues about what basic stress–strain rate laws allow platelike behavior, they did not elucidate the underlying physics leading to these rheologies or to plate generation.

More recent studies, in the last decade or so, have expanded our understanding of the physical and microscopic mechanisms behind shear localization, the depths and conditions at which these mechanisms occur, and their interaction with convective circulation. The areas of physics and chemistry involving melting, the role of water, fracture and void nucleation, and grain evolution are few examples of plate generation mechanisms that have been recently elucidated. However, much work remains to understand these processes, including how the thermal, chemical, and petrologic history of the Earth and other planets interacts with plate generation mechanisms to control tectonic and hence planet-system evolution. Moreover, observational, in particular seismic, data on the material properties and 3-D structure of plate boundaries (including ancient, dormant, active, and incipient ones) are of vital importance in constraining dynamic models and microscopic theories of plate boundary formation; for example, grain-size reduction or 'mylonitic' models of plate boundary formation are testable since they predict lack of lattice-preferred orientation and seismic anisotropy (which only occurs in conjunction with dislocation creep). As seismic coverage of the Earth continues to improve with the deployment of continental arrays (e.g., USArray) and ocean-bottom seismometers, along with more advanced technology such as receiver function techniques, the wealth of information will increase tremendously.

The theories of plate tectonics and mantle convection are far from being tried, true, and well-resolved models; indeed, they are still in their youth, and their successful unification will require years of ongoing research and advances in microscopic physics, continuum mechanics, and observational geophysics.

## References


Abbott PL (2011) *Natural Disasters*, 8th edn. New York: McGraw-Hill.

Ahmed O and Lenardic A (2010) Low viscosity channels and the stability of long wavelength convection. *Physics of the Earth and Planetary Interiors* 179(3–4): 122–126.

Ahrens TJ and Schubert G (1975a) Gabbro-eclogite reaction rate and its geophysical significance. *Reviews of Geophysics and Space Physics* 13: 383–400.

Ahrens TJ and Schubert G (1975b) Rapid formation of eclogite in a slightly wet mantle. *Earth and Planetary Science Letters* 27: 90–94.

Allégre CJ (1982) Chemical geodynamics. *Tectonophysics* 81(3–4): 109–132.

Argus DF and Gordon RG (1991) No-net-rotation model of current plate velocities incorporating plate motion model NUVEL-1. *Geophysical Research Letters* 18(11): 2039–2042.

Balachandar S, Yuen D, and Reuteler D (1995a) Localization of toroidal motion and shear heating in 3-D high Rayleigh number convection with temperature-dependent viscosity. *Geophysical Research Letters* 22: 477–480.

Balachandar S, Yuen D, Reuteler D, and Lauer G (1995b) Viscous dissipation in 3-dimensional convection with temperature-dependent viscosity. *Science* 267: 1150–1152.

Beaumont C (1976) The evolution of sedimentary basins on a viscoelastic lithosphere. *Geophysical Journal of the Royal Astronomical Society* 55: 471–497.

Becker T, Conrad C, Buffett B, and Müller R (2009) Past and present seafloor age distributions and the temporal evolution of plate tectonic heat transport. *Earth and Planetary Science Letters* 278: 233–242.

Bénard H (1900) Les tourbillons cellulaires dans une nappe liquide. *Revue générale des Sciences pures et appliquées* 11: 1261–1271, and 1309–1328.

Bénard H (1901) Les tourbillons cellulaires dans une nappe liquide transportant de la chaleur par convection en régime permanent. *Annales de Chimie et de Physique* 23: 62–144.

Bercovici D (1993) A simple model of plate generation from mantle flow. *Geophysical Journal International* 114: 635–650.

Bercovici D (1995a) On the purpose of toroidal flow in a convecting mantle. *Geophysical Research Letters* 22: 3107–3110.

Bercovici D (1995b) A source–sink model of the generation of plate tectonics from non-Newtonian mantle flow. *Journal of Geophysical Research* 100: 2013–2030.

Bercovici D (1996) Plate generation in a simple model of lithosphere–mantle flow with dynamic self-lubrication. *Earth and Planetary Science Letters* 144: 41–51.

Bercovici D (1998) Generation of plate tectonics from lithosphere-mantle flow and void-volatile self-lubrication. *Earth and Planetary Science Letters* 154: 139–151.

Bercovici D (2003) The generation of plate tectonics from mantle convection. *Earth and Planetary Science Letters* 205: 107–121.

Bercovici D (2007) Mantle dynamics, past, present and future: An overview. In: Bercovici D and Schubert G (Chief Editor) (eds.) *Treatise on Geophysics*. *Mantle Dynamics*, vol. 7, pp. 1–30. New York: Elsevier.

Bercovici D and Karato S (2003) Theoretical analysis of shear localization in the lithosphere. In: Karato S and Wenk H (eds.) *Reviews in Mineralogy and Geochemistry: Plastic Deformation of Minerals and Rocks*, vol. 51, pp. 387–420. Washington, DC: Mineralogical Society of America (ch. 13).

Bercovici D and Kelly A (1997) Nonlinear initiation of diapirs and plume heads. *Physics of the Earth and Planetary Interiors* 101: 119–130.

Bercovici D and Long MD (2014) Slab rollback instability and supercontinent dispersal. *Geophysical Research Letters* 41. http://dx.doi.org/10.1002/2014GL061251.

Bercovici D and Ricard Y (2003) Energetics of a two-phase model of lithospheric damage, shear localization and plate-boundary formation. *Geophysical Journal International* 152: 581–596.

Bercovici D and Ricard Y (2005) Tectonic plate generation and two-phase damage: Void growth versus grainsize reduction. *Journal of Geophysical Research* 110: B03401. http://dx.doi.org/10.1029/2004JB003181.

Bercovici D and Ricard Y (2012) Mechanisms for the generation of plate tectonics by two-phase grain-damage and pinning. *Physics of the Earth and Planetary Interiors* 202–203: 27–55.

Bercovici D and Ricard Y (2013) Generation of plate tectonics with two-phase grain-damage and pinning: Source–sink model and toroidal flow. *Earth and Planetary Science Letters* 365: 275–288.

Bercovici D and Ricard Y (2014) Plate tectonics, damage and inheritance. *Nature* 508: 513–516. http://dx.doi.org/10.1038/nature13072.

Bercovici D, Ricard Y, and Richards M (2000) The relation between mantle dynamics and plate tectonics: A primer. In: Richards MA, Gordon R, and van der Hilst R (eds.) *History and Dynamics of Global Plate Motions*. *Geophysical Monograph Series*, vol. 121, pp. 5–46. Washington, DC: American Geophysical Union.

Bercovici D, Ricard Y, and Schubert G (2001a) A two-phase model of compaction and damage: 1. General theory. *Journal of Geophysical Research* 106(B5): 8887–8906.

Bercovici D, Ricard Y, and Schubert G (2001b) A two-phase model of compaction and damage: 3. Applications to shear localization and plate boundary formation. *Journal of Geophysical Research* 106(B5): 8925–8940.

Bercovici D, Schubert G, and Glatzmaier G (1989a) Three-dimensional, spherical models of convection in the earth's mantle. *Science* 244: 950–955.

Bercovici D, Schubert G, and Glatzmaier G (1992) Three-dimensional, infinite Prandtl number, compressible convection in a basally heated spherical shell. *Journal of Fluid Mechanics* 239: 683–719.

Bercovici D, Schubert G, Glatzmaier G, and Zebib A (1989b) Three-dimensional thermal convection in a spherical shell. *Journal of Fluid Mechanics* 206: 75–104.

Bercovici D, Schubert G, and Ricard Y (2015) Abrupt tectonics and rapid slab detachment with grain damage. *Proceedings of the National Academy of Sciences*, http://dx.doi.org/10.1073/pnas.1415473112.

Berner R (2004) *The Phanerozoic Carbon Cycle*. Oxford: Oxford University Press.

Bird P (2003) An updated digital model of plate boundaries. *Geochemistry, Geophysics, Geosystems* 4(3): 1027. http://dx.doi.org/10.1029/2001GC000252.

Block M (1956) Surface tension as the cause for Bénard and surface deformation in a liquid film. *Nature* 178: 650–651.

Brady J (1995) Diffusion data for silicate minerals, glasses, and liquids. In: *Mineral Physics and Crystallography: A Handbook of Physical Constants*. *AGU Reference Shelf*, vol. 2, pp. 269–290. Washington, DC: American Geophysical Union.

Braun J, Chery J, Poliakov A, et al. (1999) A simple parameterization of strain localization in the ductile regime due to grain size reduction: A case study for olivine. *Journal of Geophysical Research* 104: 25167–25181.

Bridgman PW (1922) *Dimensional Analysis*. New Haven, CT: Yale University Press.

Brown M (2007) Metamorphic conditions in orogenic belts: A record of secular change. *International Geology Review* 49: 193–234.

Buffett BA and Becker TW (2012) Bending stress and dissipation in subducted lithosphere. *Journal of Geophysical Research – Solid Earth* 117. http://dxdoi.org/10.1029/2012JB009205.

Bunge H, Richards M, and Baumgardner J (1996) Effect of depth-dependent viscosity on the planform of mantle-convection. *Nature* 379: 436–438.

Bunge H, Richards M, and Baumgardner J (1997) A sensitivity study of 3-D spherical mantle convection at $10^8$ Rayleigh number: Effects of depth-dependent viscosity, heating mode, and an endothermic phase change. *Journal of Geophysical Research* 102: 11991–12007.

Busse F (1975) Patterns of convection in spherical shells. *Journal of Fluid Mechanics* 72: 67–85.

Busse F (1978) Non-linear properties of thermal convection. *Reports on Progress in Physics* 41: 1929–1967.

Busse F and Riahi N (1982) Patterns of convection in spherical shells: Part 2. *Journal of Fluid Mechanics* 123: 283–301.

Busse F and Riahi N (1988) Mixed-mode patterns of bifurcations from spherically symmetric basic states. *Nonlinearity* 1: 379–388.

Busse F and Whitehead J (1971) Instabilities of convection rolls in high Prandtl number fluid. *Journal of Fluid Mechanics* 47: 305–320.

Cadek O and Ricard Y (1992) Toroidal/poloidal energy partitioning and global lithospheric rotation during cenozoic time. *Earth and Planetary Science Letters* 109: 621–632.

Cadek O, Ricard Y, Martinec Z, and Matyska C (1993) Comparison between Newtonian and non-Newtonian flow driven by internal loads. *Geophysical Journal International* 112: 103–114.

Chandrasekhar S (1961) *Hydrodynamic and Hydromagnetic Stability*. New York: Oxford University Press.

Charbonneau D, Berta ZK, Irwin J, et al. (2009) A super-earth transiting a nearby low-mass star. *Nature* 462: 891–894.

Choblet G, Cadek O, Couturier F, and Dumoulin C (2007) OEDIPUS: A new tool to study the dynamics of planetary interiors. *Geophysical Journal International* 170(1): 9–30. http://dx.doi.org/10.1111/j.1365-246X.2007.03419.x.

Christensen U (1984a) Convection with pressure- and temperature-dependent non-Newtonian rheology. *Geophysical Journal of the Royal Astronomical Society* 77: 343–384.

Christensen U (1984b) Heat transport by variable-viscosity convection and implications for the earth's thermal evolution. *Physics of the Earth and Planetary Interiors* 35: 264–282.

Christensen U (1984c) Instability of a hot thermal boundary layer and initiation of thermo-chemical plumes. *Annales Geophysicae* 2: 311–314.

Christensen U and Harder H (1991) Three-dimensional convection with variable viscosity. *Geophysical Journal International* 104: 213–226.

Christensen U and Yuen D (1985) Layered convection induced by phase changes. *Journal of Geophysical Research* 90: 291–300.

Coltice N, Bertrand H, Rey P, Jourdan F, Phillips BR, and Ricard Y (2009) Global warming of the mantle beneath continents back to the Archaean. *Gondwana Research* 15(3–4, SI): 254–266.

Coltice N, Phillips BR, Bertrand H, Ricard Y, and Rey P (2007) Global warming of the mantle at the origin of flood basalts over supercontinents. *Geology* 35(5): 391–394.

Coltice N, Rolf T, Tackley PJ, and Labrosse S (2012) Dynamic causes of the relation between area and age of the ocean floor. *Science* 336(6079): 335–338. http://www.sciencemag.org/content/336/6079/335.abstract.

Condie K and Kroner A (2008) When did plate tectonics begin? Evidence from the geologic record. In: Condie K and Pease V (eds.) *When Did Plate Tectonics Begin on Planet Earth?* pp. 281–294. Boulder, CO: Geological Society of America, Special Paper 440.

Connerney JEP, Acuña MH, Ness NF, et al. (2005) Tectonic implications of mars crustal magnetism. *Proceedings of the National Academy of Sciences of the United States of America* 102(42): 14970–14975. http://www.pnas.org/content/102/42/14970.abstract.

Connerney JEP, Acuña MH, Wasilewski PJ, et al. (1999) Magnetic lineations in the ancient crust of mars. *Science* 284(5415): 794–798. http://www.sciencemag.org/content/284/5415/794.abstract.

Conrad C and Hager B (2001) Mantle convection with strong subduction zones. *Geophysical Journal International* 144: 271–288.

Corrieu V, Ricard Y, and Froidevaux C (1994) Radial viscosity of the earth deduced from mantle tomography. *Physics of the Earth and Planetary Interiors* 84: 3–13.

Crameri F, Tackley PJ, Meilick I, Gerya TV, and Kaus BJP (2012) A free plate surface and weak oceanic crust produce single-sided subduction on earth. *Geophysical Research Letters* 39(3: L03306). http://dx.doi.org/10.1029/2011GL050046.

Creager K and Jordan T (1984) Slab penetration into the lower mantle. *Journal of Geophysical Research* 89: 3031–3049.

Davies G (1980) Thermal histories of convective earth models and constraints on radiogenic heat production in the earth. *Journal of Geophysical Research* 85: 2517–2530.

Davies G (1988a) Ocean bathymetry and mantle convection: 1. Large-scale flow and hotspots. *Journal of Geophysical Research* 93: 10467–10480.

Davies G (1988b) Ocean bathymetry and mantle convection: 2. Small scale flow. *Journal of Geophysical Research* 93: 10481–10488.

Davies G (1988c) The role of the lithosphere in mantle convection. *Journal of Geophysical Research* 93: 10451–10466.

Davies G (1992) On the emergence of plate tectonics. *Geology* 20: 963–966.

Davies GF (2006) Gravitational depletion of the early earth's upper mantle and the viability of early plate tectonics. *Earth and Planetary Science Letters* 243(3–4): 376–382, http://www.sciencedirect.com/science/article/pii/S0012821X06001051.

Davies G (2007a) Thermal evolution of the earth. In: Stevenson D and Schubert G (Chief Editor) (eds.) *Treatise on Geophysics*. *Evolution of the Earth*, vol. 9, pp. 197–216. Amsterdam: Elsevier.

Davies GF (2007b) Controls on density stratification in the early mantle. *Geochemistry, Geophysics, Geosystems* 8(4). http://dx.doi.org/10.1029/2006GC001414.

Davies GF (2009) Effect of plate bending on the Urey ratio and the thermal evolution of the mantle. *Earth and Planetary Science Letters* 287(3–4): 513–518. http://www.sciencedirect.com/science/article/pii/S0012821X09005238.

Davies G and Richards M (1992) Mantle convection. *Journal of Geology* 100: 151–206.

De Bresser J, Peach C, Reijs J, and Spiers C (1998) On dynamic recrystallization during solid state flow: Effects of stress and temperature. *Geophysical Research Letters* 25: 3457–3460.

De Bresser J, ter Heege J, and Spiers C (2001) Grain size reduction by dynamic recrystallization: Can it result in major rheological weakening? *International Journal of Earth Sciences* 90: 28–45.

Derby B and Ashby M (1987) On dynamic recrystallization. *Scripta Metallurgica* 21: 879–884.

Dijkstra AH, Drury MR, Vissers RLM, Newman J, and Van Roermund HLM (2004) Shear zones in the upper mantle: Evidence from alpine- and ophiolite-type peridotite massifs. *Geological Society, London, Special Publications* 224(1): 11–24. http://sp.lyellcollection.org/content/224/1/11.abstract.

Doherty RD, Hughes DA, Humphreys FJ, et al. (1997) Current issues in recrystallization: A review. *Materials Science and Engineering A* 238(2): 219–274.

Driscoll P and Bercovici D (2013) Divergent evolution of Earth and Venus: Influence of degassing, tectonics, and magnetic fields. *Icarus* 226: 1447–1464. http://www.sciencedirect.com/science/article/pii/S0019103513003266.

Duffield W (1972) A naturally occurring model of global plate tectonics. *Journal of Geophysical Research* 77: 2543–2555.

Dumoulin C, Bercovici D, and Wessel P (1998) A continuous plate-tectonic model using geophysical data to estimate plate margin widths, with a seismicity based example. *Geophysical Journal International* 133: 379–389.

Duncan R and Richards M (1991) Hotspots, mantle plumes, flood basalts and true polar wander. *Reviews of Geophysics* 29: 31–50.

Escartin J, Hirth G, and Evans B (2001) Strength of slightly serpentinized peridotites: Implications for the tectonics of oceanic lithosphere. *Geology* 29: 1023–1026.

Etheridge M and Wilkie J (1979) Grainsize reduction, grain boundary sliding and the flow strength of mylonites. *Tectonophysics* 58(1–2): 159–178.

Evans DA (2009) The palaeomagnetically viable, long-lived and all-inclusive Rodinia supercontinent reconstruction. *Geological Society, London, Special Publications* 327: 371–404.

Evans B and Kohlstedt D (1995) Rheology of rocks. In: Ahrens TJ (ed.) *Rock Physics and Phase Relations: A Handbook of Physical Constants*. *AGU Reference Shelf*, vol. 3, pp. 148–165. Washington, DC: American Geophysical Union.

Evans DA and Mitchell RN (2011) Assembly and breakup of the core of Paleoproterozoic–Mesoproterozoic supercontinent Nuna. *Geology* 39(5): 443–446. http://geology.gsapubs.org/content/39/5/443.abstract.

Evans DA and Pisarevsky S (2008) Plate tectonics on the early earth? Weighing the paleomagnetic evidence. In: Condie K and Pease V (eds.) *When Did Plate Tectonics Begin on Planet Earth?* pp. 249–263. Boulder, CO: Geological Society of America, Special Paper 440.

Faccenda M, Gerya TV, and Burlini L (2009) Deep slab hydration induced by bending-related variations in tectonic pressure. *Nature Geoscience* 2(11): 790–793. http://dx.doi.org/10.1038/ngeo656.

Faccenda M, Gerya TV, Mancktelow NS, and Moresi L (2012) Fluid flow during slab unbending and dehydration: Implications for intermediate-depth seismicity, slab weakening and deep water recycling. *Geochemistry, Geophysics, Geosystems* 13: Q01010.

Fleitout L and Froidevaux C (1980) Thermal and mechanical evolution of shear zones. *Journal of Structural Geology* 2: 159–164.

Foley B and Becker T (2009) Generation of plate-like behavior and mantle heterogeneity from a spherical, visco-plastic convection model. *Geochemistry, Geophysics, Geosystems* 10(8): Q08001. http://dx.doi.org/10.1029/2009GC002378.

Foley BJ, Bercovici D, and Landuyt W (2012) The conditions for plate tectonics on super-earths: Inferences from convection models with damage. *Earth and Planetary Science Letters* 331–332: 281–290.

Forsyth D, Scheirer D, Webb S, et al. (1998) Imaging the deep seismic structure beneath a mid-ocean ridge: The melt experiment. *Science* 280: 1215–1218.

Forsyth D and Uyeda S (1975) On the relative importance of the driving forces of plate motion. *Geophysical Journal of the Royal Astronomical Society* 43: 163–200.

Forte A and Peltier W (1987) Plate tectonics and aspherical earth structure: The importance of poloidal–toroidal coupling. *Journal of Geophysical Research* 92: 3645–3679.

Fukao Y, Obayashi M, Inoue H, and Nenbai M (1992) Subducting slabs stagnant in the mantle transition zone. *Journal of Geophysical Research – Solid Earth* 97(B4): 4809–4822.

Furbish D (1997) *Fluid Physics in Geology*. New York: Oxford University Press.

Furusho M and Kanagawa K (1999) Reaction induced strain localization in a lherzolite mylonite from the Hidaka metamorphic belt of central Hokkaido, Japan. *Tectonophysics* 313: 411–432.

Gable C, O'Connell R, and Travis B (1991) Convection in three dimensions with surface plates: Generation of toroidal flow. *Journal of Geophysical Research* 96: 8391–8405.

Gerya T (2010) Dynamical instability produces transform faults at mid-ocean ridges. *Science* 329(5995): 1047–1050.

Gerya TV (2013) Three-dimensional thermomechanical modeling of oceanic spreading initiation and evolution. *Physics of the Earth and Planetary Interiors* 214: 35–52.http://www.sciencedirect.com/science/article/pii/S0031920112001835.

Gerya TV, Connolly JA, and Yuen DA (2008) Why is terrestrial subduction one-sided? *Geology* 36(1): 43–46.

Giannandrea E and Christensen U (1993) Variable viscosity convection experiments with a stress-free upper boundary and implications for the heat transport in the earth's mantle. *Physics of the Earth and Planetary Interiors* 78: 139–152.

Glatzmaier G (1988) Numerical simulations of mantle convection: Time-dependent, three-dimensional, compressible, spherical shell. *Geophysical and Astrophysical Fluid Dynamics* 43: 223–264.

Glatzmaier G, Schubert G, and Bercovici D (1990) Chaotic subduction-like downflows in a spherical model of convection in the earth's mantle. *Nature* 347: 274–277.

Gordon R, DeMets C, and Royer J (1998) Evidence for long-term diffuse deformation of the lithosphere of the equatorial Indian ocean. *Nature* 395: 370–374.

Grand S (1994) Mantle shear structure beneath the Americas and surrounding oceans. *Journal of Geophysical Research* 99: 11591–11621.

Grand S, van der Hilst R, and Widiyantoro S (1997) Global seismic tomography: A snapshot of convection in the earth. *GSA Today* 7: 1–7.

Griffith A (1921) The phenomenon of rupture and flow in solids. *Philosophical Transactions of the Royal Society of London, Series A* 221: 163–198.

Grigne C, Labrosse S, and Tackley PJ (2007) Convection under a lid of finite conductivity: Heat flux scaling and application to continents. *Journal of Geophysical Research – Solid Earth* 112(B8).

Guillou L and Jaupart C (1995) On the effect of continents on mantle convection. *Journal of Geophysical Research – Solid Earth* 100(B12): 24217–24238.

Guillou L, Mareschal J, Jaupart C, Gariépy C, Bienfait G, and Lapointe R (1994) Heat flow, gravity, and structure of the Abitibi belt, superior province, Canada: Implications for mantle heat flow. *Earth and Planetary Science Letters* 122: 103–123.

Gurnis M (1988) Large-scale mantle convection and the aggregation and dispersal of supercontinents. *Nature* 332(6166): 695–699.

Gurnis M and Hager B (1988) Controls of the structure of subducted slabs. *Nature* 335: 317–321.

Gurnis M, Hall C, and Lavier L (2004) Evolving force balance during incipient subduction. *Geochemistry, Geophysics, Geosystems* 5(7).

Gurnis M, Zhong S, and Toth J (2000) On the competing roles of fault reactivation and brittle failure in generating plate tectonics from mantle convection. In: Richards MA, Gordon R, and van der Hilst R (eds.) *History and Dynamics of Global Plate Motions*. *Geophysical Monograph Series*, vol. 121, pp. 73–94. Washington, DC: American Geophysical Union.

Hager B (1984) Subducted slabs and the geoid: Constraints on mantle rheology and flow. *Journal of Geophysical Research* 89: 6003–6015.

Hager B and O'Connell R (1978) Subduction zone dip angles and flow driven by plate motion. *Tectonophysics* 50: 111–133.

Hager B and O'Connell R (1979) Kinematic models of large-scale flow in the earth's mantle. *Journal of Geophysical Research* 84: 1031–1048.

Hager B and O'Connell R (1981) A simple global model of plate dynamics and mantle convection. *Journal of Geophysical Research* 86: 4843–4867.

Hales A (1936) Convection currents in the Earth. *Monthly Notices of the Royal Astronomical Society, Geophysical Supplement* 3: 372–379.

Hall CE, Gurnis M, Sdrolias M, Lavier LL, and Mueller RD (2003) Catastrophic initiation of subduction following forced convergence across fracture zones. *Earth and Planetary Science Letters* 212: 15–30.

Hallam A (1987) Alfred Wegener and the hypothesis of continental drift. In: *Scientific Genius and Creativity: Readings from 'Scientific American' (Reprinted from* Scientific American*, February, 1975.)*, pp. 77–85. New York: W.H. Freeman & Co.

Hamano K, Abe Y, and Genda H (2013) Emergence of two types of terrestrial planet on solidification of magma ocean. *Nature* 497(7451): 607–610. http://dx.doi.org/10.1038/nature12163.

Hamilton WB (1998) Archean tectonics and magmatism. *International Geology Review* 40: 1–39.

Hansen LN, Zimmerman ME, and Kohlstedt DL (2012) The influence of microstructure on deformation of olivine in the grain-boundary sliding regime. *Journal of Geophysical Research* 117: B09201.

Harrison TM, Blichert-Toft J, Muller W, Albarede F, Holden P, and Mojzsis SJ (2005) Heterogeneous Hadean Hafnium: Evidence of continental crust at 4.4 to 4.5 Ga. *Science* 310(5756): 1947–1950.

Heron PJ and Lowman JP (2011) The effects of supercontinent size and thermal insulation on the formation of mantle plumes. *Tectonophysics* 510(1–2): 28–38.

Herwegh M, Linckens J, Ebert A, Berger A, and Brodhag S (2011) The role of second phases for controlling microstructural evolution in polymineralic rocks: A review. *Journal of Structural Geology* 33(12): 1728–1750.

Hess H (1962) History of ocean basins. In: Engeln A, James H, and Leonard B (eds.) *Petrologic Studies – A Volume in Honor of A.F. Buddington*, pp. 599–620. New York: Geological Society America.

Hey RN, Johnson PD, Martinez F, et al. (1995) Plate boundary reorganization at a large-offset, rapidly propagating rift. *Nature* 378(6553): 167–170. http://dx.doi.org/10.1038/378167a0.

Hey R and Wilson D (1982) Propagating rift explanation for the tectonic evolution of the northeast pacific—The pseudo-movie. *Earth and Planetary Science Letters* 58(2): 167–184. http://www.sciencedirect.com/science/article/pii/0012821X82901923.

Hilairet N, Reynard B, Wang Y, et al. (2007) High-pressure creep of serpentine, interseismic deformation, and initiation of subduction. *Science* 318(5858): 1910–1913.

Hilde T, Uyeda S, and Kroenke L (1977) Evolution of the western pacific and its margins. *Tectonophysics* 38: 145–165.

Hirth G and Kohlstedt D (1996) Water in the oceanic upper mantle: Implications for rheology, melt extraction and the evolution of the lithosphere. *Earth and Planetary Science Letters* 144: 93–108.

Hirth G and Kohlstedt D (2003) Rheology of the upper mantle and the mantle wedge: A view from the experimentalists. In: Eiler J (ed.) *Subduction Factor Monograph*, vol. 138, pp. 83–105. Washington, DC: American Geophysical Union.

Hofmann A (1997) Mantle geochemistry: The message from oceanic volcanism. *Nature* 385: 219–228.

Holmes A (1931) Radioactivity and earth movements. *Geological Society of Glasgow, Transactions* 18: 559–606.

Honda S, Yuen D, Balachandar S, and Reuteler D (1993) Three-dimensional instabilities of mantle convection with multiple phase transitions. *Science* 259: 1308–1311.

Hopkins MD, Harrison TM, and Manning CE (2010) Constraints on hadean geodynamics from mineral inclusions in >4 Ga zircons. *Earth and Planetary Science Letters* 298(3–4): 367–376.

Huang J and Zhong S (2005) Sublithospheric small-scale convection and its implications for the residual topography at old ocean basins and the plate model. *Journal of Geophysical Research* 110: B05404.

Ildefonse B, Blackman D, John B, et al. (2007) Oceanic core complexes and crustal accretion at slow-spreading ridges. *Geology* 35(7): 623–626. http://geology.gsapubs.org/content/35/7/623.abstract.

Ito E, Akaogi M, Topor L, and Navrotsky A (1990) Negative pressure–temperature slopes for reactions forming $MgSiO_3$ perovskite from calorimetry. *Science* 249: 1275–1278.

Ito K and Kennedy GC (1971) An experimental study of the basalt-garnet granulite–eclogite transition. *The Structure and Physical Properties of the Earth's Crust*. *Geophysical Monograph*, vol. 14, pp. 303–314. Washington, DC: American Geophysical Union.

Jarvis G and McKenzie D (1980) Convection in a compressible fluid with infinite Prandtl number. *Journal of Fluid Mechanics* 96: 515–583.

Jaupart C, Labrosse S, and Mareschal J-C (2007) Temperatures, heat and energy in the mantle of the earth. In: Bercovici D and Schubert G (Chief Editor) (eds.) *Treatise on Geophysics*. *Mantle Dynamics*, vol. 7, pp. 253–303. New York: Elsevier.

Jellinek A and Manga M (2004) Links between long-lived hotspots, mantle plumes, D″ and plate tectonics. *Reviews of Geophysics* 42(3). http://dx.doi.org/10.1029/2003RG000144.

Jenner F, Bennett V, Yaxley G, Friend C, and Nebel O (2013) Eoarchean within-plate basalts from southwest Greenland. *Geology* 41(3): 327–330.

Jin D, Karato S, and Obata M (1998) Mechanisms of shear localization in the continental lithosphere: Inference from the deformation microstructures of peridotites from the Ivrea zone, northwestern Italy. *Journal of Structural Geology* 20: 195–209.

Kameyama M, Yuen D, and Fujimoto H (1997) The interaction of viscous heating with grain-size dependent rheology in the formation of localized slip zones. *Geophysical Research Letters* 24: 2523–2526.

Kaminski E and Ribe N (2001) A kinematic model for recrystallization and texture development in olivine polycrystals. *Earth and Planetary Science Letters* 189(3–4): 253–267. http://www.sciencedirect.com/science/article/pii/S0012821X01003569.

Karato S (1989) Grain growth kinetics in olivine aggregates. *Tectonophysics* 168: 255–273.

Karato S (2008) *Deformation of Earth Materials: An Introduction to the Rheology of Solid Earth*. New York: Cambridge University Press.

Karato S, Toriumi M, and Fujii T (1980) Dynamic recrystallization of olivine single crystals during high temperature creep. *Geophysical Research Letters* 7: 649–652.

Karato S and Wu P (1993) Rheology of the upper mantle: A synthesis. *Science* 260: 771–778.

Katz RF (2008) Magma dynamics with the enthalpy method: Benchmark solutions and magmatic focusing at mid-ocean ridges. *Journal of Petrology* 49(12): 2099–2121.

Kaula W (1980) Material properties for mantle convection consistent with observed surface fields. *Journal of Geophysical Research* 85: 7031–7044.

Kelly R and Pal D (1978) Thermal-convection with spatially periodic boundary-conditions – Resonant wavelength excitation. *Journal of Fluid Mechanics* 86: 433–456.

Kemp D and Stevenson D (1996) A tensile flexural model for the initiation of subduction. *Geophysical Journal International* 125: 73–94.

Kennet B and Engdahl E (1991) Travel times for global earthquake location and phase identification. *Geophysical Journal International* 105: 429–465.

King S (1995) The viscosity structure of the mantle. In: *Reviews of Geophysics (Supplement): U.S. Quadrennial Report to the IUGG 1991-1994*, pp. 11–17. Washington, DC: American Geophysical Union.

King S (2007) Mantle downwellings and the fate of subducting slabs: Constraints from seismology, geoid, topography, geochemistry, and petrology. In: Bercovici D and Schubert G (Chief Editor) (eds.) *Treatise on Geophysics*. *Mantle Dynamics*, vol. 7, pp. 325–370. New York: Elsevier.

King S, Gable C, and Weinstein S (1991) Models of convection driven plates: A comparison of methods and results. *Geophysical Journal International* 109: 481–487.

King S and Hager B (1990) The relationship between plate velocity and trench viscosity in Newtonian and power-law subduction calculations. *Geophysical Research Letters* 17: 2409–2412.

King SD, Lowman JP, and Gable CW (2002) Episodic tectonic plate reorganizations driven by mantle convection. *Earth and Planetary Science Letters* 203(1): 83–91.

Kohlstedt D, Evans B, and Mackwell S (1995) Strength of the lithosphere: Constraints imposed by laboratory experiments. *Journal of Geophysical Research* 100: 17587–17602.

Korenaga J (2003) Energetics of mantle convection and the fate of fossil heat. *Geophysical Research Letters* 30(8). http://dx.doi.org/10.1029/2003GL016982.

Korenaga J (2006) Archean geodynamics and the thermal evolution of earth. In: Benn K, Mareschal J-C, and Condie K (eds.) *Archean Geodynamics and Environments*. *AGU Geophysical Monograph Series*, vol. 164, pp. 7–32. Washington, DC: American Geophysical Union.

Korenaga J (2007) Thermal cracking and the deep hydration of oceanic lithosphere: A key to the generation of plate tectonics? *Journal of Geophysical Research* 112. http://dx.doi.org/10.1029/2006JB004502.

Korenaga J (2008) Urey ratio and the structure and evolution of earth's mantle. *Reviews of Geophysics* 46: RG2007. http://dx.doi.org/10.1029/2007RG000241.

Korenaga J (2010) On the likelihood of plate tectonics on super-earths: Does size matter? *Astrophysical Journal Letters* 725(1): L43–L46.

Korenaga J (2013) Initiation and evolution of plate tectonics on earth: Theories and observations. *Annual Review of Earth and Planetary Sciences* 41: 117–151.

Labrosse S (2002) Hotspots, mantle plumes and core heat loss. *Earth and Planetary Science Letters* 199(1–2): 147–156. http://www.sciencedirect.com/science/article/pii/S0012821X0200537X.

Lachenbruch A (1976) Dynamics of a passive spreading center. *Journal of Geophysical Research* 81: 1883–1902.

Lachenbruch A and Sass J (1980) Heat flow and energetics of the San Andreas fault zone. *Technical Report 80-625*, U.S. Geological Survey.

Landuyt W and Bercovici D (2009a) Formation and structure of lithospheric shear zones with damage. *Physics of the Earth and Planetary Interiors* 175: 115–126.

Landuyt W and Bercovici D (2009b) Variations in planetary convection via the effect of climate on damage. *Earth and Planetary Science Letters* 277: 29–37.

Landuyt W, Bercovici D, and Ricard Y (2008) Plate generation and two-phase damage theory in a model of mantle convection. *Geophysical Journal International* 174: 1065–1080.
Lay T, Hernlund J, and Buffett BA (2008) Core–mantle boundary heat flow. *Nature Geoscience* 1(1): 25–32. http://dx.doi.org/10.1038/ngeo.2007.44.
Le Pichon X (1968) Sea-floor spreading and continental drift. *Journal of Geophysical Research* 73(12): 3661–3697. http://dx.doi.org/10.1029/JB073i012p03661.
Lebrun J-F, Lamarche G, and Collot J-Y (2003) Subduction initiation at a strike-slip plate boundary: The cenozoic pacific-Australian plate boundary, south of New Zealand. *Journal of Geophysical Research* 108: 2453. http://dx.doi.org/10.1029/2002JB002041, B9.
Lebrun T, Massol H, Chassefière E, et al. (2013) Thermal evolution of an early magma ocean in interaction with the atmosphere. *Journal of Geophysical Research, Planets* 118(6): 1155–1176. http://dx.doi.org/10.1002/jgre.20068.
Lee K, Jiang Z, and Karato S (2002) A scanning electron microscope study of effects of dynamic recrystallization on the lattice preferred orientation in olivine. *Tectonophysics* 351: 331–341.
Lee C-TA, Lenardic A, Cooper CM, Niu F, and Levander A (2005) The role of chemical boundary layers in regulating the thickness of continental and oceanic thermal boundary layers. *Earth and Planetary Science Letters* 230(3–4): 379–395, http://www.sciencedirect.com/science/article/pii/S0012821X04007022.
Lenardic A and Crowley JW (2012) On the notion of well-defined tectonic regimes for terrestrial planets in this solar system and others. *The Astrophysical Journal* 755(2): 132. http://stacks.iop.org/0004-637X/755/i=2/a=132.
Lenardic A, Jellinek M, and Moresi L-N (2008) A climate change induced transition in the tectonic style of a terrestrial planet. *Earth and Planetary Science Letters* 271: 34–42.
Lenardic A and Kaula W (1994) Self-lubricated mantle convection: Two-dimensional models. *Geophysical Research Letters* 21: 1707–1710.
Lenardic A and Kaula W (1996) Near surface thermal/chemical boundary layer convection at infinite Prandtl number: Two-dimensional numerical experiments. *Geophysical Journal International* 126: 689–711.
Lenardic A, Moresi LN, Jellinek AM, and Manga M (2005) Continental insulation, mantle cooling, and the surface area of oceans and continents. *Earth and Planetary Science Letters* 234(3–4): 317–333.
Lenardic A, Moresi L, Jellinek AM, O'Neill CJ, Cooper CM, and Lee CT (2011) Continents, supercontinents, mantle thermal mixing, and mantle thermal isolation: Theory, numerical simulations, and laboratory experiments. *Geochemistry, Geophysics, Geosystems* 12. http://dxdoi.org/10.1029/2011GC003663.
Lenardic A, Richards MA, and Busse FH (2006) Depth-dependent rheology and the horizontal length scale of mantle convection. *Journal of Geophysical Research* 111: B07404. http://dx.doi.org/10.1029/2005JB003639.
Leng W and Zhong S (2010) Constraints on viscous dissipation of plate bending from compressible mantle convection. *Earth and Planetary Science Letters* 297(1–2): 154–164. http://www.sciencedirect.com/science/article/pii/S0012821X10003900.
Lewis C (2002) Arthur Holmes: An ingenious geoscientist. *GSA Today* 12(3): 16–17.
Linckens J, Herwegh M, Müntener O, and Mercolli I (2011) Evolution of a polymineralic mantle shear zone and the role of second phases in the localization of deformation. *Journal of Geophysical Research* 116: B06210, 21 pp.
Lister CRB (1972) On the thermal balance of a mid-ocean ridge. *Geophysical Journal of the Royal Astronomical Society* 26(5): 515–535. http://dx.doi.org/10.1111/j.1365-246X.1972.tb05766.x.
Lithgow-Bertelloni C and Richards M (1995) Cenozoic plate driving forces. *Geophysical Research Letters* 22: 1317–1320.
Lithgow-Bertelloni C and Richards MA (1998) Dynamics of cenozoic and mesozoic plate motions. *Reviews of Geophysics* 36: 27–78.
Lithgow-Bertelloni C, Richards M, Ricard Y, O'Connell R, and Engebretson D (1993) Toroidal–poloidal partitioning of plate motions since 120 MA. *Geophysical Research Letters* 20: 375–378.
Lithgow-Bertelloni C and Silver P (1998) Dynamic topography, plate driving forces and the African superswell. *Nature* 395: 269–272.
Liu L (1979) Phase transformations and the constitution of the deep mantle. In: McElhinny M (ed.) *Structure and Evolution Earth: Its Origins*, pp. 177–202. San Diego, CA: Academic Press.
Long MD and Becker T (2010) Mantle dynamics and seismic anisotropy. *Earth and Planetary Science Letters* 297(3–4): 341–354.
Long MD and Silver PG (2008) The subduction zone flow field from seismic anisotropy: A global view. *Science* 319(5861): 315–318. http://www.sciencemag.org/content/319/5861/315.abstract.
Lowman J (2011) Mantle convection models featuring plate tectonic behavior: An overview of methods and progress. *Tectonophysics* 510(1): 1–16.
Lowman J and Jarvis G (1996) Continental collisions in wide aspect ratio and high Rayleigh number two-dimensional mantle convection models. *Journal of Geophysical Research* 101(B11): 25485–25497.
Lowman J, King S, and Gable C (2003) The role of the heating mode of the mantle in periodic reorganizations of the plate velocity field. *Geophysical Journal International* 152: 455–467.
Machetel P and Weber P (1991) Intermittent layered convection in a model mantle with an endothermic phase change at 670 km. *Nature* 350: 55–57.
Malvern L (1969) *Introduction to the Mechanics of a Continuous Medium*. Englewood Cliffs, NJ: Prentice-Hall.
Martin W, Baross J, Kelley D, and Russell MJ (2008) Hydrothermal vents and the origin of life. *Nature Reviews Microbiology* 6(11): 805–814.
McKenzie D (1981) The variation of temperature with time and hydrocarbon maturation in sedimentary basins formed by extension. *Earth and Planetary Science Letters* 55(1): 87–98.
McKenzie D and Parker R (1967) The north pacific: An example of tectonics on a sphere. *Nature* 216: 1276–1280.
Mehl L and Hirth G (2008) Plagioclase preferred orientation in layered mylonites: Evaluation of flow laws for the lower crust. *Journal of Geophysical Research* 113: B05202. http://dx.doi.org/10.1029/2007JB005075.
Mojzsis SJ, Harrison TM, and Pidgeon RT (2001) Oxygen-isotope evidence from ancient zircons for liquid water at the Earth's surface 4,300 Myr ago. *Nature* 409(6817): 178–181. http://dx.doi.org/10.1038/35051557.
Molnar P and Stock J (1987) Relative motions of hotspots in the pacific, Atlantic and Indian oceans since late cretaceous time. *Nature* 327(6123): 587–591.
Monnereau M and Quéré S (2001) Spherical shell models of mantle convection with tectonic plates. *Earth and Planetary Science Letters* 184(3–4): 575–587. http://www.sciencedirect.com/science/article/pii/S0012821X00003344.
Montelli R, Nolet G, Dahlen FA, Masters G, Engdahl ER, and Hung S-H (2004) Finite-frequency tomography reveals a variety of plumes in the mantle. *Science* 303: 338–343.
Montési L and Hirth G (2003) Grain size evolution and the rheology of ductile shear zones: From laboratory experiments to postseismic creep. *Earth and Planetary Science Letters* 211: 97–110.
Moresi L and Solomatov V (1998) Mantle convection with a brittle lithosphere: Thoughts on the global tectonic style of the Earth and Venus. *Geophysical Journal International* 133: 669–682.
Morgan W (1968) Rises, trenches, great faults and crustal blocks. *Journal of Geophysical Research* 73: 1959–1982.
Morgan WJ (1972) Plate motions and deep mantle convection. *Memoir – Geological Society of America* 132: 7–22.
Morgan JP and Smith W (1992) Flattening of the seafloor depth-age curve as a response to asthenospheric flow? *Nature* 359: 524–527.
Morra G, Seton M, Quevedo L, and Müller RD (2013) Organization of the tectonic plates in the last 200 Myr. *Earth and Planetary Science Letters* 373: 93–101.
Moyen J-F and van Hunen J (2012) Short-term episodicity of Archaean plate, tectonics. *Geology,* http://dx.doi.org/10.1130/G32894.1.
Mueller S and Phillips R (1991) On the initiation of subduction. *Journal of Geophysical Research* 96: 651–665.
Nakakuki T, Hamada C, and Tagawa M (2008) Generation and driving forces of plate-like motion and asymmetric subduction in dynamical models of an integrated mantle–lithosphere system. *Physics of the Earth and Planetary Interiors* 166(3–4): 128–146. http://www.sciencedirect.com/science/article/pii/S0031920108000241.
Nataf H and VanDecar J (1993) Seismological detection of a mantle plume? *Nature* 364: 115–120.
Nicolis G (1995) *Introduction to Nonlinear Science*. Cambridge: Cambridge University Press.
Nikolaeva K, Gerya TV, and Marques FO (2010) Subduction initiation at passive margins: Numerical modeling. *Journal of Geophysical Research* 115: B03406.
O'Connell R, Gable C, and Hager B (1991) Toroidal–poloidal partitioning of lithospheric plate motion. In: Sabadini R, et al. (eds.) *Glacial Isostasy, Sea Level and Mantle Rheology*, pp. 535–551. Norwell, MA: Kluwer Academic.
Ogawa M, Schubert G, and Zebib A (1991) Numerical simulations of three-dimensional thermal convection in a fluid with strongly temperature-dependent viscosity. *Journal of Fluid Mechanics* 233: 299–328.
Olgaard D (1990) The role of second phase in localizing deformation. In: Knipe R and Rutter E (eds.) *Deformation Mechanisms, Rheology and Tectonics*, vol. 54, pp. 175–181. London: Geological Society, Special Publication.
Olson P and Bercovici D (1991) On the equipartitioning of kinetic energy in plate tectonics. *Geophysical Research Letters* 18: 1751–1754.
Olson P and Corcos G (1980) A boundary layer model for mantle convection with surface plates. *Geophysical Journal of the Royal Astronomical Society* 62: 195–219.

O'Neill C and Lenardic A (2007) Geological consequences of super-sized earths. *Geophysical Research Letters* 34: 19204–19208.
O'Rourke J and Korenaga J (2012) Terrestrial planet evolution in the stagnant-lid regime: Size effects and the formation of self-destabilizing crust. *Icarus* 221: 1043–1060.
Oxburgh E and Turcotte D (1978) Mechanisms of continental drift. *Reports on Progress in Physics* 41: 1249–1312.
Parmentier E, Turcotte D, and Torrance K (1976) Studies of finite amplitude non-Newtonian thermal convection with applications to convection in the earth's mantle. *Journal of Geophysical Research* 81: 1839–1846.
Parsons B and McKenzie D (1978) Mantle convection and the thermal structure of plates. *Journal of Geophysical Research* 83: 4485–4496.
Parsons B and Sclater J (1977) An analysis of the variation of ocean floor bathymetry with age. *Journal of Geophysical Research* 82: 803–827.
Pearson J (1958) On convection cells induced by surface tension. *Journal of Fluid Mechanics* 4: 489–500.
Pekeris C (1935) Thermal convection in the interior of the earth. *Monthly Notices of the Royal Astronomical Society, Geophysical Supplement* 3: 343–367.
Phillips BR and Coltice N (2010) Temperature beneath continents as a function of continental cover and convective wavelength. *Journal of Geophysical Research – Solid Earth* 115: B04408. http://dx.doi.org/10.1029/2009JB006600.
Pinet C, Jaupart C, Mareschal J, Gariepy C, Bienfait G, and Lapointe R (1991) Heat-flow and structure of the lithosphere in the Eastern Canadian Shield. *Journal of Geophysical Research – Solid Earth* 96(B12): 19941–19963.
Polat A, Appel PW, and Fryer BJ (2011) An overview of the geochemistry of Eoarchean to Mesoarchean ultramafic to mafic volcanic rocks, SW Greenland: Implications for mantle depletion and petrogenetic processes at subduction zones in the early Earth. *Gondwana Research* 20(2–3): 255–283.
Pollack H, Hurter S, and Johnson J (1993) Heat flow from the earth's interior: Analysis of the global data set. *Reviews of Geophysics* 31: 267–280.
Ranalli G (1995) *Rheology of the Earth*. London: Chapman and Hall.
Ranero CR, Phipps Morgan J, McIntosh K, and Reichert C (2003) Bending-related faulting and mantle serpentinization at the middle America trench. *Nature* 425(6956): 367–373. http://dx.doi.org/10.1038/nature01961.
Ratcliff J, Tackley P, Schubert G, and Zebib A (1997) Transitions in thermal convection with strongly variable viscosity. *Physics of the Earth and Planetary Interiors* 102: 201–212.
Regenauer-Lieb K, Yuen D, and Branlund J (2001) The initiation of subduction: Criticality by addition of water? *Science* 294: 578–580.
Ribe N (1992) The dynamics of thin shells with variable viscosity and the origin of toroidal flow in the mantle. *Geophysical Journal International* 110: 537–552.
Ricard Y and Bercovici D (2003) Two-phase damage theory and crustal rock failure: The theoretical 'void' limit, and the prediction of experimental data. *Geophysical Journal International* 155: 1057–1064.
Ricard Y, Bercovici D, and Schubert G (2001) A two-phase model of compaction and damage: 2. Applications to compaction, deformation, and the role of interfacial surface tension. *Journal of Geophysical Research* 106(B5): 8907–8924.
Ricard Y, Doglioni C, and Sabadini R (1991) Differential rotation between lithosphere and mantle: A consequence of lateral viscosity variations. *Journal of Geophysical Research* 96: 8407–8415.
Ricard Y, Fleitout L, and Froidevaux C (1984) Geoid heights and lithospheric stresses for a dynamic earth. *Annales Geophysicae* 2: 267–286.
Ricard Y and Froidevaux C (1986) Stretching instabilities and lithospheric boudinage. *Journal of Geophysical Research* 91: 8314–8324.
Ricard Y and Froidevaux C (1991) Seismic imaging, plate velocities and geoid, the direct and inverse problem. In: Sabadini R and Lambeck K (eds.) *Glacial Isostasy, Sea-Level and Mantle Rheology*, pp. 553–569. Dordrecht: Kluwer Academic.
Ricard Y, Richards MA, Lithgow-Berteloni C, and Stunf YL (1993) A geodynamic model of mantle mass heterogeneities. *Journal of Geophysical Research* 98: 21895–21909.
Ricard Y and Vigny C (1989) Mantle dynamics with induced plate tectonics. *Journal of Geophysical Research* 94: 17543–17559.
Ricard Y, Vigny C, and Froidevaux C (1989) Mantle heterogeneities, geoid and plate motion: A Monte Carlo inversion. *Journal of Geophysical Research* 94: 13739–13754.
Ricard Y and Wuming B (1991) Inferring the mantle viscosity and its three dimensional structure from geoid, topography and plate velocities. *Geophysical Journal* 105: 561–571.
Richards MA and Engebretson DC (1992) Large-scale mantle convection and the history of subduction. *Nature* 355(6359): 437–440.
Richards M and Hager B (1984) Geoid anomalies in a dynamic earth. *Journal of Geophysical Research* 89: 5487–6002.
Richards M and Lithgow-Bertelloni C (1996) Plate motion changes, the Hawaiian–Emperor bend, and the apparent success and failure of geodynamical models. *Earth and Planetary Science Letters* 137: 19–27.
Richards M, Yang W-S, Baumgardner J, and Bunge H-P (2001) Role of a low-viscosity zone in stabilizing plate tectonics: Implications for comparative terrestrial planetology. *Geochemistry, Geophysics, Geosystems* 2: 1026. http://dx.doi.org/10.1029/2000GC000115.
Ringwood A (1972) Phase transformations and mantle dynamics. *Earth and Planetary Science Letters* 14(2): 233–241. http://www.sciencedirect.com/science/article/pii/0012821X7290012X.
Ringwood A and Green D (1966) An experimental investigation of the gabbro-eclogite transformation and some geophysical implications. *Tectonophysics* 3(5): 383–427.http://www.sciencedirect.com/science/article/pii/0040195166900096.
Rolf T, Coltice N, and Tackley PJ (2012) Linking continental drift, plate tectonics and the thermal state of the Earth's mantle. *Earth and Planetary Science Letters* 351: 134–146.
Rolf T and Tackley PJ (2011) Focussing of stress by continents in 3D spherical mantle convection with self-consistent plate tectonics. *Geophysical Research Letters* 38(18): L18301. http://dx.doi.org/10.1029/2011GL048677.
Rozel A, Ricard Y, and Bercovici D (2011) A thermodynamically self-consistent damage equation for grain size evolution during dynamic recrystallization. *Geophysical Journal International* 184(2): 719–728.
Runcorn S (1962a) Convection currents in the earth's mantle. *Nature* 195: 1248–1249.
Runcorn S (1962b) Towards a theory of continental drift. *Nature* 193: 311–314.
Russo R and Silver PG (1994) Trench-parallel flow beneath the Nazca plate from seismic anisotropy. *Science* 263: 1105–1111.
Schmeling S and Jacoby W (1981) On modeling the lithosphere in mantle convection with non-linear rheology. *Journal of Geophysics* 50: 89–100.
Schubert G (1980) Self-driven motions of plates and descending slabs. In: Davies P and Runcorn S (eds.) *Mechanisms of Continental Drift and Plate Tectonics*, pp. 151–158. New York: Academic Press.
Schubert G, Froidevaux C, and Yuen D (1976) Oceanic lithosphere and asthenosphere: Thermal and mechanical structure. *Journal of Geophysical Research* 81: 3525–3540.
Schubert G and Sandwell D (1995) A global survey of possible subduction sites on Venus. *Icarus* 117(1): 173–196.
Schubert G, Stevenson D, and Cassen P (1980) Whole planet cooling and the radiogenic heat source contents of the earth and moon. *Journal of Geophysical Research* 85: 2531–2538.
Schubert G and Turcotte D (1972) One-dimensional model of shallow mantle convection. *Journal of Geophysical Research* 77: 945–951.
Schubert G, Turcotte D, and Olson P (2001) *Mantle Convection in the Earth and Planets*. Cambridge: Cambridge University Press.
Schubert G, Turcotte D, and Yuen D (1975) Role of phase transitions in a dynamic mantle. *Geophysical Journal of the Royal Astronomical Society* 42: 705–735.
Schubert G and Zhang K (1997) Foundering of the lithosphere at the onset of subduction. *Geophysical Research Letters* 24: 1527–1529.
Sclater J, Jaupart C, and Galson D (1980) The heat flow through the oceanic and continental crust and the heat loss of the earth. *Reviews of Geophysics and Space Physics* 18: 269–311.
Sharp WD and Clague DA (2006) 50-Ma Initiation of Hawaiian–Emperor bend records major change in Pacific plate motion. *Science* 313(5791): 1281–1284.
Shen Y, Solomon S, Bjarnason I, and Wolfe C (1998) Seismic evidence for a lower mantle origin of the iceland plume. *Nature* 395: 62–65.
Shimizu I (1998) Stress and temperature dependence of recrystallized grain size: A subgrain misorientation model. *Geophysical Research Letters* 25: 4237–4240.
Shirey S, Kamber B, Whitehouse M, Mueller P, and Basu A (2008) A review of the isotopic and trace element evidence for mantle and crustal processes in the Hadean and Archean: Implications for the onset of plate tectonic subduction. In: Condie K and Pease V (eds.) *When Did Plate Tectonics Begin on Planet Earth?* pp. 1–29. Boulder, CO: Geological Society of America, Special Paper 440.
Shirey SB and Richardson SH (2011) Start of the Wilson cycle at 3 Ga shown by diamonds from subcontinental mantle. *Science* 333: 434–436.
Silver P, Carlson R, and Olson P (1988) Deep slabs, geochemical heterogeneity, and the large-scale structure of mantle convection: An investigation of an enduring paradox. *Annual Review of Earth and Planetary Sciences* 16: 477–541.
Sizova E, Gerya T, Brown M, and Perchuk LL (2010) Subduction styles in the precambrian: Insight from numerical experiments. *Lithos* 116(3–4): 209–229.
Skemer P, Warren JM, Kelemen PB, and Hirth G (2010) Microstructural and rheological evolution of a mantle shear zone. *Journal of Petrology* 51: 43–53.

Sleep N (1990) Hotspots and mantle plumes: Some phenomenology. *Journal of Geophysical Research* 95: 6715–6736.

Solomatov V (1995) Scaling of temperature dependent and stress dependent viscosity convection. *Physics of Fluids* 7: 266–274.

Sornette D and Pisarenko V (2003) Fractal plate tectonics. *Geophysical Research Letters* 30(3: 1105). http://dx.doi.org/10.1029/2002GL015043.

Sotin C and Labrosse S (1999) Three-dimensional thermal convection in an iso-viscous, infinite Prandtl number fluid heated from within and from below: Applications to the transfer of heat through planetary mantles. *Physics of the Earth and Planetary Interiors* 112(3–4): 171–190. http://www.sciencedirect.com/science/article/pii/S0031920199000047.

Southam G and Westall F (2007) Geology, life and habitability. In: Spohn T and Schubert G (Editor-in-Chief) (eds.) *Treatise on Geophysics*. *Planets and Moons*, vol. 10, pp. 421–437. Amsterdam: Elsevier.

Spiegelman M and McKenzie D (1987) Simple 2-D models for melt extraction at mid-ocean ridges and island arcs. *Earth and Planetary Science Letters* 83: 137–152.

Squyres SW, Grotzinger JP, Arvidson RE, et al. (2004) In situ evidence for an ancient aqueous environment at Meridiani Planum, Mars. *Science* 306(5702): 1709–1714. http://www.sciencemag.org/content/306/5702/1709.abstract.

Stein C, Schmalzl J, and Hansen U (2004) The effect of rheological parameters on plate behaviour in a self-consistent model of mantle convection. *Physics of the Earth and Planetary Interiors* 142: 225–255.

Stein C and Stein S (1992) A model for the global variation in oceanic depth and heat flow with lithospheric age. *Nature* 359: 123–129.

Steinberger B and O'Connell R (1998) Advection of plumes in mantle flow: Implications for hotspot motion, mantle viscosity and plume distribution. *Geophysical Journal International* 132: 412–434.

Stern RJ (2004) Subduction initiation: Spontaneous and induced. *Earth and Planetary Science Letters* 226: 275–292.

Stern R and Bloomer S (1992) Subduction zone infancy: Examples from the eocene Izu-Bonin-Mariana and Jurassic California arcs. *Geological Society of America Bulletin* 104: 1621–1636.

Strutt JW (Lord Rayleigh) (1916) On convective currents in a horizontal layer of fluid when the higher temperature is on the under side. *Philosophical Magazine* 32: 529–546.

Su W and Dziewonski A (1992) On the scale of mantle heterogeneity. *Physics of the Earth and Planetary Interiors* 74: 29–54.

Tackley P (1996a) Effects of strongly variable viscosity on three-dimensional compressible convection in planetary mantles. *Journal of Geophysical Research* 101: 3311–3332.

Tackley P (1996b) On the ability of phase transitions and viscosity layering to induce long-wavelength heterogeneity in the mantle. *Geophysical Research Letters* 23: 1985–1988.

Tackley P (1998) Self-consistent generation of tectonic plates in three-dimensional mantle convection. *Earth and Planetary Science Letters* 157: 9–22.

Tackley P (2000a) Mantle convection and plate tectonics: Toward and integrated physical and chemical theory. *Science* 288: 2002–2007.

Tackley P (2000b) Self-consistent generation of tectonic plates in time-dependent, three-dimensional mantle convection simulations: 1. Pseudoplastic yielding. *Geochemistry, Geophysics, Geosystems* 1: 1021. http://dx.doi.org/10.1029/2000GC000036.

Tackley P (2000c) Self-consistent generation of tectonic plates in time-dependent, three-dimensional mantle convection simulations: 2. Strain weakening and asthenosphere. *Geochemistry, Geophysics, Geosystems* 1: 1026. http://dx.doi.org/10.1029/2000GC000043.

Tackley P (2000d) The quest for self-consistent generation of plate tectonics in mantle convection models. In: Richards MA, Gordon R, and van der Hilst R (eds.) *History and Dynamics of Global Plate Motions*. *Geophysical Monograph Series*, vol. 121, pp. 47–72. Washington, DC: American Geophysical Union.

Tackley P, Ammann M, Brodholt J, Dobson D, and Valencia D (2013) Mantle dynamics in super-earths: Post-perovskite rheology and self-regulation of viscosity. *Icarus* 225(1): 50–61. http://www.sciencedirect.com/science/article/pii/S0019103513001231.

Tackley P, Stevenson D, Glatzmaier GA, and Schubert G (1993) Effects of an endothermic phase transition at 670 km depth in a spherical model of convection in the earth's mantle. *Nature* 361: 699–704.

Tackley P, Stevenson D, Glatzmaier GA, and Schubert G (1994) Effects of a multiple phase transitions in a 3 dimensional spherical model of convection in earth's mantle. *Journal of Geophysical Research* 99: 15877–15901.

Thatcher W and England P (1998) Ductile shear zones beneath strike-slip faults: Implications for the thermomechanics of the San Andreas Fault zone. *Journal of Geophysical Research* 103: 891–905.

Thielmann M and Kaus BJP (2012) Shear heating induced lithospheric-scale localization: Does it result in subduction? *Earth and Planetary Science Letters* 359–360: 1–13.

Thompson B (Count Rumford) (1797) The propagation of heat in fluids. *Bibliotheque Britannique (Science et Arts)* 90: 97–200, Reprinted in Brown, 1967.

Thorkelson DJ (1996) Subduction of diverging plates and the principles of slab window formation. *Tectonophysics* 255(1–2): 47–63. http://www.sciencedirect.com/science/article/pii/0040195195001069.

Torsvik T, Smethurst M, Meert J, et al. (1996) Continental break-up and collision in the Neoproterozoic and Palaeozoic – A tale of Baltica and Laurentia. *Earth Science Reviews* 40(3–4): 229–258. http://www.sciencedirect.com/science/article/pii/0012825296000086.

Toth G and Gurnis M (1998) Dynamics of subduction initiation at preexisting fault zones. *Journal of Geophysical Research* 103: 18053–18067.

Tozer D (1972) The present thermal state of the terrestrial planets. *Physics of the Earth and Planetary Interiors* 6: 182–197.

Tozer D (1985) Heat transfer and planetary evolution. *Geophysical Surveys* 7: 213–246.

Trompert R and Hansen U (1998) Mantle convection simulations with rheologies that generate plate-like behavior. *Nature* 395: 686–689.

Turcotte DL (1993) An episodic hypothesis for Venusian tectonics. *Journal of Geophysical Research, Planets* 98(E9): 17061–17068. http://dx.doi.org/10.1029/93JE01775.

Turcotte D, Morein G, Roberts D, and Malamud B (1999) Catastrophic resurfacing and episodic subduction on Venus. *Icarus* 139(1): 49–54. http://www.sciencedirect.com/science/article/pii/S0019103599960840.

Turcotte D and Morgan JP (1992) The physics of magma migration and mantle flow beneath a mid-ocean ridge. In: Morgan JP, Blackman D, and Sinton J (eds.) *Mantle Flow and Melt-Generation at Mid-Ocean Ridges*. *Geophysical Monograph Series*, vol. 71, pp. 155–182. Washington, DC: American Geophysical Union.

Turcotte D and Oxburgh E (1967) Finite amplitude convection cells and continental drift. *Journal of Fluid Mechanics* 28: 29–42.

Turcotte D and Oxburgh E (1972) Mantle convection and the new global tectonics. *Annual Review of Fluid Mechanics* 4: 33–66.

Turcotte D and Schubert G (2002) *Geodynamics*. Cambridge: Cambridge University Press.

Urai J, Means W, and Lister G (1986) Dynamic recrystallization in minerals. In: Hobbs B and Heard H (eds.) *Mineral and Rock Deformation: Laboratory Studies*, pp. 166–199. Washington, DC: American Geophysical Union.

Valencia D and O'Connell RJ (2009) Convection scaling and subduction on earth and super-earths. *Earth and Planetary Science Letters* 286(3–4): 492–502.

Valencia D, O'Connell R, and Sasselov D (2007) Inevitability of plate tectonics on super-earths. *Astrophysics Journal* 670: L45–L48.

Valley JW, Peck WH, King EM, and Wilde SA (2002) A cool early earth. *Geology* 30(4): 351–354.http://geology.gsapubs.org/content/30/4/351.abstract.

van der Hilst R, Engdahl R, Spakman W, and Nolet G (1991) Tomographic imaging of subducted lithosphere below northwest pacific island arcs. *Nature* 353: 37–43.

van der Hilst R, Widiyantoro S, and Engdahl E (1997) Evidence for deep mantle circulation from global tomography. *Nature* 386: 578–584.

van Heck H and Tackley P (2008) Planforms of self-consistently generated plates in 3D spherical geometry. *Geophysical Research Letters* 35: L19312. http://dx.doi.org/10.1029/2008GL035190.

van Heck H and Tackley P (2011) Plate tectonics on super-earths: Equally or more likely than on earth. *Earth and Planetary Science Letters* 310(3–4): 252–261.

van Hunen J and Moyen J-F (2012) Archean subduction: Fact or fiction? *Annual Review of Earth and Planetary Sciences* 40(1): 195–219. http://www.annualreviews.org/doi/abs/10.1146/annurev-earth-042711-105255.

van Hunen J and van den Berg AP (2008) Plate tectonics on the early earth: Limitations imposed by strength and buoyancy of subducted lithosphere. *Lithos* 103(1–2): 217–235.

Vigny C, Ricard Y, and Froidevaux C (1991) The driving mechanism of plate tectonics. *Tectonophysics* 187: 345–360.

Vine F and Matthews D (1963) Magnetic anomalies over oceanic ridges. *Nature* 199: 947–949.

Walker J, Hayes P, and Kasting J (1981) A negative feedback mechanism for the long-term stabilization of Earth's surface temperature. *Journal of Geophysical Research* 86: 9776–9782.

Warren JM and Hirth G (2006) Grain size sensitive deformation mechanisms in naturally deformed peridotites. *Earth and Planetary Science Letters* 248(1–2): 438–450.

Watts A, Karner G, and Steckler M (1982) Lithosphere flexure and the evolution of sedimentary basins. *Philosophical Transactions of the Royal Society of London, Series A: Mathematical, Physical and Engineering Sciences* 305: 249–281.

Weertman J and Weertman J (1975) High temperature creep of rock and mantle viscosity. *Annual Review of Earth and Planetary Sciences* 3: 293–315.

Wegener A (1924) *The Origin of Continents and Oceans*. London: Methuen and Co.

Weinstein S (1993) Catastrophic overturn of the earth's mantle driven by multiple phase changes and internal heating. *Geophysical Research Letters* 20: 101–104.

Weinstein S (1996) Thermal convection in a cylindrical annulus with a non-Newtonian outer surface. *PAGEOPH* 146: 551–572.

Weinstein S (1998) The effect of convection planform on the toroidal–poloidal energy ratio. *Earth and Planetary Science Letters* 155: 87–95.

Weinstein S and Christensen U (1991) Convection planforms in a fluid with a temperature-dependent viscosity beneath a stress-free upper boundary. *Geophysical Research Letters* 18: 2035–2038.

Weinstein S and Olson P (1989) The proximity of hotspots to convergent and divergent plate boundaries. *Geophysical Research Letters* 16: 433–436.

Weinstein S and Olson P (1990) Planforms in thermal convection with internal heat sources at large Rayleigh and Prandtl numbers. *Geophysical Research Letters* 17: 239–242.

Weinstein S and Olson P (1992) Thermal convection with non-Newtonian plates. *Geophysical Journal International* 111: 515–530.

Wessel P and Kroenke LW (2008) Pacific absolute plate motion since 145 Ma: An assessment of the fixed hot spot hypothesis. *Journal of Geophysical Research - Solid Earth* 113(B6). http://dx.doi.org/10.1029/2007JB005499.

White D (1988) The planforms and onset of convection with temperature-dependent viscosity. *Journal of Fluid Mechanics* 191: 247–286.

White S, Burrows S, Carreras J, Shaw N, and Humphreys F (1980) On mylonites in ductile shear zones. *Journal of Structural Geology* 2: 175–187.

Whitehead J (1976) Convection models: Laboratory versus mantle. *Tectonophysics* 35: 215–228.

Whitehead J and Gans R (1974) A new, theoretically tractable earthquake model. *Geophysical Journal of the Royal Astronomical Society* 39: 11–28.

Whitehead J and Parsons B (1978) Observations of convection at Rayleigh numbers up to 760,000 in a fluid with a large Prandtl number. *Geophysical and Astrophysical Fluid Dynamics* 19: 201–217.

Wilson J (1966) Did the Atlantic close and then re-open? *Nature* 211: 676–681.

Wolfe C, Bjarnason I, VanDecar J, and Solomon S (1997) Seismic structure of the iceland mantle plume. *Nature* 385: 245–247.

Wolfe C, Solomon S, Laske G, et al. (2009) Mantle shear-wave velocity structure beneath the Hawaiian hotspot. *Science* 326: 1388–1390.

Yin A (2012) Structural analysis of the Valles Marineris fault zone: Possible evidence for large-scale strike-slip faulting on mars. *Lithosphere* 4(4): 286–330.

Yoshida M (2013) Mantle temperature under drifting deformable continents during the supercontinent cycle. *Geophysical Research Letters* 40(4): 681–686.

Yuen D, Fleitout L, Schubert G, and Froidevaux C (1978) Shear deformation zones along major transform faults and subducting slabs. *Geophysical Journal of the Royal Astronomical Society* 54(1): 93–119.

Zhang S and Yuen D (1995) Intense local toroidal motion generated by variable viscosity compressible convection in 3-D spherical shell. *Geophysical Research Letters* 23: 3135–3138.

Zhong S and Gurnis M (1993) Dynamic feedback between a continent-like raft and thermal-convection. *Journal of Geophysical Research – Solid Earth* 98(B7): 12219–12232.

Zhong S and Gurnis M (1995a) Mantle convection with plates and mobile, faulted plate margins. *Science* 267: 838–843.

Zhong S and Gurnis M (1995b) Towards a realistic simulation of plate margins in mantle convection? *Geophysical Research Letters* 22: 981–984.

Zhong S and Gurnis M (1996) Interaction of weak faults and non-Newtonian rheology produces plate tectonics in a 3d model of mantle flow. *Nature* 383: 245–247.

Zhong S, Gurnis M, and Moresi L (1998) Role of faults, nonlinear rheology, and viscosity structure in generating plates from instantaneous mantle flow models. *Journal of Geophysical Research* 103: 15255–15268.

Zhong S, Zuber M, Moresi L, and Gurnis M (2000) Role of temperature-dependent viscosity and surface plates in spherical shell models of mantle convection. *Journal of Geophysical Research* 105: 11063–11082.

Zindler A and Hart S (1986) Chemical geodynamics. *Annual Review of Earth and Planetary Sciences* 14: 493–571.